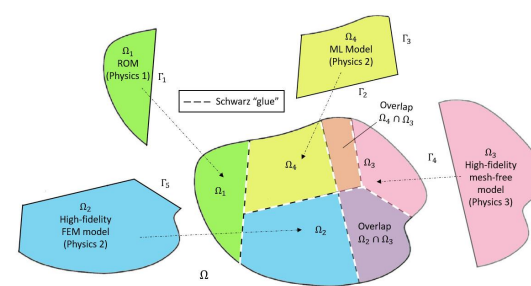
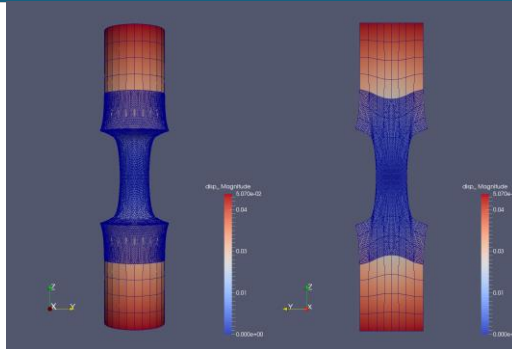
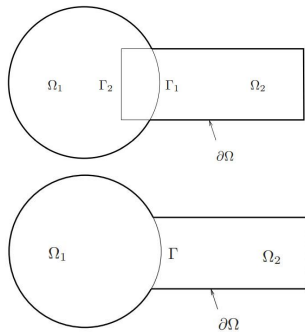


# Domain decomposition-based coupling of intrusive and non-intrusive reduced order models via the Schwarz alternating method



Irina Tezaur<sup>1</sup>, Chris Wentland<sup>1</sup>, Francesco Rizzi<sup>2</sup>, Joshua Barnett<sup>3</sup>, Ian Moore<sup>1</sup>, Eric Parish<sup>1</sup>, Anthony Gruber<sup>1</sup>, Alejandro Mota<sup>1</sup>

<sup>1</sup>Sandia National Laboratories, <sup>2</sup>NexGen Analytics, <sup>3</sup>Cadence Design Systems

Large-Scale Scientific Computations (LSSC) 2025  
Sozopol, Bulgaria. June 16-20, 2025.

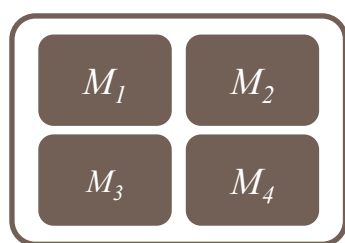
SAND2025-06760C



# Motivation: Multi-scale & Multi-physics Coupling for Predictive Digital Twins

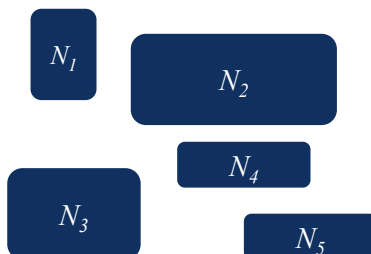


There exist established **rigorous mathematical theories** for **coupling** multi-scale and multi-physics components based on **traditional discretization methods** (“Full Order Models” or FOMs).



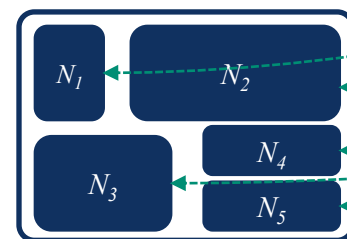
## Complex System Model

- PDEs, ODEs
- Nonlocal integral
- Classical DFT
- Atomistic, ...



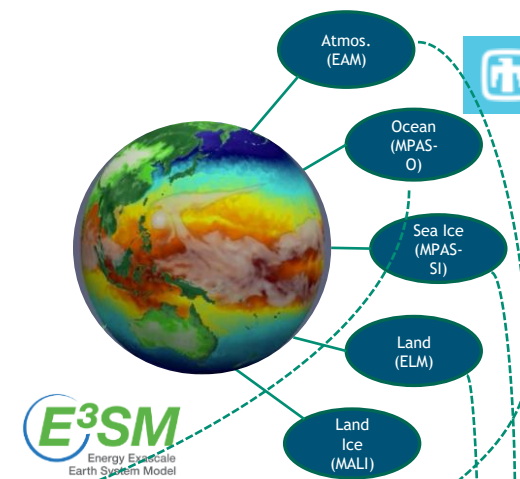
## Traditional Methods

- Mesh-based (FE, FV, FD)
- Meshless (SPH, MLS)
- Implicit, explicit
- Eulerian, Lagrangian...



## Coupled Numerical Model

- Monolithic (Lagrange multipliers)
- Partitioned (loose) coupling
- Iterative (Schwarz, optimization)

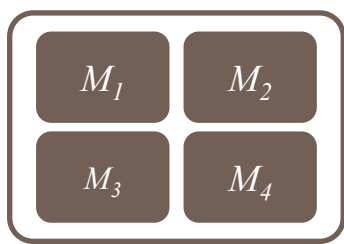




# Motivation: Multi-scale & Multi-physics Coupling for Predictive Digital Twins

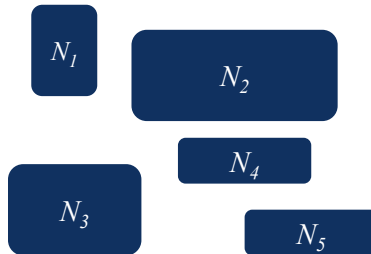


There exist established **rigorous mathematical theories** for **coupling** multi-scale and multi-physics components based on **traditional discretization methods** (“Full Order Models” or FOMs).



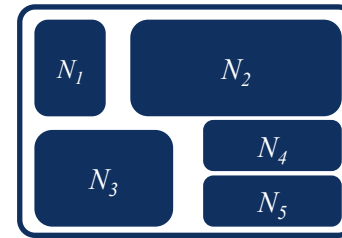
## Complex System Model

- PDEs, ODEs
- Nonlocal integral
- Classical DFT
- Atomistic, ...



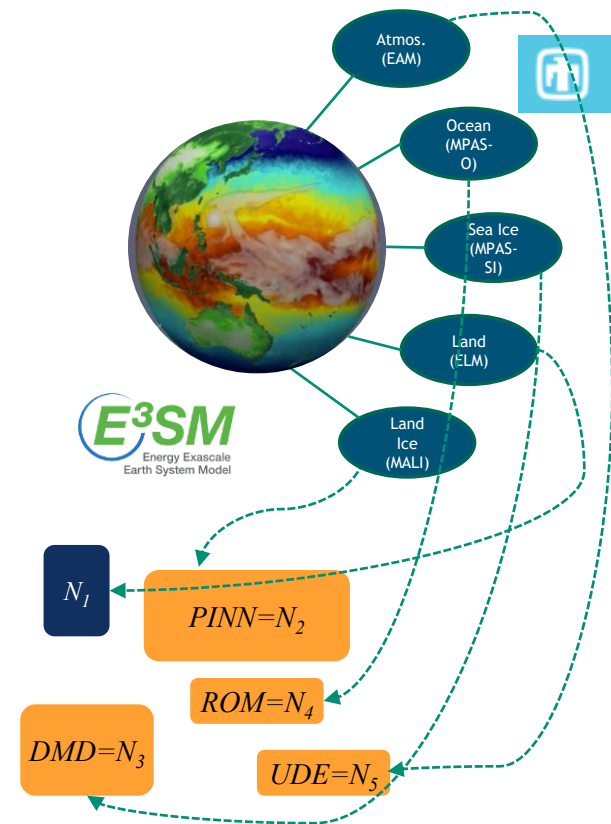
## Traditional Methods

- Mesh-based (FE, FV, FD)
- Meshless (SPH, MLS)
- Implicit, explicit
- Eulerian, Lagrangian, ...



## Coupled Numerical Model

- Monolithic (Lagrange multipliers)
- Partitioned (loose) coupling
- Iterative (Schwarz, optimization)



## Traditional + Data-Driven Methods

- PINNs
- Neural ODEs
- Projection-based ROMs, ...

Unfortunately, existing algorithmic and software infrastructures are **ill-equipped** to handle plug-and-play integration of **non-traditional, data-driven models**!





# Projects on Coupling for Predictive Hybrid Models



$$\int \mathcal{M}^2 dt$$



## Three projects:

- **FHNM:** Flexible Heterogeneous Numerical Methods [LDRD, FY22-FY24]
- **M2dt:** Multi-faceted Mathematics for Predictive Digital Twins [ASCR, FY23-FY27]
- **AHEAD:** Adaptive Hybrid modElS via domAin Decomposition [LDRD, FY25-FY27]

## Principal research objective:

- Develop rigorous methods to enable the “**plug-and-play**” coupling of **standard and data-driven models** from the following classes
  - *Class A:* intrusive projection-based ROMs
  - *Class B:* machine-learned models
  - *Class C:* flow map approximation models, i.e., dynamic model decomposition (DMD)
  - *Class D:* non-intrusive operator inference (OpInf) ROMs



U.S. DEPARTMENT OF  
**ENERGY**

Office of Science

## Three classes of coupling methods:

- Alternating Schwarz-based coupling [FHNM, M2dt, AHEAD]
- Optimization-based coupling [FHNM, M2dt]
- Coupling via **generalized mortar methods** [FHNM, M2dt]



# Projects on Coupling for Predictive Hybrid Models



$$\int \mathcal{M}^2 dt$$



## Three projects:

- **FHNM:** Flexible Heterogeneous Numerical Methods [LDRD, FY22-FY24]
- **M2dt:** Multi-faceted Mathematics for Predictive Digital Twins [ASCR, FY23-FY27]
- **AHEAD:** Adaptive Hybrid modELs via domAin Decomposition [LDRD, FY25-FY27]

## Principal research objective:

- Develop rigorous methods to enable the “**plug-and-play**” coupling of **standard and data-driven models** from the following classes
  - *Class A:* intrusive projection-based ROMs → this talk
  - *Class B:* machine-learned models
  - *Class C:* flow map approximation models, i.e., dynamic model decomposition (DMD)
  - *Class D:* non-intrusive operator inference (OpInf) ROMs → this talk



U.S. DEPARTMENT OF  
**ENERGY**

Office of Science

## Three classes of coupling methods:

- Alternating **Schwarz-based** coupling [FHNM, M2dt, AHEAD] → this talk
- **Optimization-based** coupling [FHNM, M2dt]
- Coupling via **generalized mortar methods** [FHNM, M2dt]



# Projects on Coupling for Predictive Hybrid Models



$$\int \mathcal{M}^2 dt$$



## Three projects:

- **FHNM**: Flexible Heterogeneous Numerical Methods [LDRD, FY22-FY24]
- **M2dt**: Multi-faceted Mathematics for Predictive Digital Twins [ASCR, FY23-FY27]
- **AHEAD**: Adaptive Hybrid modELs via domAin Decomposition [LDRD, FY25-FY27]

## Principal research objective:

- Develop rigorous methods to enable the “**plug-and-play**” coupling of **standard and data-driven models** from the following classes
  - *Class A*: intrusive projection-based ROMs → this talk, 4<sup>th</sup> talk in MS (Y. Choi)
  - *Class B*: machine-learned models → 5<sup>th</sup> talk in MS (J. Actor)
  - *Class C*: flow map approximation models, i.e., dynamic model decomposition (DMD)
  - *Class D*: non-intrusive operator inference (OpInf) ROMs → this talk, 6<sup>th</sup> talk in MS (V. Gosea)



U.S. DEPARTMENT OF  
**ENERGY**

Office of Science

## Three classes of coupling methods:

- Alternating **Schwarz**-based coupling [FHNM, M2dt, AHEAD] → this talk
- **Optimization**-based coupling [FHNM, M2dt]
- Coupling via **generalized mortar methods** [FHNM, M2dt]



# Projects on Coupling for Predictive Hybrid Models



$$\int \mathcal{M}^2 dt$$



## Three projects:

- **FHNM**: Flexible Heterogeneous Numerical Methods [LDRD, FY22-FY24]
- **M2dt**: Multi-faceted Mathematics for Predictive Digital Twins [ASCR, FY23-FY27]
- **AHEAD**: Adaptive Hybrid modELs via domAin Decomposition [LDRD, FY25-FY27]

## Principal research objective:

- Develop rigorous methods to enable the “**plug-and-play**” coupling of **standard** and **data-driven models** from the following classes
  - *Class A*: intrusive projection-based ROMs → this talk, 4<sup>th</sup> talk in MS (Y. Choi)
  - *Class B*: machine-learned models → 5<sup>th</sup> talk in MS (J. Actor)
  - *Class C*: flow map approximation models, i.e., dynamic model decomposition (DMD)
  - *Class D*: non-intrusive operator inference (OpInf) ROMs → this talk, 6<sup>th</sup> talk in MS (V. Gosea)



U.S. DEPARTMENT OF  
**ENERGY**

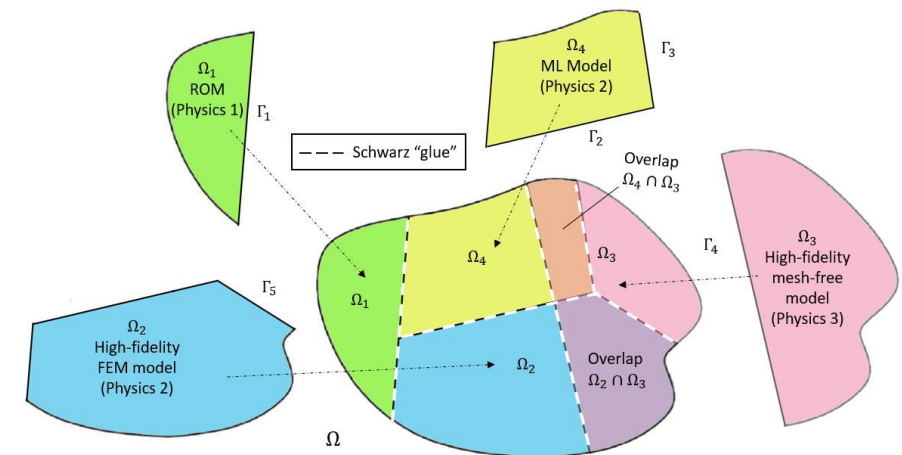
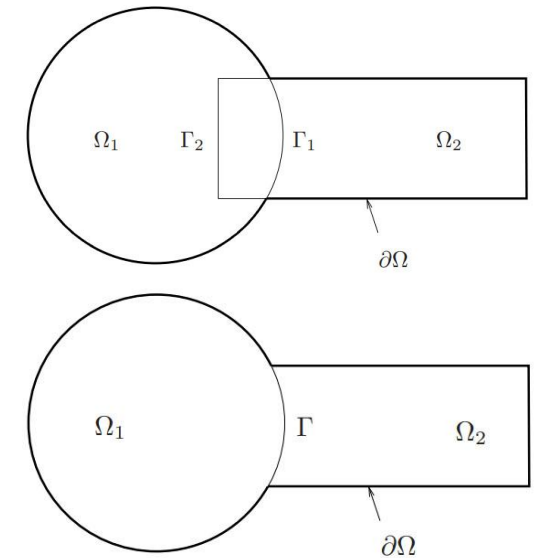
Office of Science

## Three classes of coupling methods:

- Alternating Schwarz-based coupling [FHNM, M2dt, AHEAD] → this talk
- **Optimization-based coupling** → 2<sup>nd</sup> talk in MS (I. Prusak)
- Coupling via **generalized mortar methods** [FHNM, M2dt] → 3<sup>rd</sup> talk in MS (P. Kuberry)

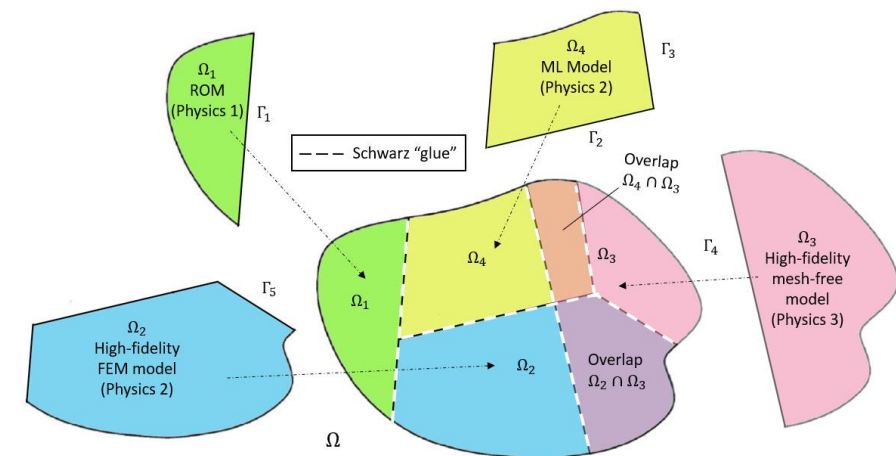
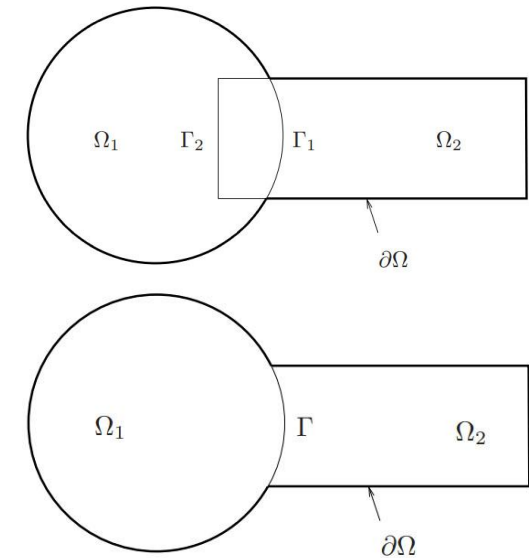


- The Schwarz Alternating Method (SAM) for Domain Decomposition-Based Coupling
- Part 1: SAM-based Coupling of Intrusive Projection-based ROMs
  - Projection-based ROM Overview
  - SAM-based Coupling Workflow
  - Numerical Examples
- Part 2: SAM-based Coupling of Non-Intrusive OpInf ROMs
  - OpInf ROM Overview
  - SAM-based Coupling Workflow
  - Numerical Examples
- Summary & Ongoing/Future Work



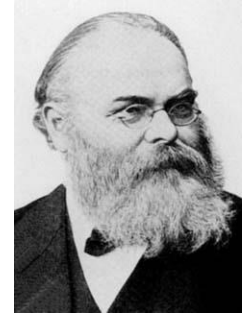


- The Schwarz Alternating Method (SAM) for Domain Decomposition-Based Coupling
- Part 1: SAM-based Coupling of Intrusive Projection-based ROMs
  - Projection-based ROM Overview
  - SAM-based Coupling Workflow
  - Numerical Examples
- Part 2: SAM-based Coupling of Non-Intrusive OpInf ROMs
  - OpInf ROM Overview
  - SAM-based Coupling Workflow
  - Numerical Examples
- Summary & Ongoing/Future Work





# Schwarz Alternating Method for Domain Decomposition



H. Schwarz (1843-1921)



- Proposed in 1870 by H. Schwarz for solving Laplace PDE on irregular domains.

**Crux of Method:** if the solution is known in regularly shaped domains, use those as pieces to iteratively build a solution for the more complex domain.

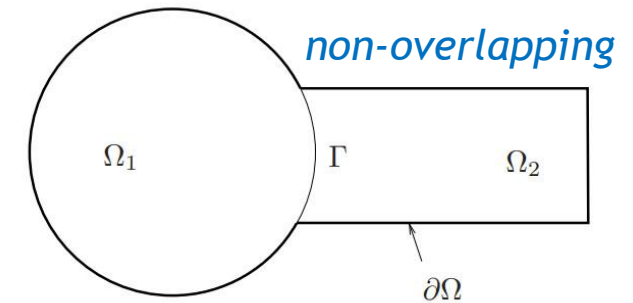
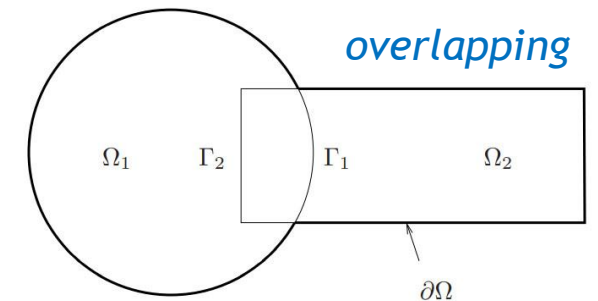
## Basic Schwarz Algorithm

### *Initialize:*

- Solve PDE by any method on  $\Omega_1$  w/ initial guess for transmission BCs on  $\Gamma_1$ .

### *Iterate until convergence:*

- Solve PDE by any method on  $\Omega_2$  w/ transmission BCs on  $\Gamma_2$  based on values just obtained for  $\Omega_1$ .
- Solve PDE by any method on  $\Omega_1$  w/ transmission BCs on  $\Gamma_1$  based on values just obtained for  $\Omega_2$ .



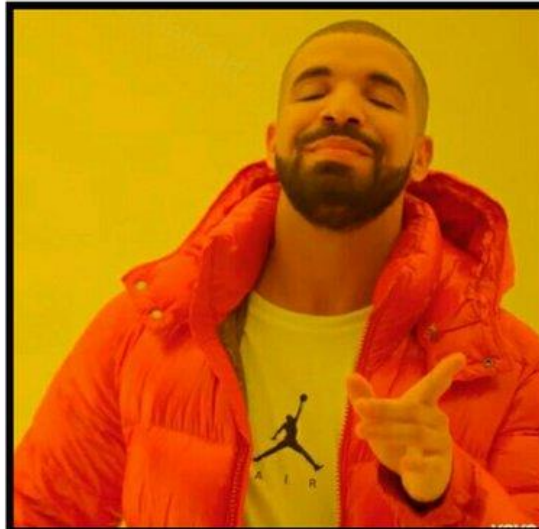
- Schwarz alternating method most commonly used as a ***preconditioner*** for Krylov iterative methods to solve linear algebraic equations.

**Novelty:** we are using the Schwarz alternating method as a ***discretization method*** for solving multi-scale or multi-physics partial differential equations (PDEs).





AS A *PRECONDITIONER*  
FOR THE LINEARIZED  
SYSTEM



AS A *SOLVER* FOR THE  
COUPLED  
FULLY NONLINEAR  
PROBLEM

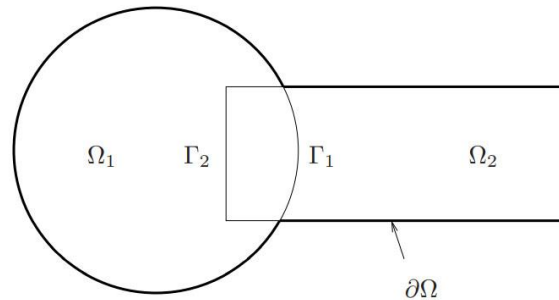


## Overlapping Domain Decomposition

$$\begin{cases} N(\mathbf{u}_1^{(n+1)}) = f, & \text{in } \Omega_1 \\ \mathbf{u}_1^{(n+1)} = \mathbf{g}, & \text{on } \partial\Omega_1 \setminus \Gamma_1 \\ \mathbf{u}_1^{(n+1)} = \mathbf{u}_2^{(n)} & \text{on } \Gamma_1 \end{cases}$$

$$\begin{cases} N(\mathbf{u}_2^{(n+1)}) = f, & \text{in } \Omega_2 \\ \mathbf{u}_2^{(n+1)} = \mathbf{g}, & \text{on } \partial\Omega_2 \setminus \Gamma_2 \\ \mathbf{u}_2^{(n+1)} = \mathbf{u}_1^{(n+1)} & \text{on } \Gamma_2 \end{cases}$$

Part 2 of Talk



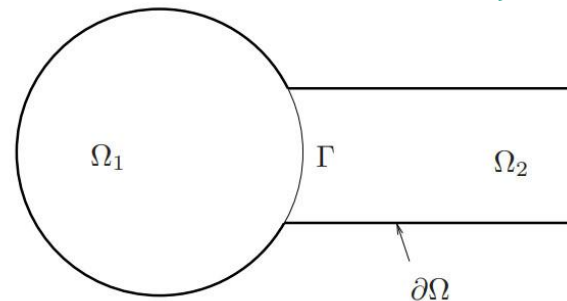
$$\text{Model PDE: } \begin{cases} N(\mathbf{u}) = \mathbf{f}, & \text{in } \Omega \\ \mathbf{u} = \mathbf{g}, & \text{on } \partial\Omega \end{cases}$$

- Dirichlet-Dirichlet transmission BCs [Schwarz 1870; Lions 1988; Mota *et al.* 2017; Mota *et al.* 2022] guarantee convergence

## Non-overlapping Domain Decomposition

$$\begin{cases} N(\mathbf{u}_1^{(n+1)}) = f, & \text{in } \Omega_1 \\ \mathbf{u}_1^{(n+1)} = \mathbf{g}, & \text{on } \partial\Omega_1 \setminus \Gamma \\ \mathbf{u}_1^{(n+1)} = \lambda_{n+1}, & \text{on } \Gamma \end{cases}$$

$$\begin{cases} N(\mathbf{u}_2^{(n+1)}) = f, & \text{in } \Omega_2 \\ \mathbf{u}_2^{(n+1)} = \mathbf{g}, & \text{on } \partial\Omega_2 \setminus \Gamma \\ \nabla \mathbf{u}_2^{(n+1)} \cdot \mathbf{n} = \nabla \mathbf{u}_1^{(n+1)} \cdot \mathbf{n}, & \text{on } \Gamma \end{cases}$$



Part 1 of Talk

$$\lambda_{n+1} = \theta \mathbf{u}_2^{(n)} + (1 - \theta) \lambda_n, \text{ on } \Gamma, \text{ for } n \geq 1$$

- Relevant for multi-material and multi-physics coupling\*
- Usually requires alternating Dirichlet-Neumann [Zanolli *et al.* 1987] or Robin-Robin transmission BCs [Lions 1990] for convergence
- $\theta \in [0,1]$ : relaxation parameter (can help convergence)

\* For certain discretizations, non-overlapping DD + Dirichlet-Dirichlet transmission BCs is convergent [Wentland *et al.*, 2025]!

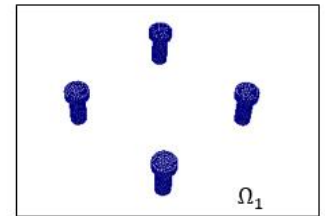
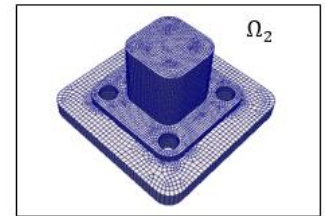
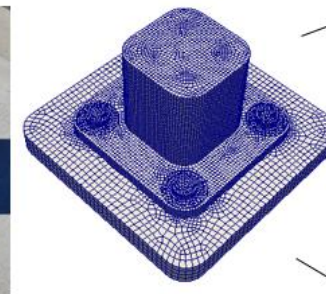


### Model Solid Mechanics PDEs:

$$\text{Quasistatic: } \operatorname{Div} \mathbf{P} + \rho_0 \mathbf{B} = \mathbf{0} \quad \text{in } \Omega$$

$$\text{Dynamic: } \operatorname{Div} \mathbf{P} + \rho_0 \mathbf{B} = \rho_0 \ddot{\boldsymbol{\varphi}} \quad \text{in } \Omega \times I$$

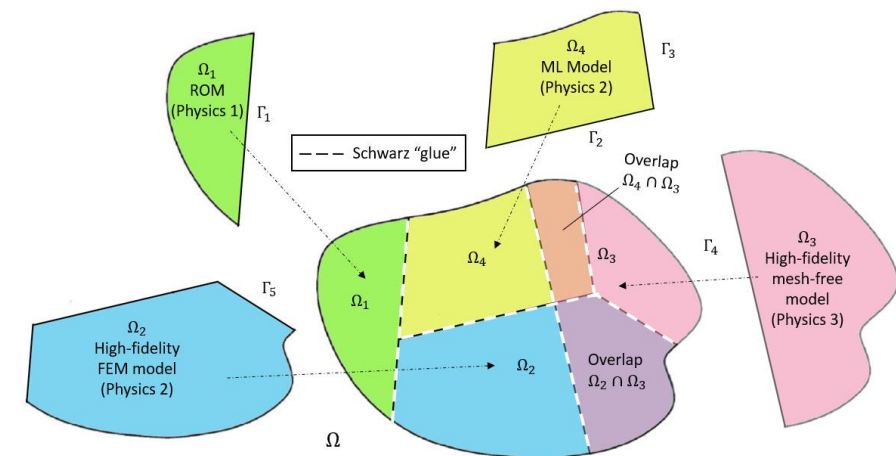
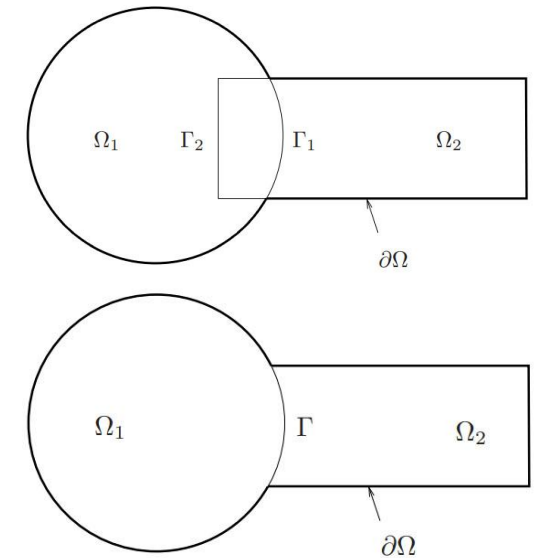
- Coupling is *concurrent* (two-way).
- *Ease of implementation* into existing massively-parallel HPC codes.
- *Scalable, fast, robust* (we target *real* engineering problems, e.g., analyses involving failure of bolted components!).
- Coupling does not introduce *nonphysical artifacts*.
- *Theoretical* convergence properties/guarantees<sup>1</sup>.
- “*Plug-and-play*” framework:
  - Ability to couple regions with *different non-conformal meshes*, *different element types* and *different levels of refinement* to simplify task of *meshing complex geometries*.
  - Ability to use *different solvers/time-integrators* in different regions.



<sup>1</sup> Mota et al. 2017; Mota et al. 2022. <sup>2</sup> <https://github.com/sandialabs/LCM>.



- The Schwarz Alternating Method (SAM) for Domain Decomposition-Based Coupling
- **Part 1: SAM-based Coupling of Intrusive Projection-based ROMs**
  - Projection-based ROM Overview
  - SAM-based Coupling Workflow
  - Numerical Examples
- Part 2: SAM-based Coupling of Non-Intrusive OpInf ROMs
  - OpInf ROM Overview
  - SAM-based Coupling Workflow
  - Numerical Examples
- Summary & Ongoing/Future Work



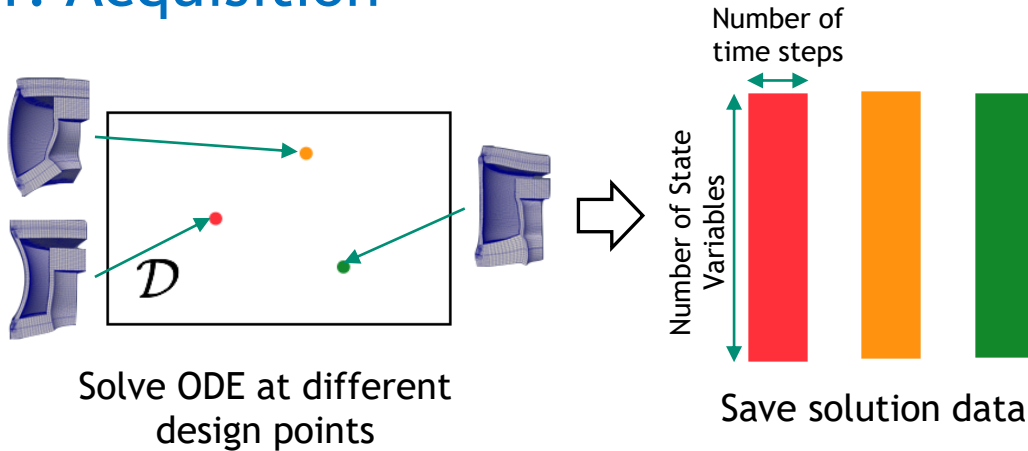




Full Order Model (FOM):  $\frac{du}{dt} = f(u; t, \mu)$

\* Least-Squares Petrov-Galerkin

## 1. Acquisition



## 2. Learning

Proper Orthogonal Decomposition (POD):

$$\mathbf{X} = \begin{bmatrix} \text{red} & \text{orange} & \text{green} \end{bmatrix} = \begin{bmatrix} \Phi & \mathbf{U} \end{bmatrix} \begin{bmatrix} \Sigma & \mathbf{V}^T \end{bmatrix}$$

ROM = projection-based Reduced Order Model

## 3. Projection-Based Reduction

Choose ODE temporal discretization

$$\frac{du}{dt} = f(u; t, \mu) \Downarrow r^n(u^n; \mu) = 0, \quad n = 1, \dots, T$$

Reduce the number of unknowns

$$\mathbf{u}(t) \approx \tilde{\mathbf{u}}(t) = \Phi \hat{\mathbf{u}}(t)$$

Minimize residual

$$\min_{\hat{\mathbf{v}}} \left\| \begin{bmatrix} S \\ \hat{\mathbf{v}} \end{bmatrix} \right\|_2 = \min_{\hat{\mathbf{v}}} \left\| \begin{bmatrix} S \\ \hat{\mathbf{v}} \end{bmatrix} \right\|_2 = \min_{\hat{\mathbf{v}}} \left\| \begin{bmatrix} S \\ \hat{\mathbf{v}} \end{bmatrix} \right\|_2$$



HROM = Hyper-reduced ROM



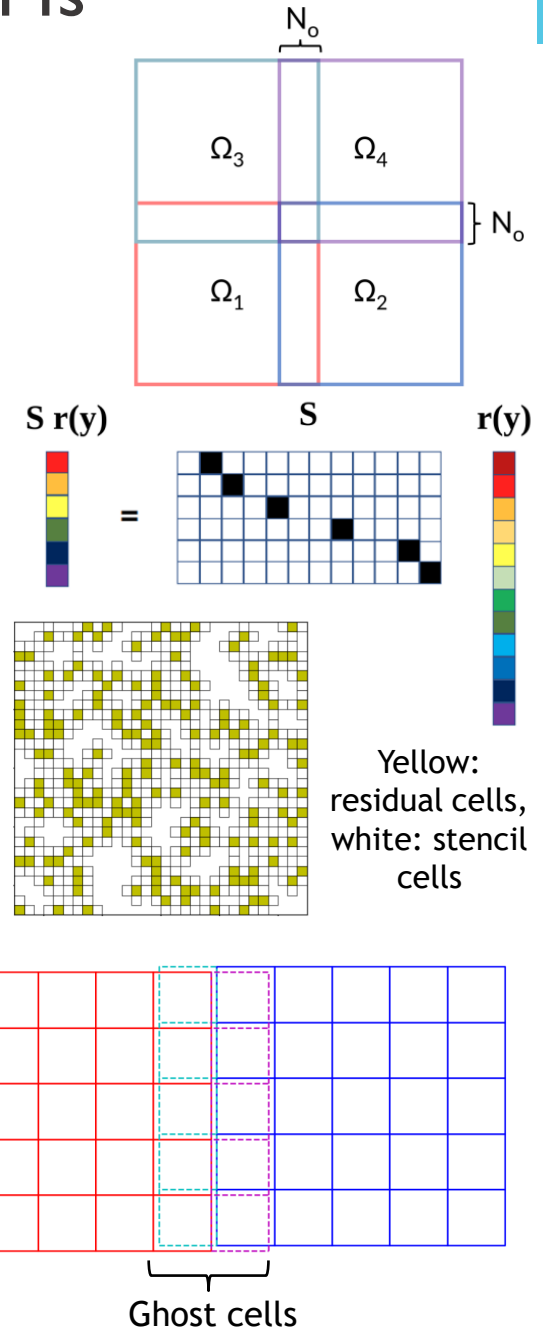
# SAM-based Coupling for Intrusive Projection-based ROMs

## Offline stage:

- Perform **FOM** simulation on a spatial domain  $\Omega$  and **collect**  $s$  snapshots
- Create **domain decomposition** of  $\Omega$  into  $d$  **overlapping** or **non-overlapping** subdomains  $\Omega_i$  with  $N_o$  overlap cells (could be 0).
- Compute **POD basis**  $\Phi_i$  on each  $\Omega_i$  by restricting the snapshots to  $\Omega_i$ .
- For nonlinear problems, compute **sample mesh**  $S_i$  on each  $\Omega_i$ .
  - **Collocation**: minimize the residual at a small subset of DOFs  $N_s \ll N$ .
  - *Key question: how to sample Schwarz boundaries given fixed budget of sample mesh points?*

## Online stage:

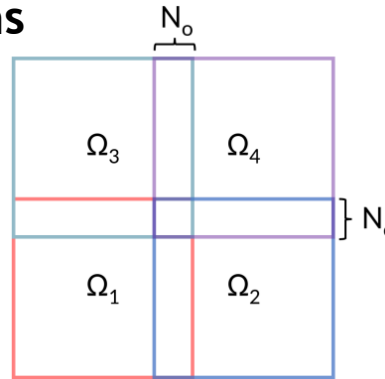
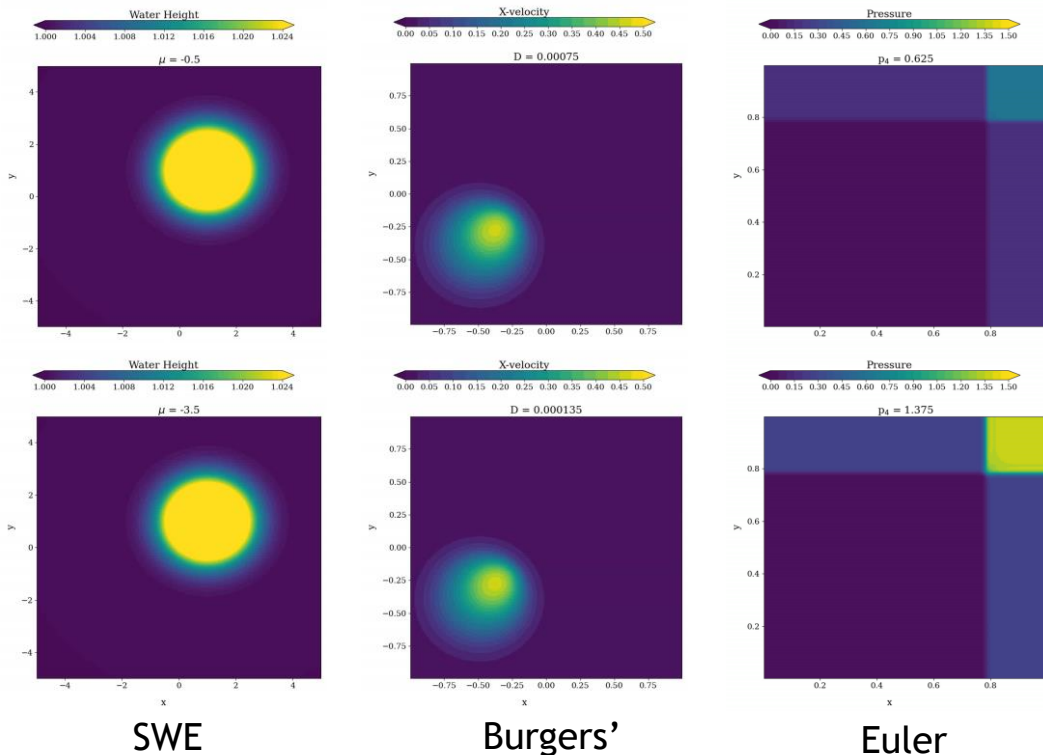
- Construct POD/LSPG ROM in each subdomain  $\Omega_i$ , transmit Schwarz BCs, apply Schwarz iteration procedure.
  - *Key question: how to impose Schwarz BCs in ROMs?*
    - ❖ *Often discretization specific.*
    - ❖ *This talk: cell-centered finite volume (CCFV) discretizations. BCs imposed approximately by fictitious ghost cells.*





# Numerical Examples

- Nonlinear hyperbolic fluid systems in Pressio/Pressio demo-apps\*
  - 2D shallow water equations (SWE), vary Coriolis parameter ( $\mu$ )
  - 2D viscous Burgers' equations, vary diffusion parameter ( $D$ )
  - 2D Euler equations, vary upper right pressure ( $p_4$ ) in IC
- Wave/shock propagation across interfaces  $\Rightarrow$  high Kolmogorov  $n$ -width
- FOM discretization: first-order CCFV method, 300x300 mesh, BDF1
- Consider decompositions of  $\Omega$  into four subdomains



**All results  
predictive: 5  
training points, 4  
(interpolative)  
testing points**

**SWE**

$$\frac{\partial h}{\partial t} + \frac{\partial hu}{\partial x} + \frac{\partial hv}{\partial y} = 0$$

$$\frac{\partial(hu)}{\partial t} + \frac{\partial}{\partial x} \left( hu^2 + \frac{1}{2}gh^2 \right) + \frac{\partial(huv)}{\partial y} = -\mu v$$

$$\frac{\partial(hv)}{\partial t} + \frac{\partial(hvu)}{\partial x} + \frac{\partial}{\partial y} \left( hv^2 + \frac{1}{2}gh^2 \right) = \mu u$$

**Burgers'**

$$\frac{\partial u}{\partial t} + \frac{1}{2} \left( \frac{\partial u^2}{\partial x} + \frac{\partial uv}{\partial y} \right) = D \left( \frac{\partial^2 u}{\partial x^2} + \frac{\partial^2 u}{\partial y^2} \right)$$

$$\frac{\partial v}{\partial t} + \frac{1}{2} \left( \frac{\partial uv}{\partial x} + \frac{\partial v^2}{\partial y} \right) = D \left( \frac{\partial^2 v}{\partial x^2} + \frac{\partial^2 v}{\partial y^2} \right)$$

**Euler**

$$\frac{\partial \rho}{\partial t} + \frac{\partial \rho u}{\partial x} + \frac{\partial \rho v}{\partial y} = 0$$

$$\frac{\partial(\rho u)}{\partial t} + \frac{\partial}{\partial x} (\rho u^2 + p) + \frac{\partial(\rho uv)}{\partial y} = 0$$

$$\frac{\partial(\rho v)}{\partial t} + \frac{\partial(\rho vu)}{\partial x} + \frac{\partial}{\partial y} (\rho v^2 + p) = 0$$

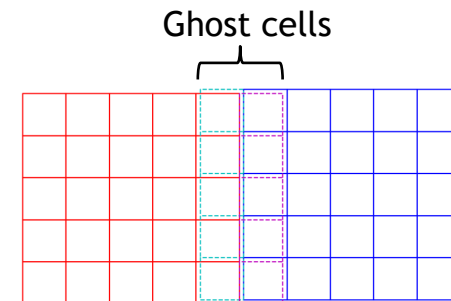
$$\frac{\partial(\rho E)}{\partial t} + \frac{\partial}{\partial x} ((E + p)u) + \frac{\partial}{\partial y} ((E + p)v) = 0$$

\* <https://pressio.github.io>,  
<https://github.com/Pressio/pressio-schwarz>

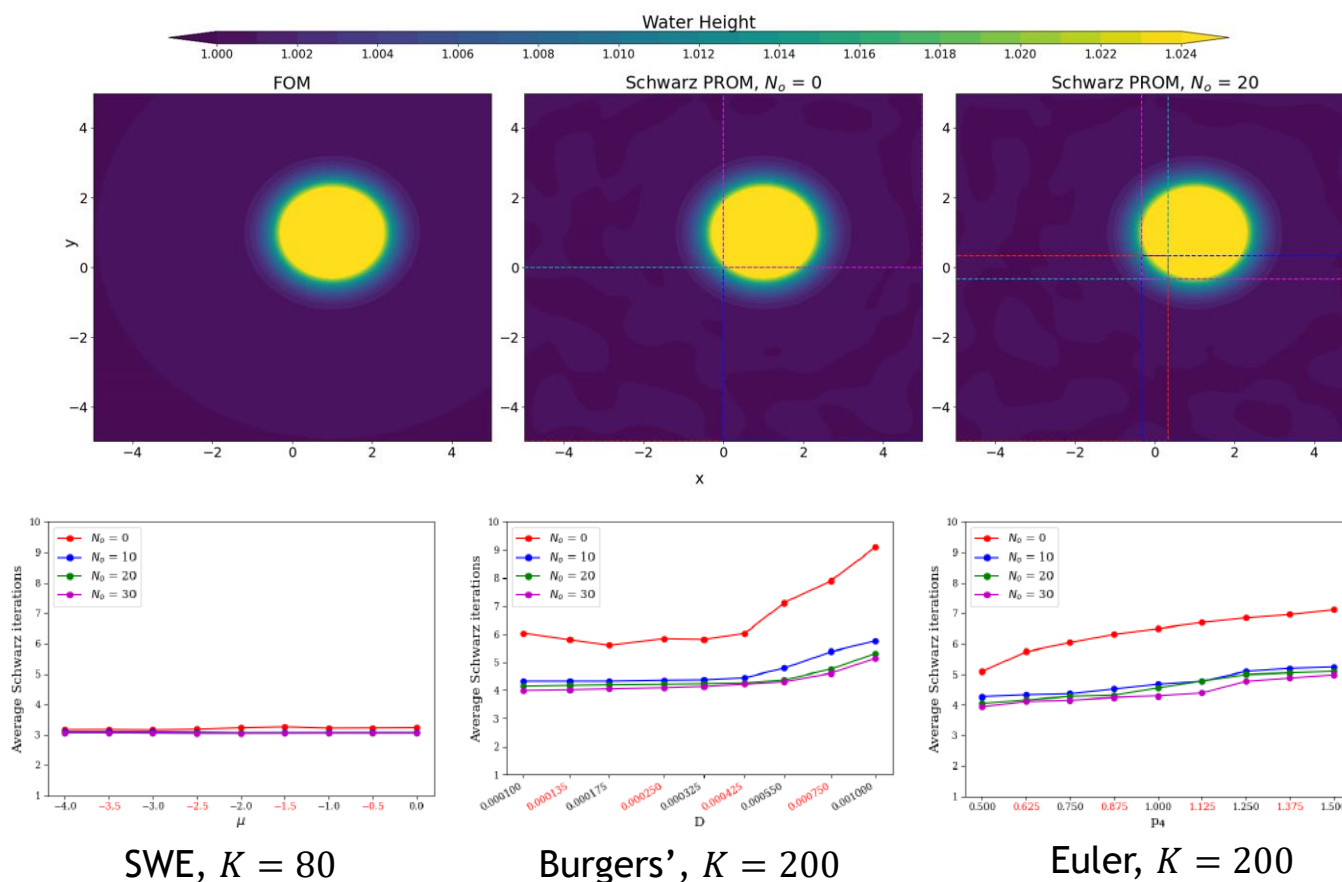


# Impact of Subdomain Overlap\*

**Key result:** non-overlapping Schwarz iteration converges without a degradation in accuracy when using **Dirichlet-Dirichlet Schwarz BCs!**



- This result is **not true** in general [Barnett et al., 2022; Mota et al., 2017; Mota et al. 2022]!
  - Generally need **alternating Dirichlet-Neumann** or **Robin-Robin BCs** for non-overlapping Schwarz convergence.
  - Dirichlet-Dirichlet works here due to **implied overlap** introduced into otherwise non-overlapping DD by ghost cells.
- More Schwarz iterations** are required for convergence with no overlap (as expected)
- Non-overlapping incurs **negligible convergence penalty** for smooth problems (SWE)
- Non-overlapping Schwarz **avoids duplicate calculations** in overlap region
- It becomes **more difficult to transmit shock** across non-overlapping interface (Burgers, Euler)



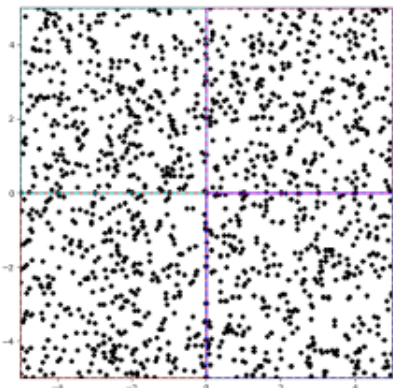
\* See [Wentland et al., 2025] for more details.



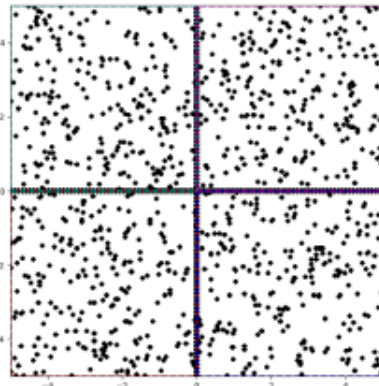
# Impact of Boundary Sampling for Hyper-Reduction\*



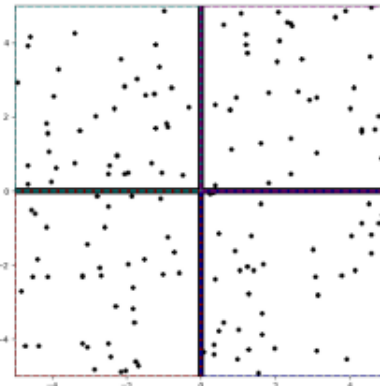
**Key result:** given a fixed “budget” of sample mesh points, there is a (problem-dependent) optimal number of sample mesh points to allocate to the Schwarz boundaries vs. the subdomain interiors.



$N_b = 30$



$N_b = 3$



$N_b = 1$

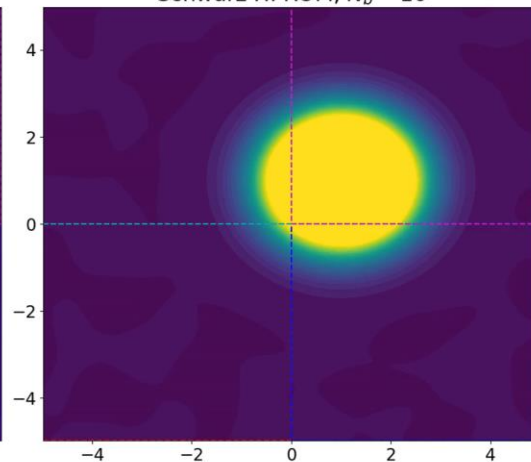
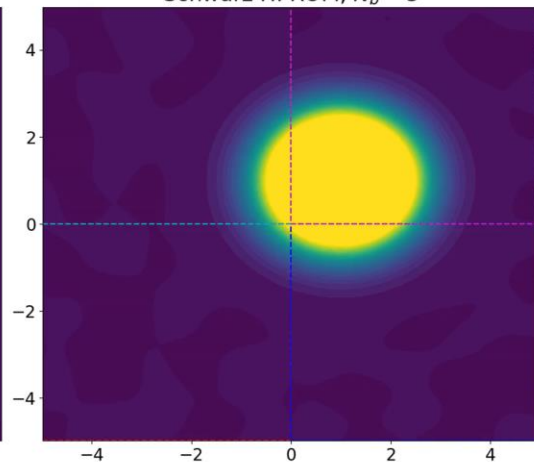
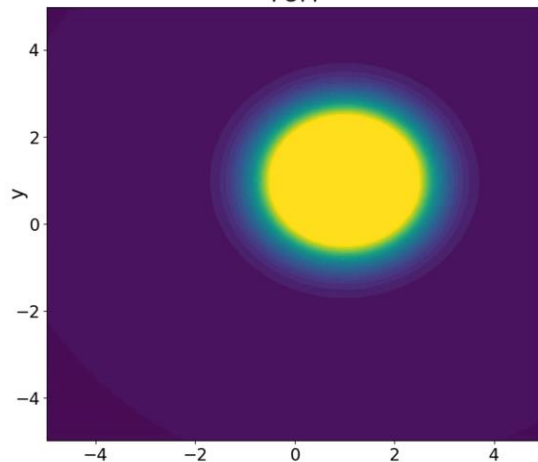
- $N_b$  = fixed interval at which Schwarz boundaries are sampled
- For a fixed budget of sample mesh points  $N_S$ , boundary points draw points away from interior (figure left)
- Failure to deliberately sample the Schwarz boundary will also always lead to instabilities (movie left)



FOM

Schwarz HPROM,  $N_b = 5$

Schwarz HPROM,  $N_b = 10$



\* See [Wentland et al., 2025] for more details.



Top row: SWE  
Middle row: Burgers'  
Bottom row: Euler

**Key result: predictive hyper-reduced ROMs (HROMs) with non-overlapping Dirichlet-Dirichlet Schwarz coupling are indistinguishable from corresponding monolithic ROMs/FOMs.**

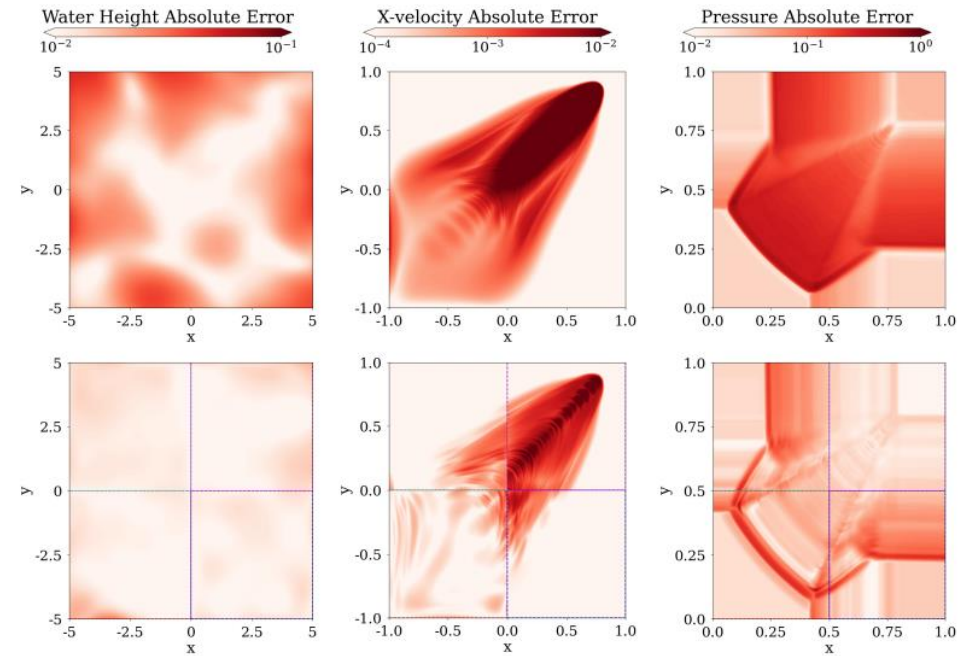
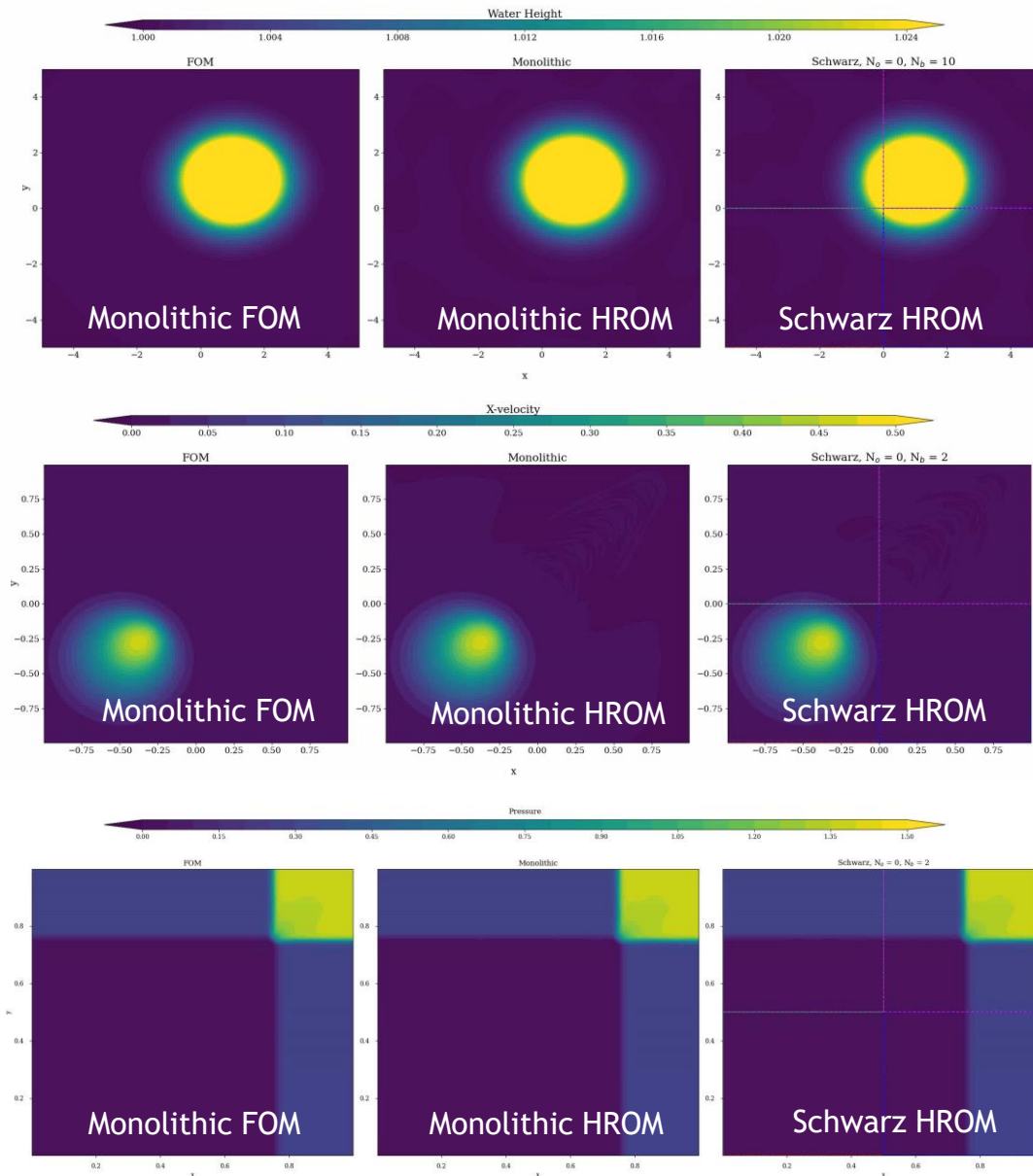


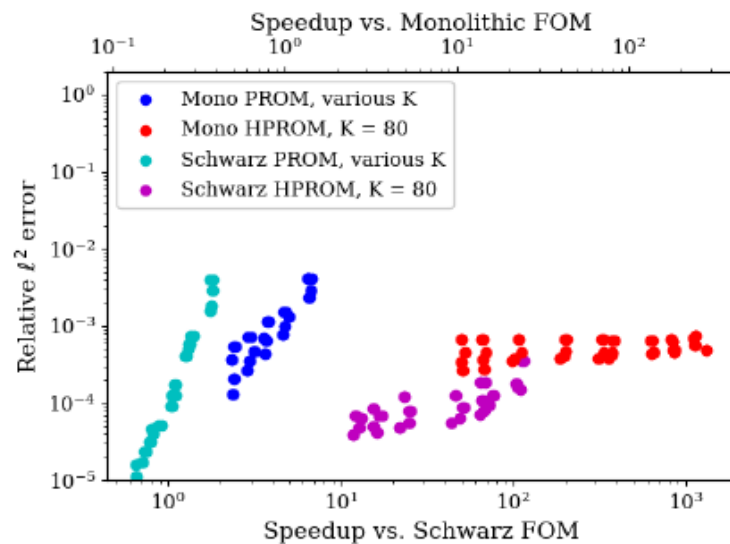
Figure above: average absolute spatial error fields for representative monolithic (top) and decomposed (bottom) hyper-reduced ROM with no overlap. Subdomain interfaces are marked with dashed lines.

\* See [Wentland et al., 2025] for more details.

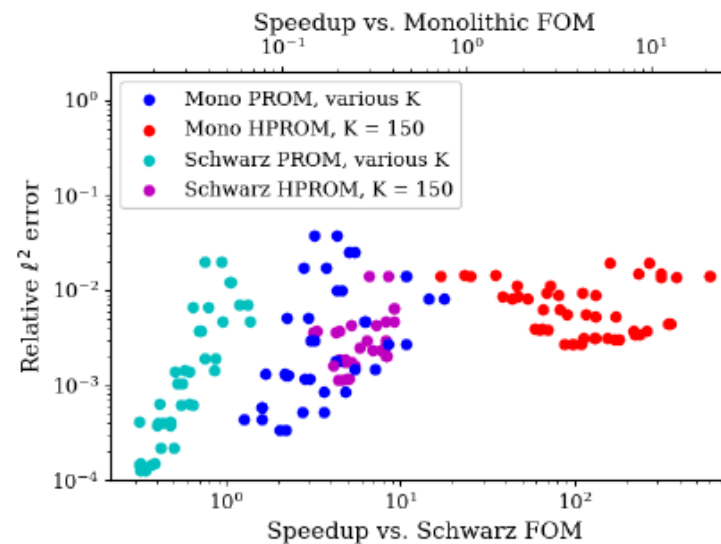


**Key result:** additive Schwarz enables speed-ups over corresponding coupled Schwarz FOM and sometimes over monolithic FOM.

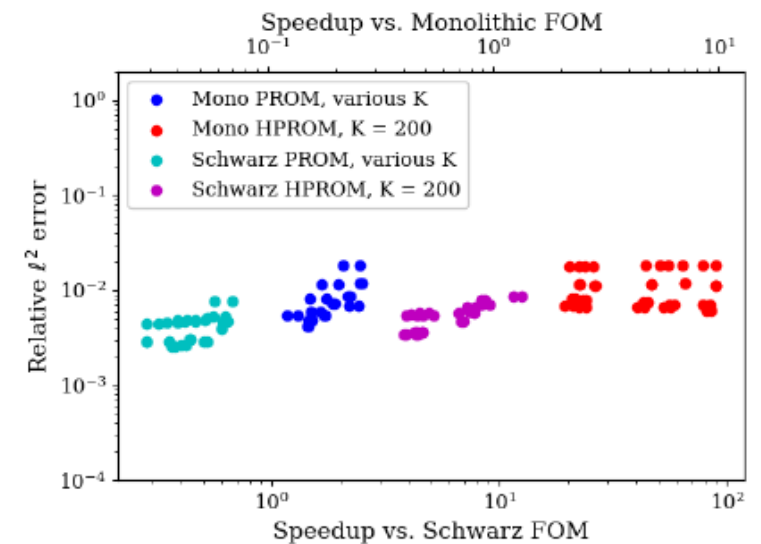
- Hyper-reduced ROMs generally achieve **cost savings** w.r.t. corresponding coupled Schwarz FOM
- **Cost savings** using Schwarz ROMs over corresponding **monolithic FOM** are possible for **SWE** problem
  - **Coupled Schwarz FOMs** are often only viable options for Sandia analysts due to meshing challenges
  - **Next step:** try to improve this via **adaptive Schwarz ROMs**



SWE



Burgers'



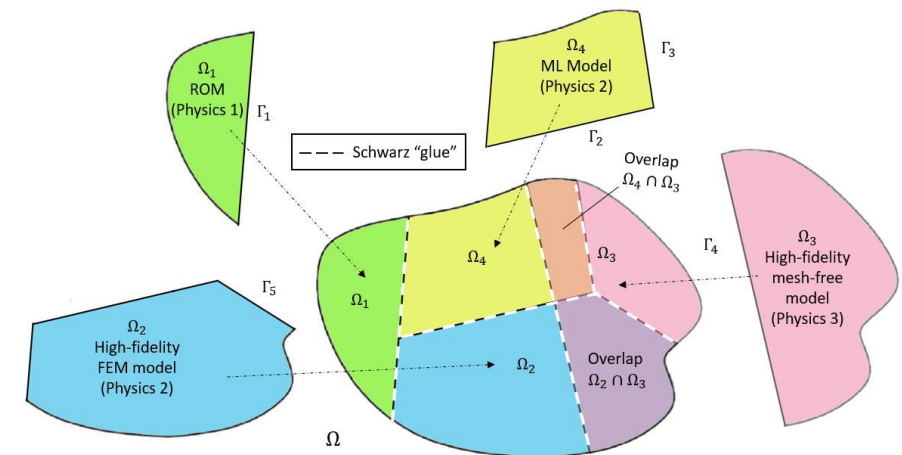
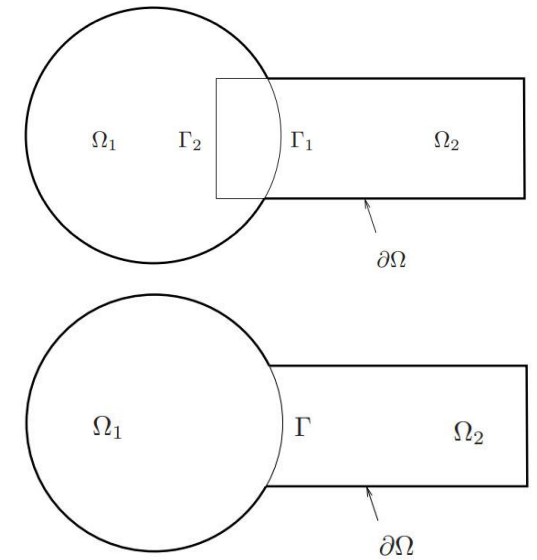
Euler

Red parameter values are predictive.

\* See [Wentland et al., 2025] for more details.



- The Schwarz Alternating Method (SAM) for Domain Decomposition-Based Coupling
- Part 1: SAM-based Coupling of Intrusive Projection-based ROMs
  - Projection-based ROM Overview
  - SAM-based Coupling Workflow
  - Numerical Examples
- Part 2: SAM-based Coupling of Non-Intrusive OpInf ROMs
  - OpInf ROM Overview
  - SAM-based Coupling Workflow
  - Numerical Examples
- Summary & Ongoing/Future Work



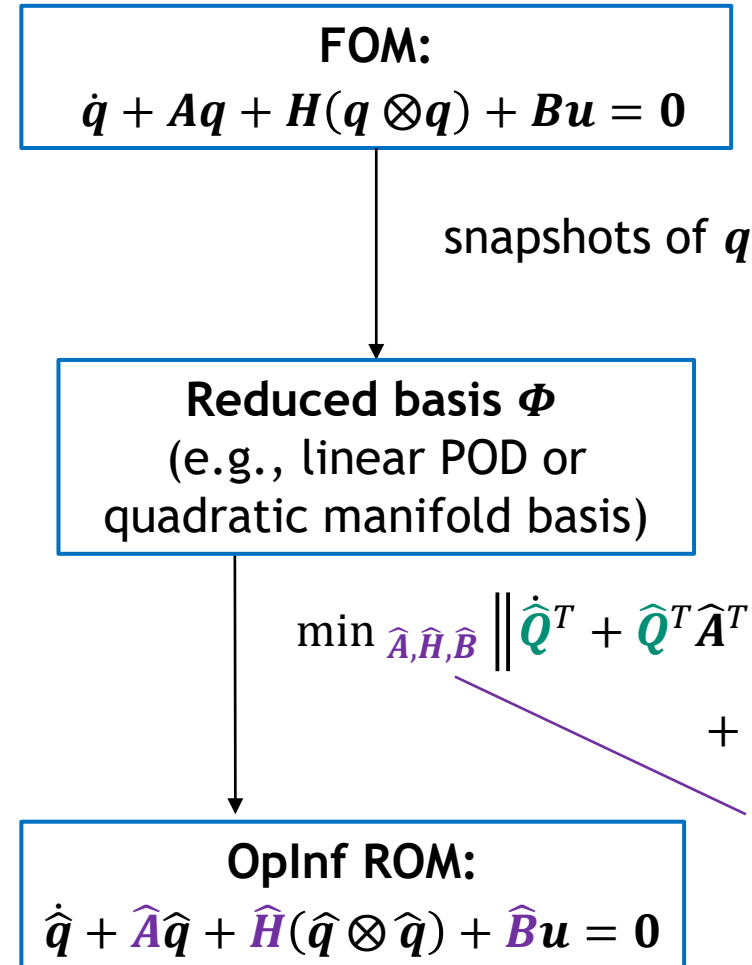




**Key Idea Behind OpInf:** circumvent the burden of implementing intrusive ROMs in HPC codes by **combining projection-based ROM and machine learning (ML)**.

### Nuances:

- OpInf can be applied to **nonlinear problems** by transforming the nonlinear PDEs into PDEs with a polynomial functional form (“**lifting**” [Qian et al., 2019]) or assuming a **polynomial functional form** for the ROM
- The OpInf least-squares (LS) minimization problem often requires **regularization** to be solvable, e.g., Tikhonov regularization
- **Structure preservation** (e.g., symmetry constraints) can be incorporated into the OpInf LS minimization problem



\* [Peherstorfer & Willcox, 2016] + many subsequent refs

$\hat{Q}$ : snapshots generated from projected simulation data  $q$

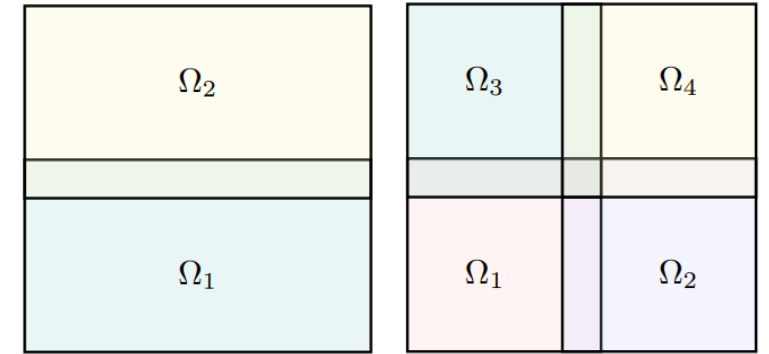
$\hat{A}, \hat{H}, \hat{B}$ : low-dimensional operators defining ROM dynamical system





## Offline stage:

- Perform **FOM** simulation on a spatial domain  $\Omega$  and **collect**  $s$  **snapshots**
- Create **DD** of  $\Omega$  into  $d$  **overlapping subdomains**  $\Omega_i$ .
- Compute **POD basis**  $\Phi_i$  on each  $\Omega_i$  by restricting the snapshots to  $\Omega_i$ .
- Assume a **functional form** for your ROM in  $\Omega_i$ , informed by the functional form of the corresponding FOM
  - *Key question: how to impose Schwarz BCs in OpInf ROMs?*



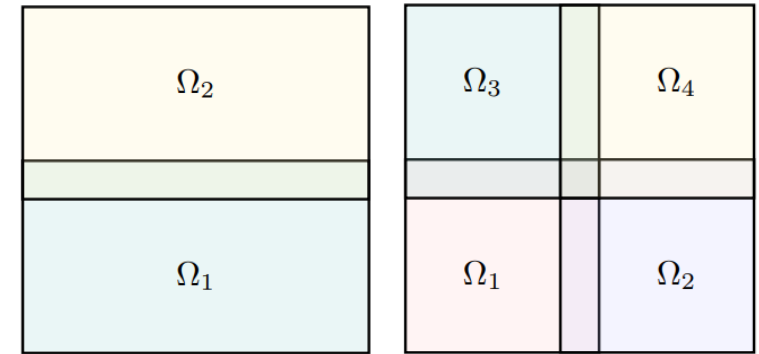
**OpInf ROM in  $\Omega_i$ :**

$$\dot{\hat{q}}_i + \hat{A}_i \hat{q}_i + \hat{H}_i(\hat{q}_i \otimes \hat{q}_i) = 0$$



## Offline stage:

- Perform **FOM** simulation on a spatial domain  $\Omega$  and **collect**  $s$  **snapshots**
- Create **DD** of  $\Omega$  into  $d$  **overlapping subdomains**  $\Omega_i$ .
- Compute **POD basis**  $\Phi_i$  on each  $\Omega_i$  by restricting the snapshots to  $\Omega_i$ .
- Assume a **functional form** for your ROM in  $\Omega_i$ , informed by the functional form of the corresponding FOM
  - **Key question: how to impose Schwarz BCs in OpInf ROMs?**
    - ❖ **Boundary transmission enters through learned source term  $\hat{\mathbf{B}}_i \mathbf{g}_i$  added to OpInf ROM dynamical system**



OpInf ROM + Schwarz BCs in  $\Omega_i$ :

$$\hat{\mathbf{q}}_i + \hat{\mathbf{A}}_i \hat{\mathbf{q}}_i + \hat{\mathbf{H}}_i(\hat{\mathbf{q}}_i \otimes \hat{\mathbf{q}}_i) + \underbrace{\hat{\mathbf{B}}_i \mathbf{g}_i}_{\text{Schwarz Dirichlet BC term}} = \mathbf{0}$$

Motivated by  
implementation of  
Dirichlet BCs in FEM

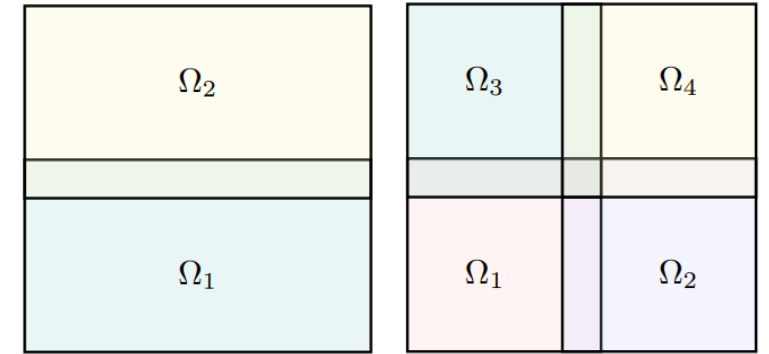
Schwarz  
Dirichlet BC  
term





## Offline stage:

- Perform **FOM** simulation on a spatial domain  $\Omega$  and **collect**  $s$  **snapshots**
- Create **DD** of  $\Omega$  into  $d$  **overlapping subdomains**  $\Omega_i$ .
- Compute **POD basis**  $\Phi_i$  on each  $\Omega_i$  by restricting the snapshots to  $\Omega_i$ .
- Assume a **functional form** for your ROM in  $\Omega_i$ , informed by the functional form of the corresponding FOM
  - **Key question: how to impose Schwarz BCs in OpInf ROMs?**
    - ❖ *Boundary transmission enters through **learned source term**  $\hat{\mathbf{B}}_i \mathbf{g}_i$  added to OpInf ROM dynamical system*
    - ❖ *Further reduction achieved by expanding  $\mathbf{g}_i$  in its own POD basis  $\Phi_i^g$  and approximating  $\hat{\mathbf{B}}_i \mathbf{g}_i \approx \hat{\mathbf{B}}_i \hat{\mathbf{g}}_i = \tilde{\mathbf{B}}_i \mathbf{g}_i$  where  $\hat{\mathbf{g}}_i = \Phi_i^g \mathbf{g}_i$*



OpInf ROM + Schwarz BCs in  $\Omega_i$ :

$$\hat{\mathbf{q}}_i + \hat{\mathbf{A}}_i \hat{\mathbf{q}}_i + \hat{\mathbf{H}}_i(\hat{\mathbf{q}}_i \otimes \hat{\mathbf{q}}_i) + \underbrace{\tilde{\mathbf{B}}_i \mathbf{g}_i}_{\text{Schwarz Dirichlet BC term}} = \mathbf{0}$$

Motivated by  
implementation of  
Dirichlet BCs in FEM

Schwarz  
Dirichlet BC  
term





## Offline stage:

- Perform **FOM** simulation on a spatial domain  $\Omega$  and **collect  $s$  snapshots**
- Create **DD** of  $\Omega$  into  $d$  **overlapping subdomains**  $\Omega_i$ .
- Compute **POD basis**  $\Phi_i$  on each  $\Omega_i$  by restricting the snapshots to  $\Omega_i$ .
- Assume a **functional form** for your ROM in  $\Omega_i$ , informed by the functional form of the corresponding FOM

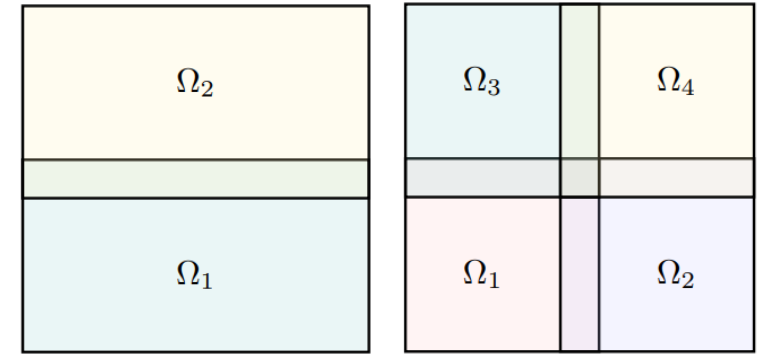
➤ **Key question: how to impose Schwarz BCs in OpInf ROMs?**

- ❖ *Boundary transmission enters through **learned source term**  $\tilde{\mathbf{B}}_i \mathbf{g}_i$  added to OpInf ROM dynamical system*
- ❖ *Further reduction achieved by expanding  $\mathbf{g}_i$  in its own POD basis  $\Phi_i^g$  and approximating  $\tilde{\mathbf{B}}_i \mathbf{g}_i \approx \tilde{\mathbf{B}}_i \hat{\mathbf{g}}_i = \tilde{\mathbf{B}}_i^g \mathbf{g}_i$  where  $\hat{\mathbf{g}}_i = \Phi_i^g \mathbf{g}_i$*

- Compute OpInf operators  $\hat{\mathbf{A}}_i, \hat{\mathbf{H}}_i$  and  $\tilde{\mathbf{B}}_i$  in each subdomain  $\Omega_i$  by solving regularized OpInf LS minimization problem

## Online stage:

- Apply **Schwarz iteration procedure**, with Schwarz BC transfer via pre-learned boundary contributions  $\tilde{\mathbf{B}}_i \mathbf{g}_i$



**OpInf ROM + Schwarz BCs in  $\Omega_i$ :**

$$\hat{\mathbf{q}}_i + \hat{\mathbf{A}}_i \hat{\mathbf{q}}_i + \hat{\mathbf{H}}_i (\hat{\mathbf{q}}_i \otimes \hat{\mathbf{q}}_i) + \underbrace{\tilde{\mathbf{B}}_i \mathbf{g}_i}_{\text{Schwarz Dirichlet BC term}} = 0$$

Motivated by  
implementation of  
Dirichlet BCs in FEM

Schwarz  
Dirichlet BC  
term

*[Farcas et al., 2023] coupling formulation is **similar** but solves each subdomain problem **once** rather than iterating to convergence.*



# Numerical Examples



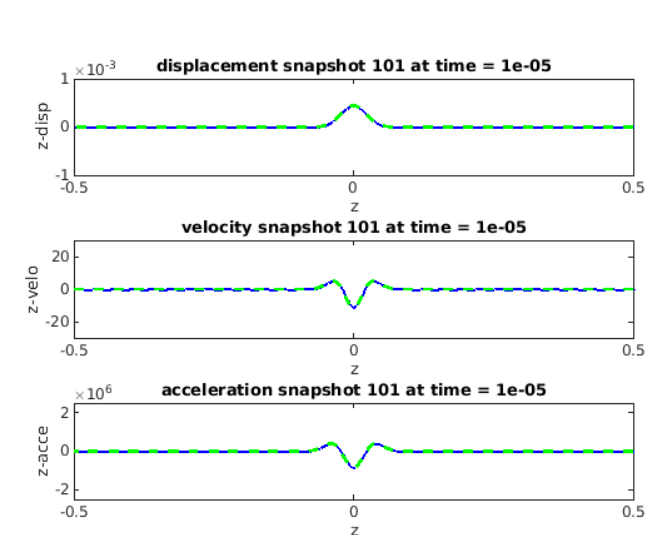
*Solid dynamics weak variational form:*

$$\int_I \left[ \int_{\Omega} (\text{Div } \mathbf{P} + \rho_0 \mathbf{B} - \rho_0 \ddot{\boldsymbol{\varphi}}) \cdot \boldsymbol{\xi} \, dV + \int_{\partial_T \Omega} \mathbf{T} \cdot \boldsymbol{\xi} \, dS \right] dt = 0$$

*Semi-discrete form:*

$$\mathbf{M} \ddot{\mathbf{u}} + \mathbf{f}^{\text{int}}(\mathbf{u}, \dot{\mathbf{u}}) = \mathbf{f}^{\text{ext}}$$

- **Dynamic finite deformation solid mechanics problem**
  - 3D linear elastic notched cylinder problem
  - 3D hyperelastic torsion problem
- **Wave propagation and large deformation**  $\Rightarrow$  difficult for ROMs/coupling!
- **FOM discretization:** FEM in space, implicit Newmark in time
  - Implementation in *Norma* Julia code\*, which relies on Python Oplnf package\*\*
- Consider **overlapping** DDs of  $\Omega$  into **two** or **three** subdomains
- Evaluate **FOM-ROM** couplings only for now
- ROM = **linear**, **quadratic** or **cubic** Oplnf model (Oplnf, QOplnf, COplnf)



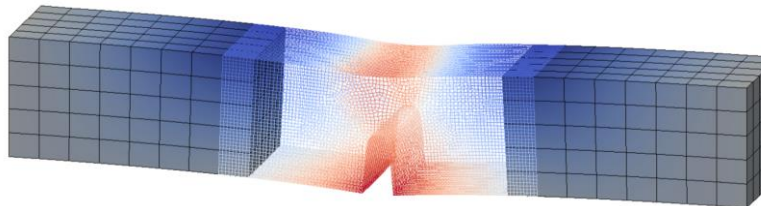
1D linear elastic wave



3D notched cylinder



3D torsion



3D laser weld

Results are **preliminary** and focus on **verification/initial prototyping** of Oplnf ROMs and FOM-Oplnf ROM coupling via **overlapping SAM** in *Norma*

\* <https://github.com:sandialabs/Norma.jl>

\*\* <https://pypi.org/project/oplnf>

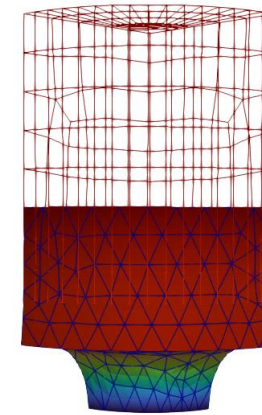


# 3D Linear Elastic Notched Cylinder Problem

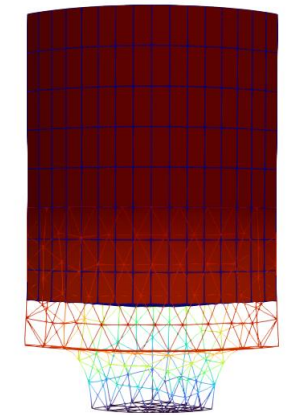
- Geometry is *linear elastic notched cylinder* pulled from top *dynamically* to time  $T_{max} = 1.5$  at rate of  $0.0064t$  with  $\Delta t = 0.005$
- Demonstration of SAM's ability to *couple disparate meshes, element types* and *models*: TET10 + FOM (notched region) and HEX8 + Linear Oplnf with  $M = 30$  modes (top region)
- Linear Oplnf* trained on 301 snapshots in time
- Reproductive* problem for now

**Key result:** regularization parameter  $\gamma$  influences accuracy & convergence. Coupled models are remarkably accurate! Schwarz is *not* introducing coupling error/artifacts.

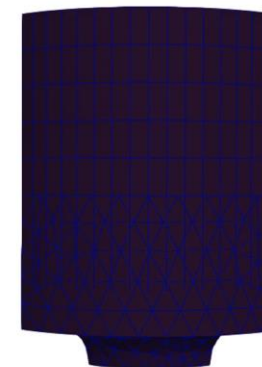
	Mean/max # Schwarz iters	Max z-disp rel error $\Omega_1$	Max z-disp rel error $\Omega_2$
FOM-FOM	5.83/9	—	—
FOM-Oplnf ( $\gamma = 1 \times 10^{-6}$ )	5.09/8	2.9e-3	4.2e-3
FOM-Oplnf ( $\gamma = 1 \times 10^{-7}$ )	5.48/9	3.8e-4	4.3e-4
FOM-Oplnf ( $\gamma = 1 \times 10^{-8}$ )	5.54/9	1.3e-4	2.2e-4
FOM-Oplnf ( $\gamma = 1 \times 10^{-9}$ )	5.52/9	3.1e-5	3.6e-5



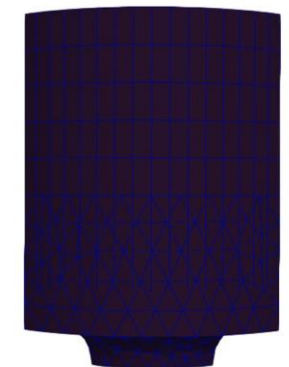
$\Omega_1$  (TET10 + FOM)



$\Omega_2$  (HEX8 + Oplnf)



FOM-FOM



FOM-Oplnf

*Movies above:* z-displacement solutions for FOM-FOM and FOM-Oplnf ( $M = 30$ ,  $\gamma = 1 \times 10^{-6}$ )



# 3D Hyperelastic Torsion Problem



- **Dynamic nonlinear hyperelastic bar** subjected to high degree of **torsion** (initial velocity =  $(-ayz, axz, 0)$ ).
- **Saint-Venant Kirchhoff** material model, which gives rise to PDEs with **cubic nonlinearities**.
- **Overlapping** DD of  $\Omega$  into **two subdomains**, discretized with **nonconformal HEX8 meshes**
- Evaluated **predictive FOM-Oplnf** couplings with **linear, quadratic** and **cubic Oplnf ROMs** built from 2K snapshots (train for  $a = 5000, 6000, 7000, 8000$ , predict for  $a = 5500$ )
- **Displacement relative errors at final time** ( $M = 30$  QOplnf): 12.5% in  $\Omega_1$  and 9.38% in  $\Omega_2$



$\Omega_1$  (HEX8 + FOM)



$\Omega_2$  (HEX8 + Oplnf)

FOM-FOM



FOM-Oplnf ( $M = 30$ )



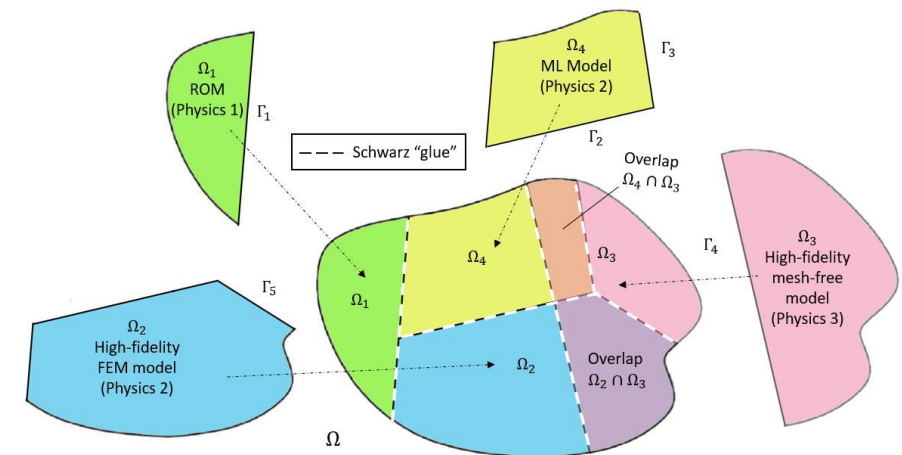
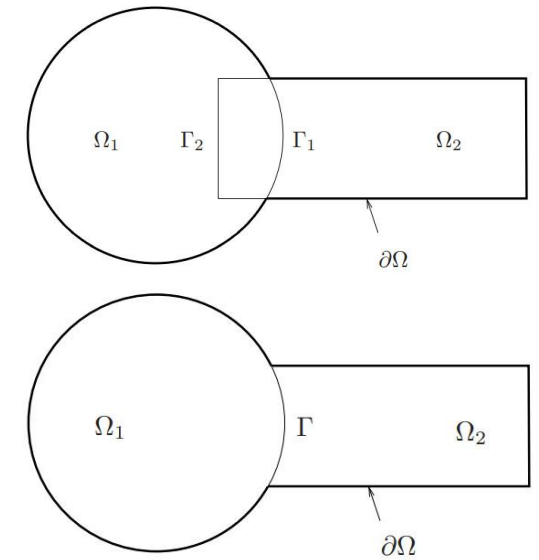
FOM-QOplnf ( $M = 30$ )



**Key result:** quadratic and cubic Oplnf models can produce **stable** and **accurate** solutions (whereas linear Oplnf blows up) but are very **sensitive** to  $\gamma$ .



- The Schwarz Alternating Method (SAM) for Domain Decomposition-Based Coupling
- Part 1: SAM-based Coupling of Intrusive Projection-based ROMs
  - Projection-based ROM Overview
  - SAM-based Coupling Workflow
  - Numerical Examples
- Part 2: SAM-based Coupling of Non-Intrusive OpInf ROMs
  - OpInf ROM Overview
  - SAM-based Coupling Workflow
  - Numerical Examples
- Summary & Ongoing/Future Work



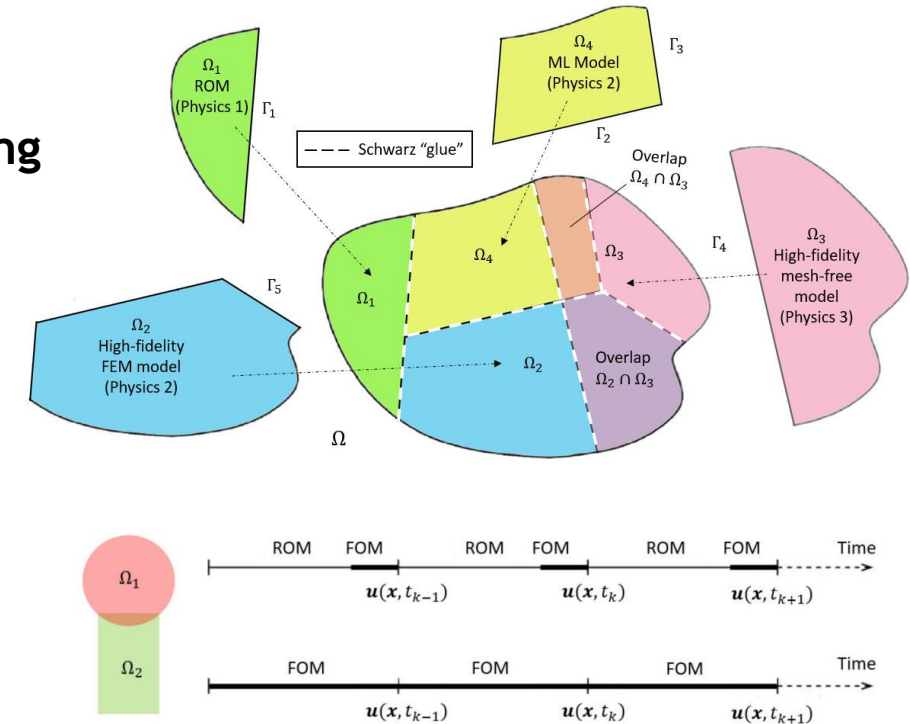


**Summary:** the Schwarz alternating method is effective at coupling subdomain-local FOMs and (intrusive or nonintrusive) ROMs and does *not* introduce artifacts or numerical instabilities if applied correctly.



## Ongoing & future work:

- Improve **robustness** and **stability** of Oplnf ROMs + Schwarz via **filtering** and/or **stabilization** (with T. Iliescu, Virginia Tech)
- Develop **automated workflow** to **optimize** DD and SAM parameters
- Extend Schwarz + Oplnf ROM to **parametric problems**
- Extend Schwarz + Oplnf ROM to **non-intrusive kernel-based ROMs**
- Extend SAM to **fully nonlinear neural network-based ROMs**
- Develop **non-overlapping SAM** for non-intrusive ROMs
- Incorporate **structure preservation** into non-intrusive Schwarz ROMs
- **Implement FOM-ROM coupling in SIERRA/SM production code.**
- Development of **automated criteria** to determine appropriate use of less refined or reduced-order models without sacrificing accuracy, enabling **real-time transitions** between different model fidelities



→ **Newest project: AHEAD LDRD**



# Team & Acknowledgments



U.S. DEPARTMENT OF  
**ENERGY**

Office of Science



Irina Tezaur



Chris Wentland



Francesco Rizzi



Joshua Barnett



Alejandro Mota



Will Snyder  
*Former Intern from  
Virginia Tech  
[Schwarz + PINNs]*



Ian Moore  
*Intern from  
Virginia Tech  
[Schwarz + OpInf]*



Eric Parish



Anthony Gruber



Cam Rodriguez  
*New Intern from  
Columbia U  
[Schwarz + OpInf]*





- [1] A. Mota, I. Tezaur, C. Alleman. “The Schwarz Alternating Method in Solid Mechanics”, *Comput. Meth. Appl. Mech. Engng.* 319 (2017), 19-51.
- [2] A. Mota, I. Tezaur, G. Phlipot. “The Schwarz Alternating Method for Dynamic Solid Mechanics”, *Comput. Meth. Appl. Mech. Engng.* 121 (21) (2022) 5036-5071.
- [3] J. Barnett, I. Tezaur, A. Mota. “The Schwarz alternating method for the seamless coupling of nonlinear reduced order models and full order models”, ArXiv pre-print, 2022. <https://arxiv.org/abs/2210.12551>
- [4] W. Snyder, I. Tezaur, C. Wentland. “Domain decomposition-based coupling of physics-informed neural networks via the Schwarz alternating method”, ArXiv pre-print, 2023. <https://arxiv.org/abs/2311.00224>
- [5] A. Mota, D. Koliesnikova, I. Tezaur. “A Fundamentally New Coupled Approach to Contact Mechanics via the Dirichlet-Neumann Schwarz Alternating Method”, ArXiv pre-print, 2023. <https://arxiv.org/abs/2311.05643>
- [6] C. Wentland, F. Rizzi, J. Barnett, I. Tezaur. “The role of interface boundary conditions and sampling strategies for Schwarz-based coupling of projection-based reduced order models, *J. Comp. Appl. Math*, 2025 (in press). <https://doi.org/10.1016/j.cam.2025.116584>
- [7] I. Moore, C. Wentland, A. Gruber, I. Tezaur. “Domain decomposition-based coupling of Operator Inference reduced order models via the Schwarz alternating method”, ArXiv pre-print, 2024. <https://arxiv.org/pdf/2409.01433>
- [8] Pressio: <https://pressio.github.io>
- [9] Pressio demo-apps: <https://github.com/Pressio/pressio-demoapps>
- [10] Pressio demo-apps + Schwarz: <https://github.com/Pressio/pressio-schwarz>
- [11] Norma: <https://sandialabs/Norma.jl>



[ikalash@sandia.gov](mailto:ikalash@sandia.gov)  
[www.sandia.gov/~ikalash](http://www.sandia.gov/~ikalash)



## Start of Backup Slides

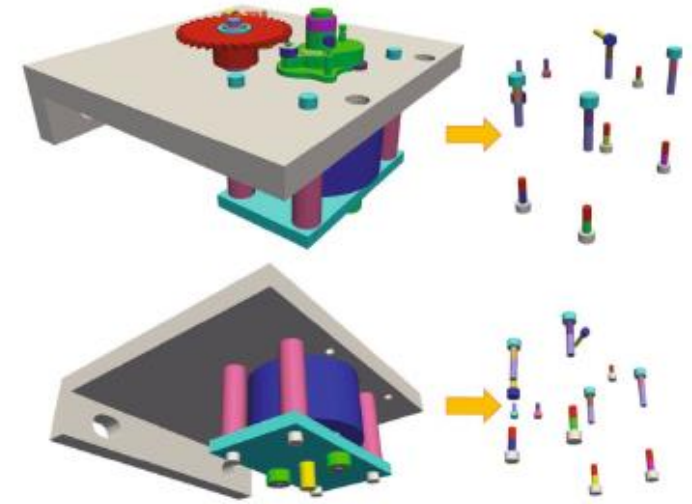


# Motivation: Multi-scale & Multi-physics Modeling & Simulation

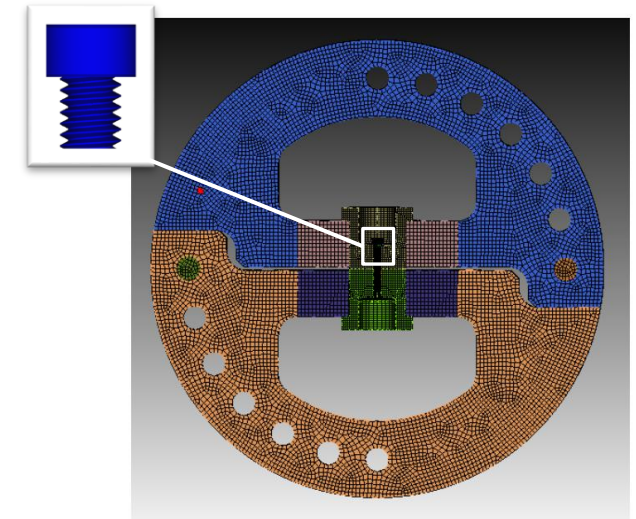
**Key challenge:** analysts using **high-fidelity models** to study multi-scale and/or multi-physics systems face **significant delays**.

## Bottlenecks/Issues:

- **Mesh generation** is the “single biggest bottleneck in [mod/sim] analyses” [Sandia Lab News, 2020]
  - Generating a **single mesh** can take **weeks** → **months**
- High-fidelity full order model (FOM) simulations require **long runtimes**
  - Data-driven **reduced order models (ROMs)** can reduce runtime burdens, but:
    - ❖ Can suffer from **lack of robustness, stability and accuracy** in the predictive regime
    - ❖ **Cannot be easily refined** to achieve a specified level of accuracy like conventional discretizations
    - ❖ Can take **years** to implement in HPC codes



Ratcheting mechanism [Parish *et al.*, 2024]



Fixture model with fastener held in by bushings [Murugesan *et al.*, 2020]



# Solution: Hybrid Domain Decomposition-based Coupling



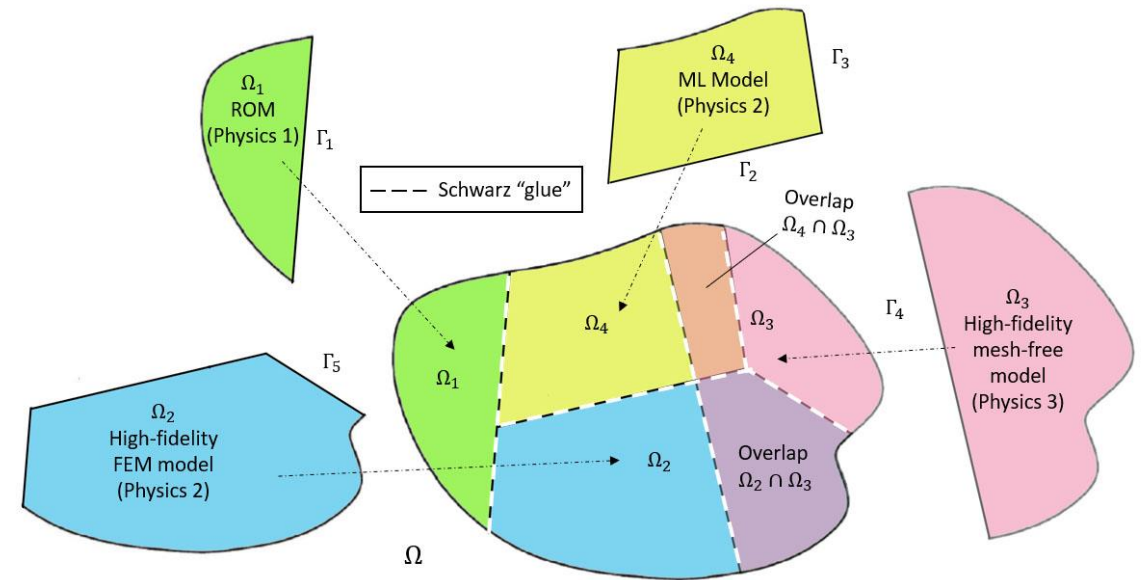
**Hypothesis:** the aforementioned hurdles can be overcome through the development of a rigorous, minimally-intrusive coupling method that creates “hybrid” (ROM+FOM) models based on an optimal domain decomposition (DD).



**MESHING CHALLENGES  
PRECLUDE ANALYSES;  
DATA-DRIVEN ROMS LACK  
STABILITY & ACCURACY  
FOR PREDICTIONS**



**MITIGATE BOTH  
CHALLENGES WITH  
OPTIMAL DOMAIN  
DECOMPOSITION-  
BASED HYBRID MODELS**



Example sample DD and ROM/FOM assignment.



# Flexible Heterogeneous Numerical Methods (fHNM) and Multi-faceted Mathematics for Predictive Digital Twins (M2dt) Projects



$$\int \mathcal{M}^2 dt$$

## Principal research objective:

- Discover mathematical principles guiding the assembly of standard and data-driven numerical models in stable, accurate and physically consistent ways.

## Principal research goals:

- “Mix-and-match” standard and data-driven models from three-classes
  - *Class A*: projection-based reduced order models (ROMs) *This talk.*
  - *Class B*: machine-learned models, i.e., Physics-Informed Neural Networks (PINNs)
  - *Class C*: flow map approximation models, i.e., dynamic model decomposition (DMD) models
- Ensure well-posedness & physical consistency of resulting heterogeneous models.
- Solve such heterogeneous models efficiently.

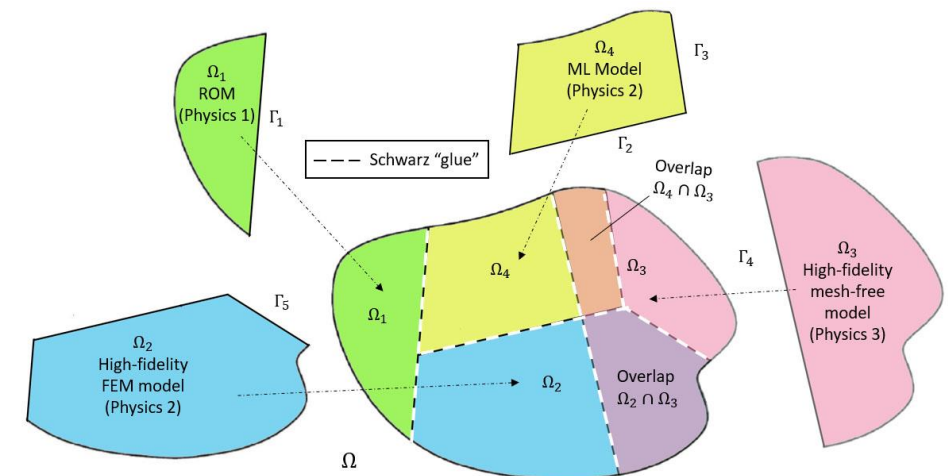


Office of Science



## Three coupling methods:

- Alternating Schwarz-based coupling *This talk.*
- Optimization-based coupling
- Coupling via generalized mortar methods







### Multiplicative Overlapping Schwarz

$$\begin{cases} N(\mathbf{u}_1^{(n+1)}) = f, & \text{in } \Omega_1 \\ \mathbf{u}_1^{(n+1)} = \mathbf{g}, & \text{on } \partial\Omega_1 \setminus \Gamma_1 \\ \mathbf{u}_1^{(n+1)} = \mathbf{u}_2^{(n)} & \text{on } \Gamma_1 \end{cases}$$

$$\begin{cases} N(\mathbf{u}_2^{(n+1)}) = f, & \text{in } \Omega_2 \\ \mathbf{u}_2^{(n+1)} = \mathbf{g}, & \text{on } \partial\Omega_2 \setminus \Gamma_2 \\ \mathbf{u}_2^{(n+1)} = \mathbf{u}_1^{(n+1)} & \text{on } \Gamma_2 \end{cases}$$

*Part 2 of Talk*

### Additive Overlapping Schwarz

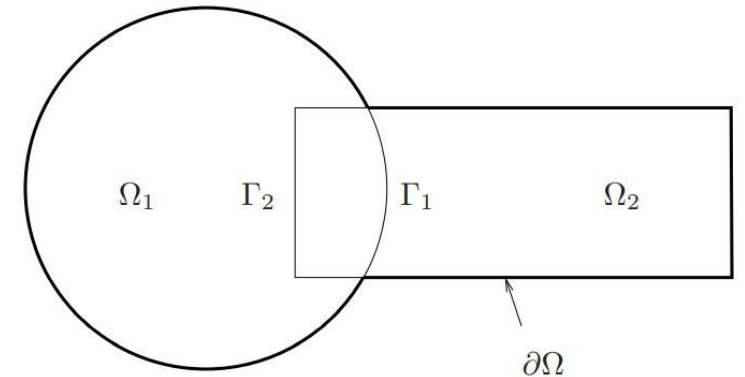
$$\begin{cases} N(\mathbf{u}_1^{(n+1)}) = f, & \text{in } \Omega_1 \\ \mathbf{u}_1^{(n+1)} = \mathbf{g}, & \text{on } \partial\Omega_1 \setminus \Gamma_1 \\ \mathbf{u}_1^{(n+1)} = \mathbf{u}_2^{(n)} & \text{on } \Gamma_1 \end{cases}$$

$$\begin{cases} N(\mathbf{u}_2^{(n+1)}) = f, & \text{in } \Omega_2 \\ \mathbf{u}_2^{(n+1)} = \mathbf{g}, & \text{on } \partial\Omega_2 \setminus \Gamma_2 \\ \mathbf{u}_2^{(n+1)} = \mathbf{u}_1^{(n+1)} & \text{on } \Gamma_2 \end{cases}$$

*Part 1 of Talk*

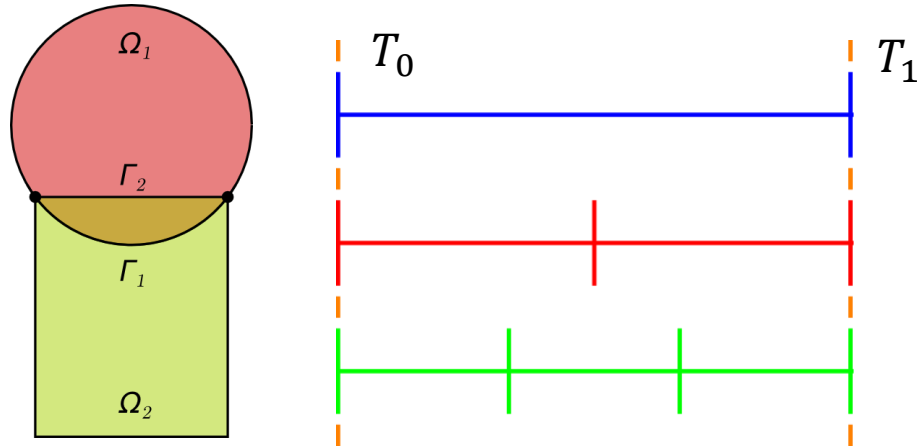
*Model PDE:*

$$\begin{cases} N(\mathbf{u}) = f, & \text{in } \Omega \\ \mathbf{u} = \mathbf{g}, & \text{on } \partial\Omega \end{cases}$$



- **Multiplicative Schwarz:** solves subdomain problems **sequentially** (in serial)
- **Additive Schwarz:** advance subdomains in **parallel**, communicate boundary condition data later
  - Typically requires a few more **Schwarz iterations**, but does not degrade **accuracy**
  - **Parallelism** helps balance additional **cost** due to Schwarz iterations
  - Applicable to both **overlapping** and **non-overlapping** Schwarz





Controller time stepper

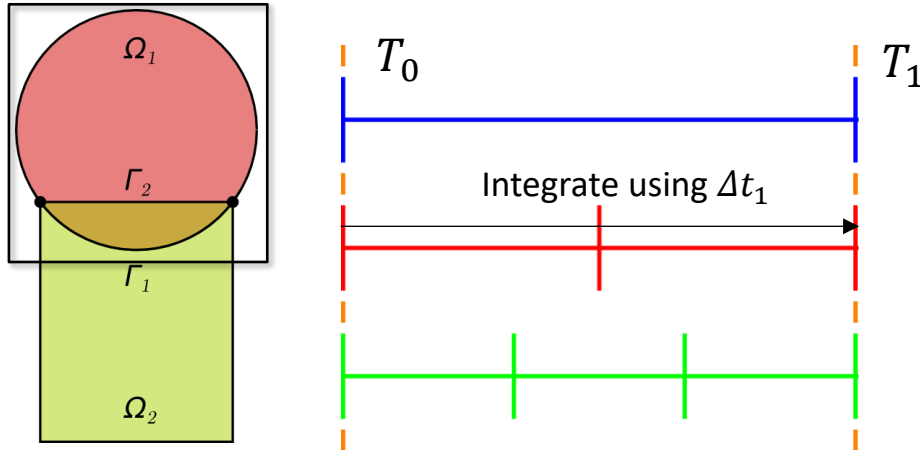
Time integrator for  $\Omega_1$

Time integrator for  $\Omega_2$

**Step 0:** Initialize  $i = 0$  (controller time index).

$$\text{Model PDE: } \begin{cases} \dot{\mathbf{u}} + N(\mathbf{u}) = \mathbf{f}, & \text{in } \Omega \\ \mathbf{u}(\mathbf{x}, t) = \mathbf{g}(t), & \text{on } \partial\Omega \\ \mathbf{u}(\mathbf{x}, 0) = \mathbf{u}_0, & \text{in } \Omega \end{cases}$$





Controller time stepper

Time integrator for  $\Omega_1$

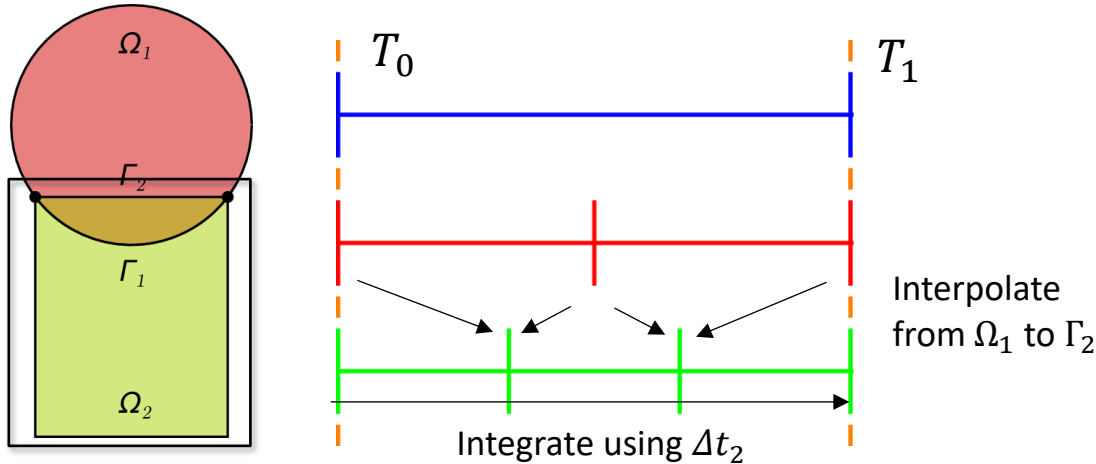
Time integrator for  $\Omega_2$

**Step 0:** Initialize  $i = 0$  (controller time index).

**Step 1:** Advance  $\Omega_1$  solution from time  $T_i$  to time  $T_{i+1}$  using time-stepper in  $\Omega_1$  with time-step  $\Delta t_1$ , using solution in  $\Omega_2$  interpolated to  $\Gamma_1$  at times  $T_i + n\Delta t_1$ .

$$\text{Model PDE: } \begin{cases} \dot{\mathbf{u}} + N(\mathbf{u}) = \mathbf{f}, & \text{in } \Omega \\ \mathbf{u}(\mathbf{x}, t) = \mathbf{g}(t), & \text{on } \partial\Omega \\ \mathbf{u}(\mathbf{x}, 0) = \mathbf{u}_0, & \text{in } \Omega \end{cases}$$





Controller time stepper

Time integrator for  $\Omega_1$

Time integrator for  $\Omega_2$

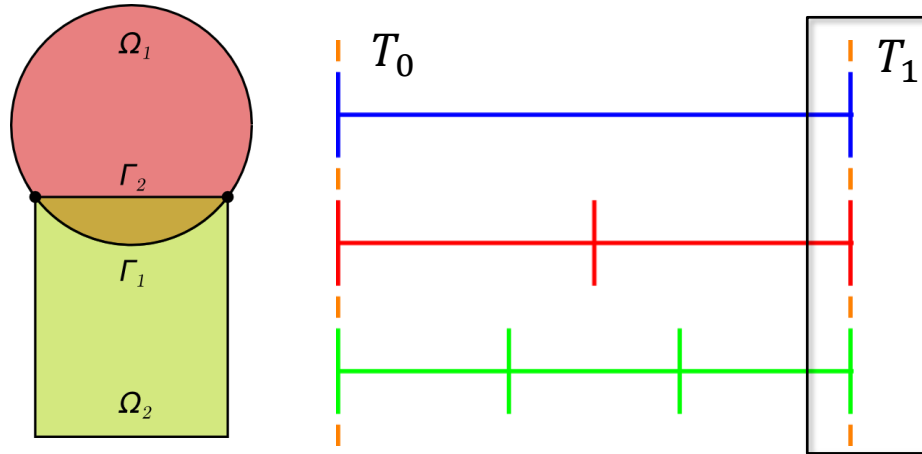
**Step 0:** Initialize  $i = 0$  (controller time index).

**Step 1:** Advance  $\Omega_1$  solution from time  $T_i$  to time  $T_{i+1}$  using time-stepper in  $\Omega_1$  with time-step  $\Delta t_1$ , using solution in  $\Omega_2$  interpolated to  $\Gamma_1$  at times  $T_i + n\Delta t_1$ .

**Step 2:** Advance  $\Omega_2$  solution from time  $T_i$  to time  $T_{i+1}$  using time-stepper in  $\Omega_2$  with time-step  $\Delta t_2$ , using solution in  $\Omega_1$  interpolated to  $\Gamma_2$  at times  $T_i + n\Delta t_2$ .

$$\text{Model PDE: } \begin{cases} \dot{\mathbf{u}} + N(\mathbf{u}) = \mathbf{f}, & \text{in } \Omega \\ \mathbf{u}(\mathbf{x}, t) = \mathbf{g}(t), & \text{on } \partial\Omega \\ \mathbf{u}(\mathbf{x}, 0) = \mathbf{u}_0, & \text{in } \Omega \end{cases}$$





Controller time stepper

Time integrator for  $\Omega_1$

Time integrator for  $\Omega_2$

**Step 0:** Initialize  $i = 0$  (controller time index).

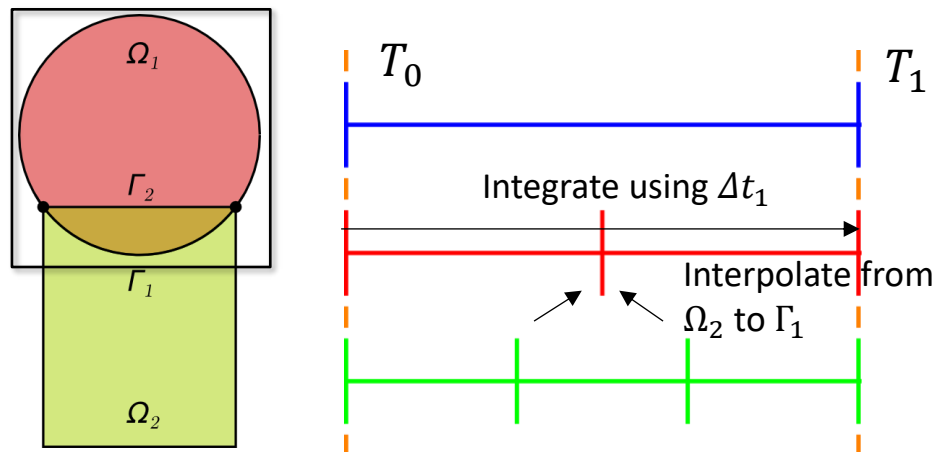
**Step 1:** Advance  $\Omega_1$  solution from time  $T_i$  to time  $T_{i+1}$  using time-stepper in  $\Omega_1$  with time-step  $\Delta t_1$ , using solution in  $\Omega_2$  interpolated to  $\Gamma_1$  at times  $T_i + n\Delta t_1$ .

**Step 2:** Advance  $\Omega_2$  solution from time  $T_i$  to time  $T_{i+1}$  using time-stepper in  $\Omega_2$  with time-step  $\Delta t_2$ , using solution in  $\Omega_1$  interpolated to  $\Gamma_2$  at times  $T_i + n\Delta t_2$ .

**Step 3:** Check for convergence at time  $T_{i+1}$ .

$$\text{Model PDE: } \begin{cases} \dot{\mathbf{u}} + N(\mathbf{u}) = \mathbf{f}, & \text{in } \Omega \\ \mathbf{u}(\mathbf{x}, t) = \mathbf{g}(t), & \text{on } \partial\Omega \\ \mathbf{u}(\mathbf{x}, 0) = \mathbf{u}_0, & \text{in } \Omega \end{cases}$$





Controller time stepper

Time integrator for  $\Omega_1$

Time integrator for  $\Omega_2$

**Step 0:** Initialize  $i = 0$  (controller time index).

**Step 1:** Advance  $\Omega_1$  solution from time  $T_i$  to time  $T_{i+1}$  using time-stepper in  $\Omega_1$  with time-step  $\Delta t_1$ , using solution in  $\Omega_2$  interpolated to  $\Gamma_1$  at times  $T_i + n\Delta t_1$ .

**Step 2:** Advance  $\Omega_2$  solution from time  $T_i$  to time  $T_{i+1}$  using time-stepper in  $\Omega_2$  with time-step  $\Delta t_2$ , using solution in  $\Omega_1$  interpolated to  $\Gamma_2$  at times  $T_i + n\Delta t_2$ .

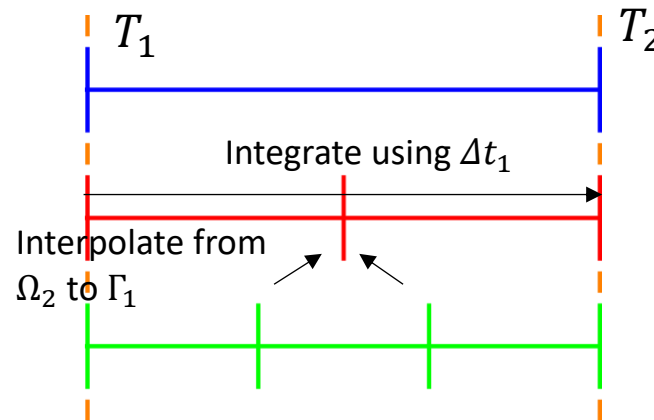
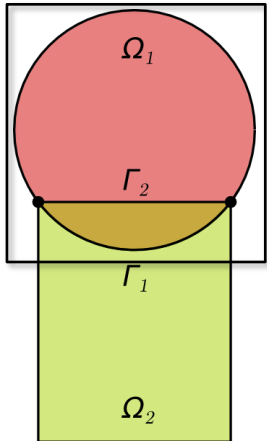
**Step 3:** Check for convergence at time  $T_{i+1}$ .

➤ If unconverged, return to Step 1.

**Model PDE:**

$$\begin{cases} \dot{\mathbf{u}} + N(\mathbf{u}) = \mathbf{f}, & \text{in } \Omega \\ \mathbf{u}(\mathbf{x}, t) = \mathbf{g}(t), & \text{on } \partial\Omega \\ \mathbf{u}(\mathbf{x}, 0) = \mathbf{u}_0, & \text{in } \Omega \end{cases}$$





Controller time stepper

Time integrator for  $\Omega_1$

Time integrator for  $\Omega_2$

Can use ***different integrators*** with ***different time steps*** within each domain!

**Step 0:** Initialize  $i = 0$  (controller time index).

**Step 1:** Advance  $\Omega_1$  solution from time  $T_i$  to time  $T_{i+1}$  using time-stepper in  $\Omega_1$  with time-step  $\Delta t_1$ , using solution in  $\Omega_2$  interpolated to  $\Gamma_1$  at times  $T_i + n\Delta t_1$ .

**Step 2:** Advance  $\Omega_2$  solution from time  $T_i$  to time  $T_{i+1}$  using time-stepper in  $\Omega_2$  with time-step  $\Delta t_2$ , using solution in  $\Omega_1$  interpolated to  $\Gamma_2$  at times  $T_i + n\Delta t_2$ .

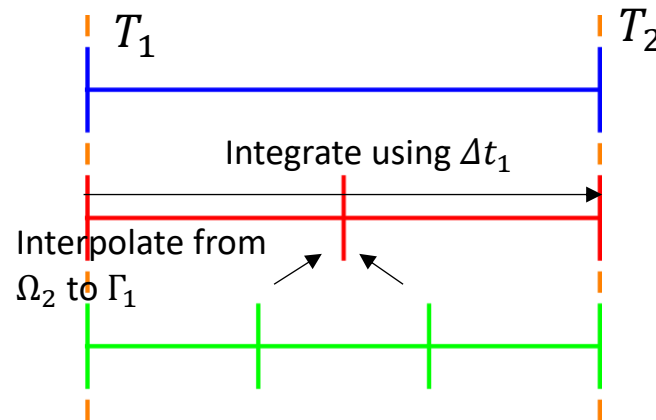
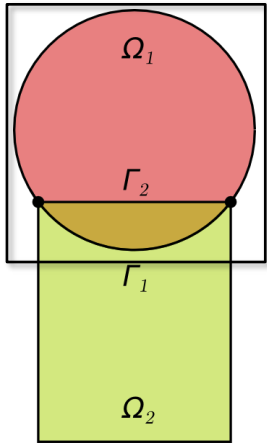
**Step 3:** Check for convergence at time  $T_{i+1}$ .

- If unconverged, return to Step 1.
- If converged, set  $i = i + 1$  and return to Step 1.

**Model PDE:**

$$\begin{cases} \dot{\mathbf{u}} + N(\mathbf{u}) = \mathbf{f}, & \text{in } \Omega \\ \mathbf{u}(x, t) = \mathbf{g}(t), & \text{on } \partial\Omega \\ \mathbf{u}(x, 0) = \mathbf{u}_0, & \text{in } \Omega \end{cases}$$





Controller time stepper

Time integrator for  $\Omega_1$

Time integrator for  $\Omega_2$

Time-stepping procedure is **equivalent** to doing Schwarz on **space-time domain** [Mota *et al.* 2022].

**Step 0:** Initialize  $i = 0$  (controller time index).

**Step 1:** Advance  $\Omega_1$  solution from time  $T_i$  to time  $T_{i+1}$  using time-stepper in  $\Omega_1$  with time-step  $\Delta t_1$ , using solution in  $\Omega_2$  interpolated to  $\Gamma_1$  at times  $T_i + n\Delta t_1$ .

**Step 2:** Advance  $\Omega_2$  solution from time  $T_i$  to time  $T_{i+1}$  using time-stepper in  $\Omega_2$  with time-step  $\Delta t_2$ , using solution in  $\Omega_1$  interpolated to  $\Gamma_2$  at times  $T_i + n\Delta t_2$ .

**Step 3:** Check for convergence at time  $T_{i+1}$ .

- If unconverged, return to Step 1.
- If converged, set  $i = i + 1$  and return to Step 1.

**Model PDE:**

$$\begin{cases} \dot{\mathbf{u}} + N(\mathbf{u}) = \mathbf{f}, & \text{in } \Omega \\ \mathbf{u}(x, t) = \mathbf{g}(t), & \text{on } \partial\Omega \\ \mathbf{u}(x, 0) = \mathbf{u}_0, & \text{in } \Omega \end{cases}$$



# Schwarz for Multi-scale FOM-FOM Coupling in Solid Mechanics<sup>1</sup>

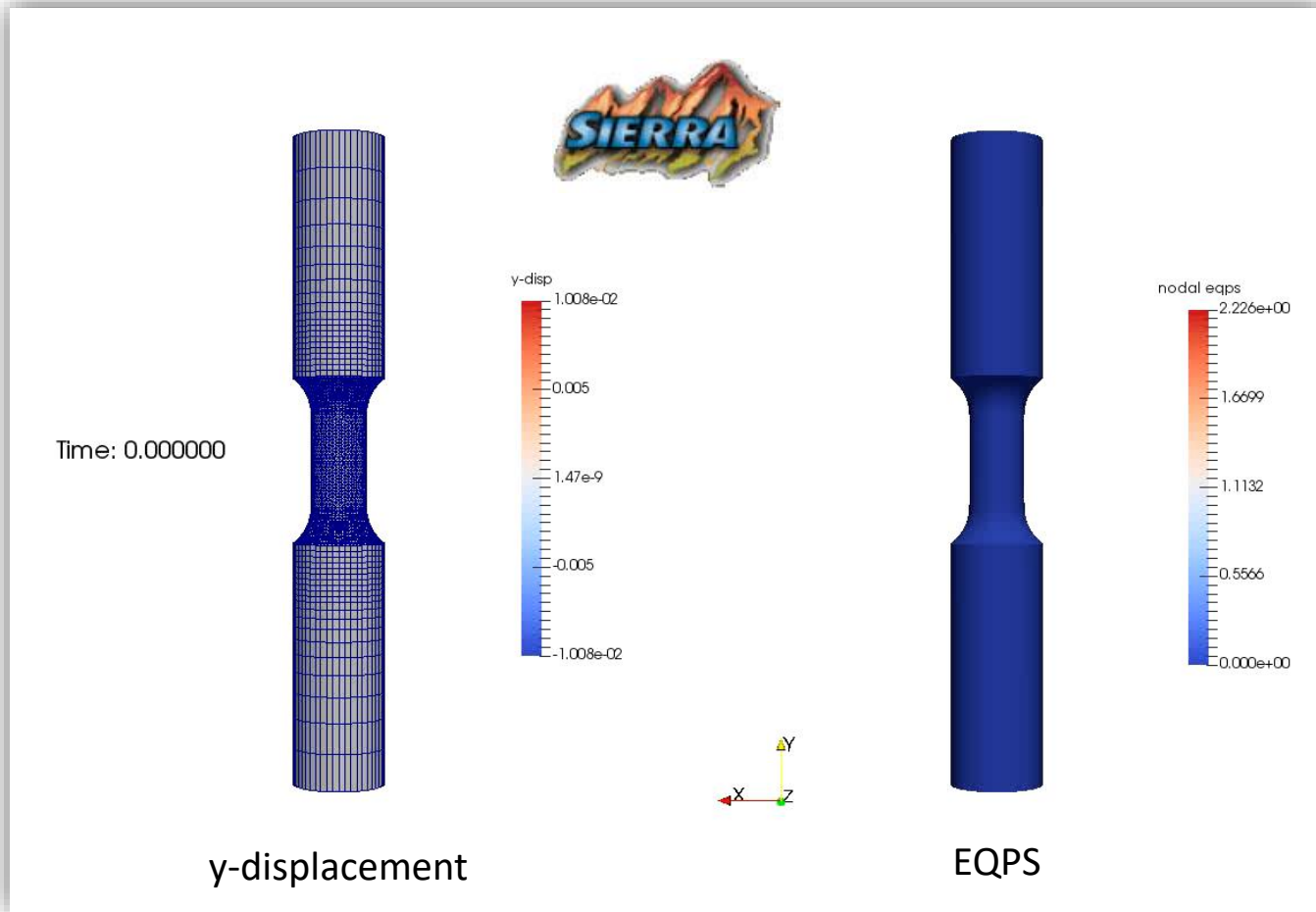
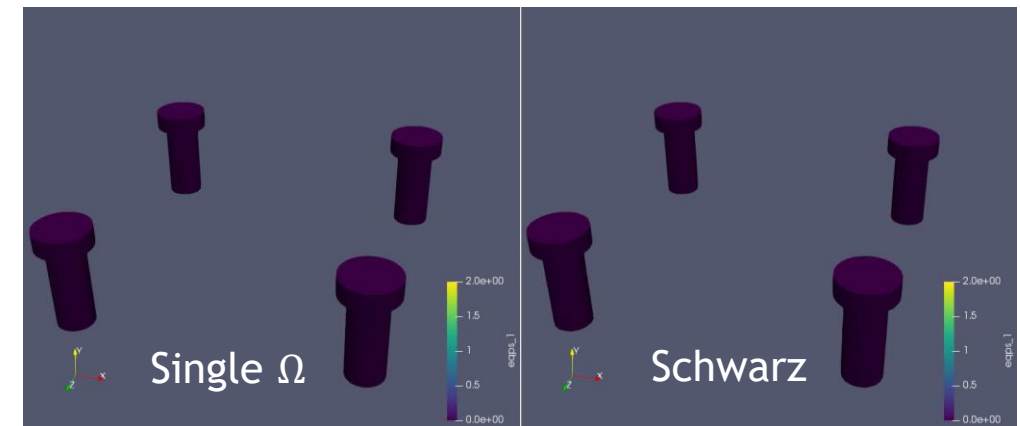


*Figure above:* tension specimen simulation coupling composite TET10 elements with HEX elements in Sierra/SM.

*Figures right:* bolted joint simulation coupling composite TET10 elements with HEX elements in Sierra/SM.



<sup>1</sup> Mota *et al.* 2017; Mota *et al.* 2022.

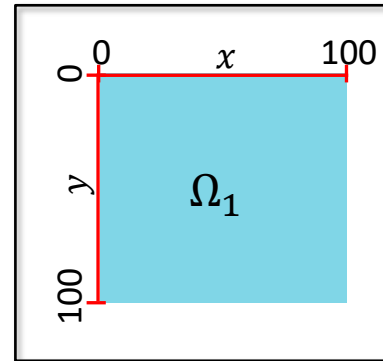


# 2D Inviscid Burgers Equation



Popular analog for fluid problems where **shocks** are possible, and particularly **difficult** for conventional projection-based ROMs

$$\begin{aligned}\frac{\partial u}{\partial t} + \frac{1}{2} \left( \frac{\partial(u^2)}{\partial x} + \frac{\partial(uv)}{\partial y} \right) &= 0.02 \exp(\mu_2 x) \\ \frac{\partial v}{\partial t} + \frac{1}{2} \left( \frac{\partial(vu)}{\partial x} + \frac{\partial(v^2)}{\partial y} \right) &= 0 \\ u(0, y, t; \boldsymbol{\mu}) &= \mu_1 \\ u(x, y, 0) = v(x, y, 0) &= 1\end{aligned}$$



## Problem setup:

- $\Omega = (0, 100)^2$ ,  $t \in [0, 25]$
- Two parameters  $\boldsymbol{\mu} = (\mu_1, \mu_2)$ . **Training:** uniform sampling of  $\mu_1 \times \mu_2 = [4.25, 5.50] \times [0.015, 0.03]$  by a  $3 \times 3$  grid. **Testing:** query unsampled point  $\boldsymbol{\mu} = [4.75, 0.02]$

## FOM discretization:

- Spatial discretization given by a **Godunov-type scheme** with  $N = 250$  elements in each dimension
- Implicit **trapezoidal method** with fixed  $\Delta t = 0.05$

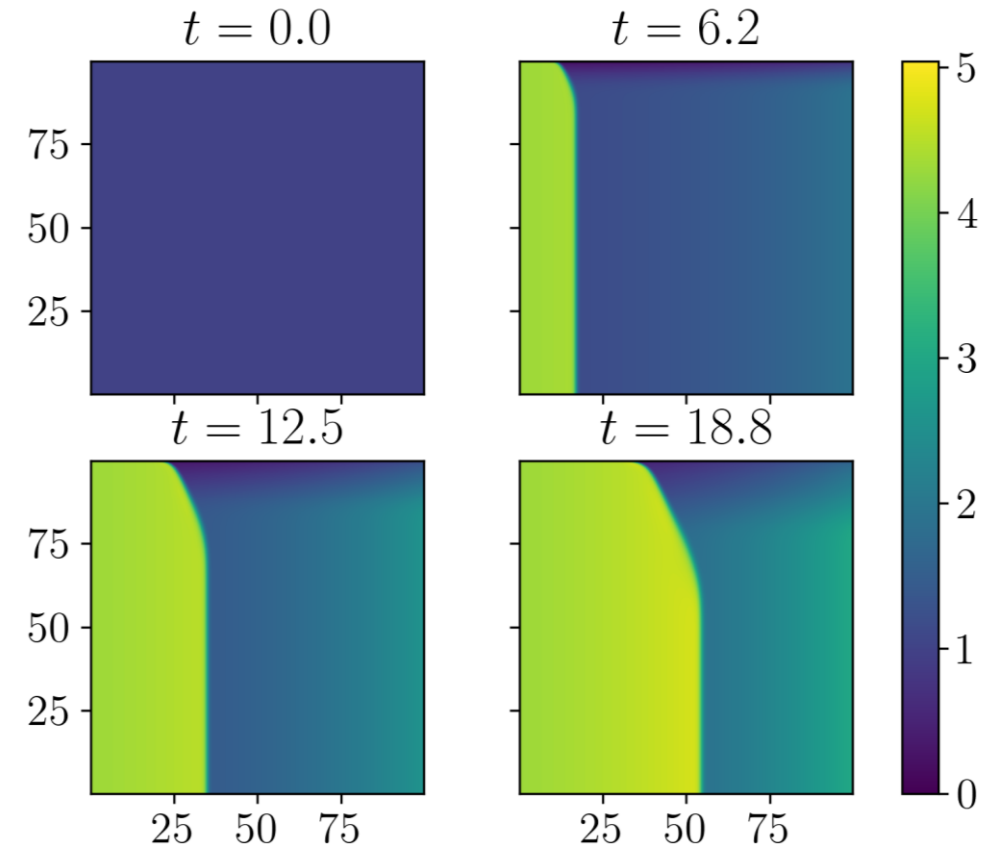


Figure above: solution of  $u$  component at various times



# Schwarz Coupling Details

## Choice of domain decomposition

- Overlapping DD of  $\Omega$  into 4 subdomains coupled via multiplicative Schwarz
- Solution in  $\Omega_1$  is most difficult to capture by ROM

## Snapshot collection and reduced basis construction

- Single-domain FOM on  $\Omega$  used to generate snapshots/POD modes

## Enforcement of boundary conditions (BCs) in ROM at Schwarz boundaries

- BCs imposed strongly via Method 1 of [Gunzburger *et al.*, 2007] at indices  $i_{\text{Dir}}$

$$\mathbf{q}(t) \approx \bar{\mathbf{q}} + \Phi \hat{\mathbf{q}}(t)$$

- POD modes made to satisfy homogeneous DBCs:  $\Phi(\mathbf{i}_{\text{Dir}}, :) = \mathbf{0}$
- BCs imposed by modifying  $\bar{\mathbf{q}}$ :  $\bar{\mathbf{q}}(\mathbf{i}_{\text{Dir}}) \leftarrow \chi_q$

## Choice of hyper-reduction

- Energy Conserving Sampling & Weighting (ECSW) method for hyper-reduction
- All points on Schwarz boundaries are included in the sample mesh

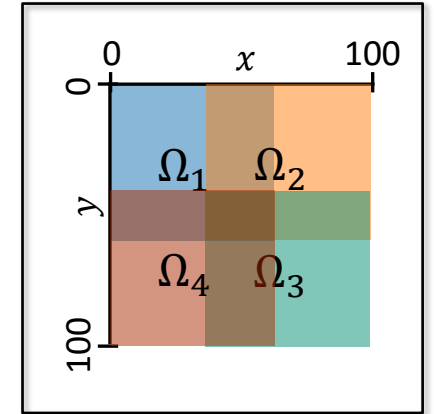


Figure above: 4 subdomain overlapping DD

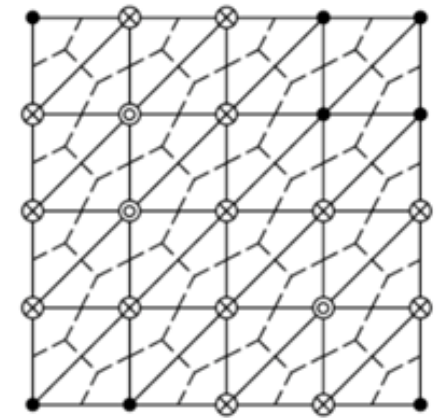
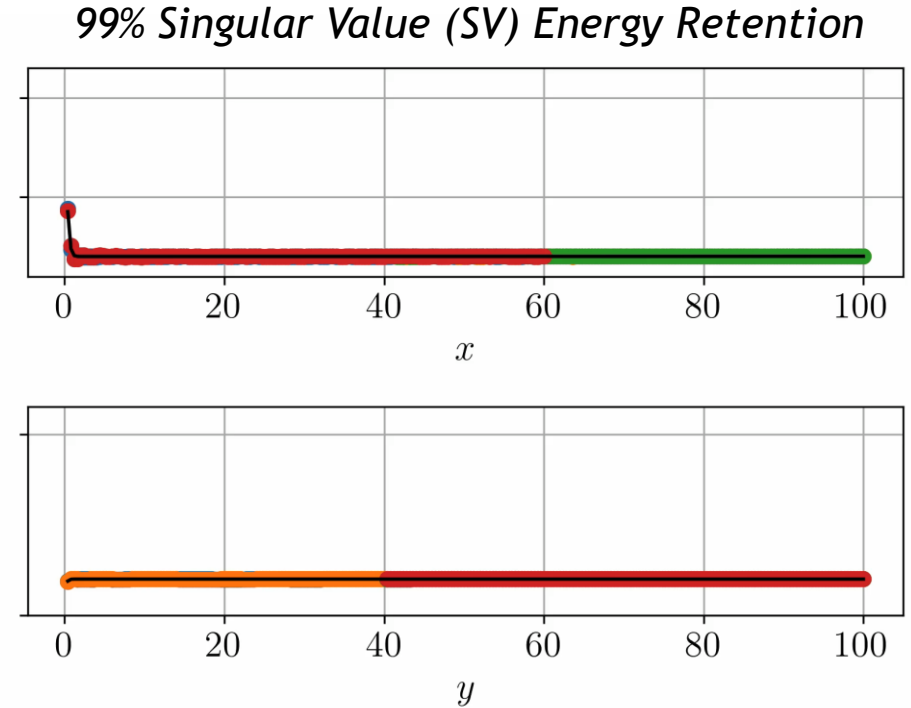
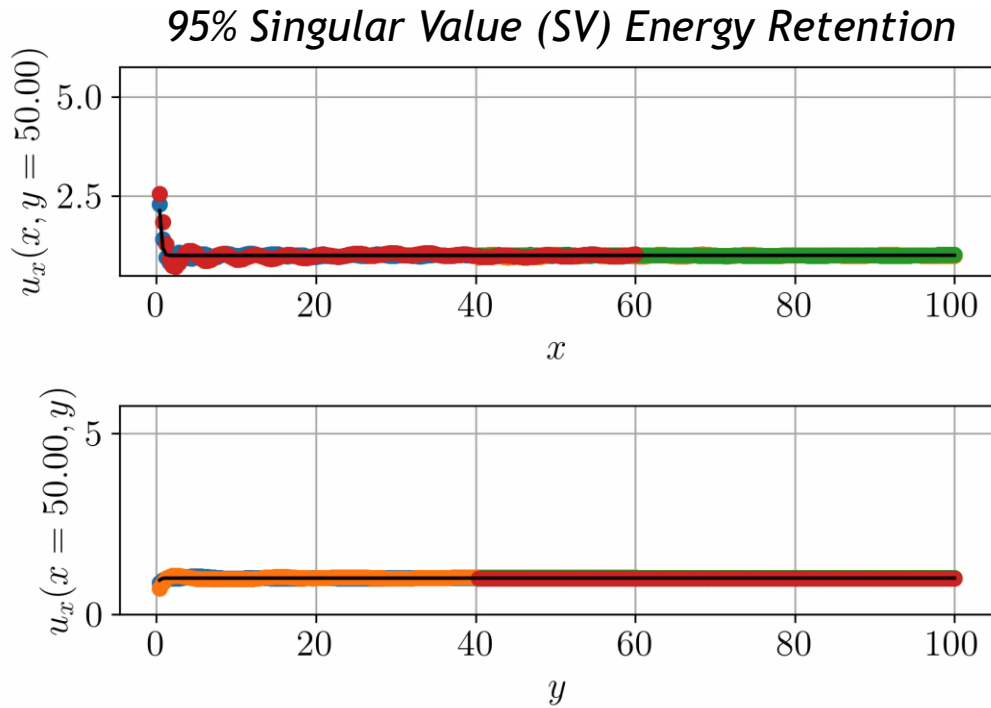
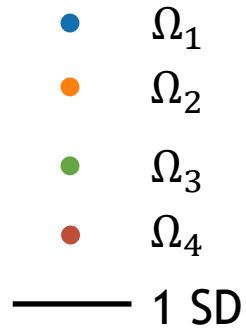


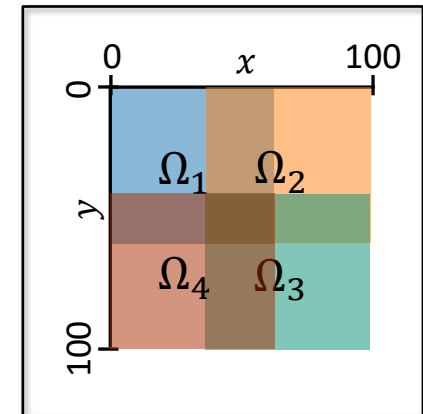
Figure above: ECSW augmented reduced mesh





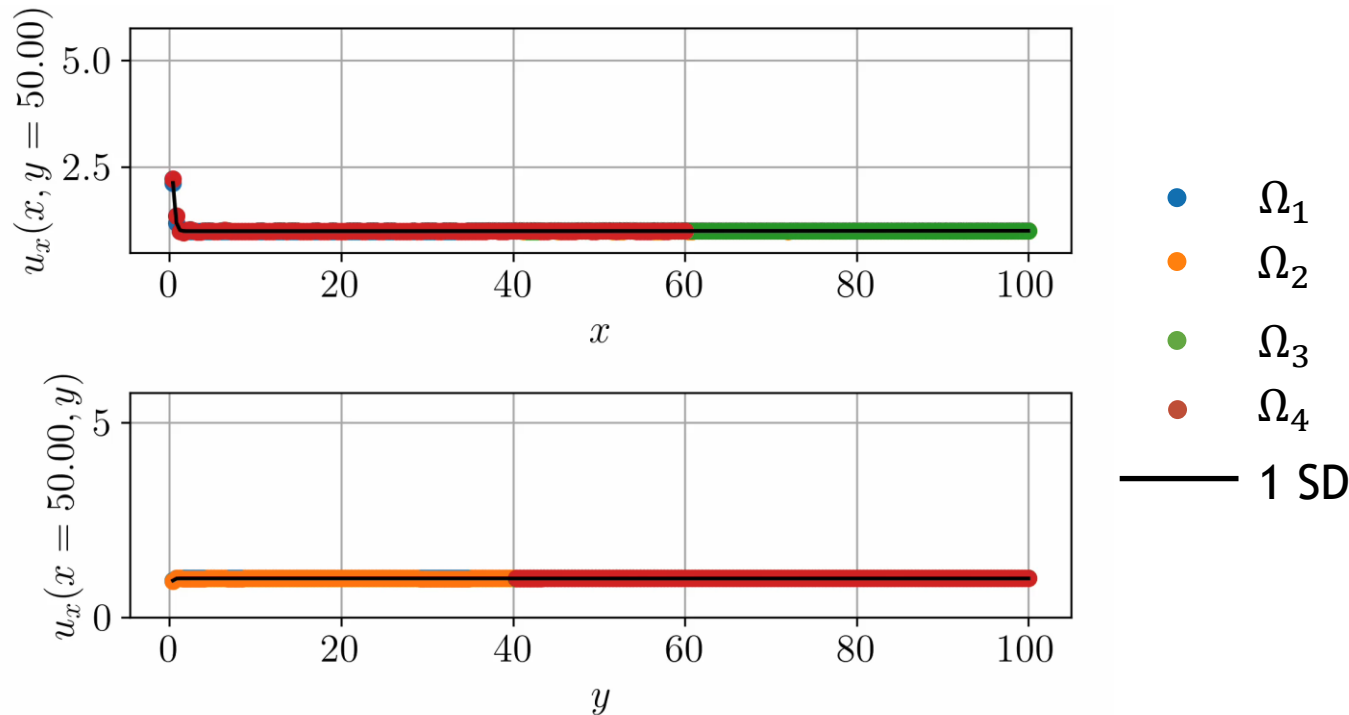
- Method converges in **only 3 Schwarz iterations** per controller time-step
- Errors  $O(1\%)$  or less**
- $1.47\times$  speedup** over all-FOM coupling for 95% SV energy retention case

Subdomains	95% SV Energy			99% SV Energy		
	$M$	MSE (%)	CPU time (s)	$M$	MSE (%)	CPU time (s)
$\Omega_1$	57	1.1	85	146	0.18	295
$\Omega_2$	44	1.2	56	120	0.18	216
$\Omega_3$	24	1.4	43	60	0.16	89
$\Omega_4$	32	1.9	61	66	0.25	100
<b>Total</b>			<b>245</b>			<b>700</b>





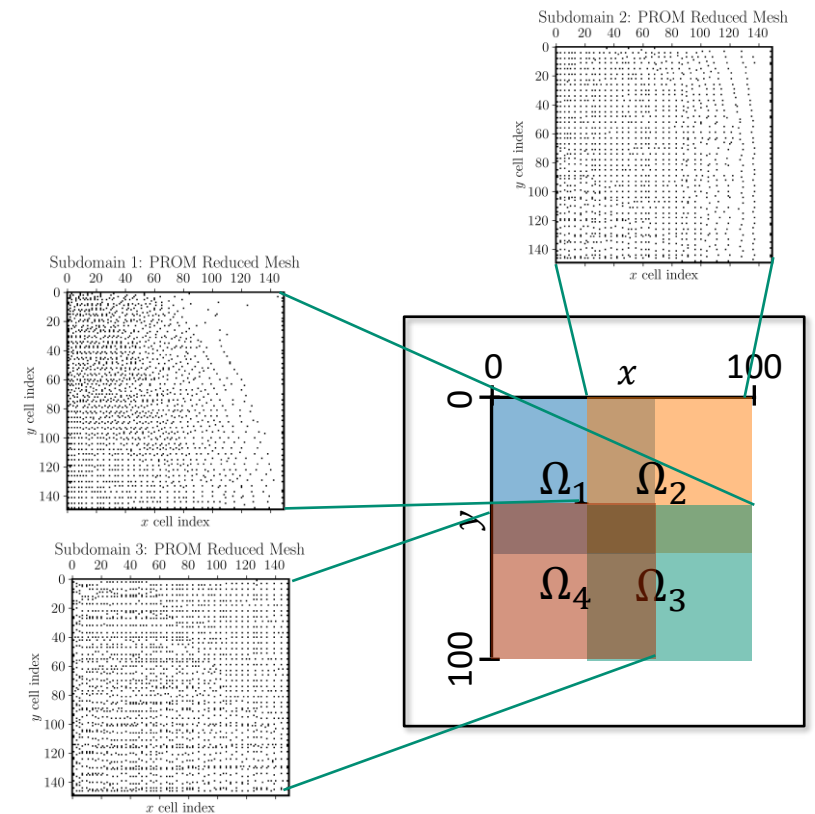
# FOM-HROM-HROM-HROM Coupling



- FOM in  $\Omega_1$  as this is “hardest” subdomain for ROM
- HROMs in  $\Omega_2, \Omega_3, \Omega_4$  capture 99% snapshot energy
- Method converges in 3 Schwarz iterations per controller time-step
- Errors  $O(0.1\%)$  with 0 error in  $\Omega_1$
- $2.26\times$  speedup achieved over all-FOM coupling

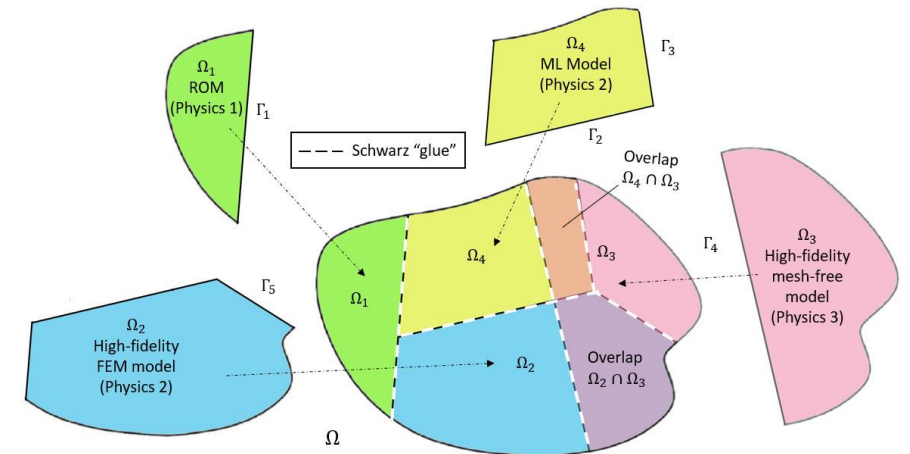
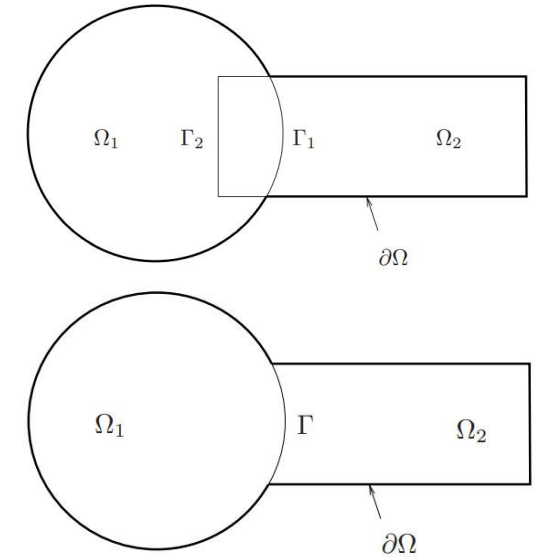
Further speedups possible via code optimizations, additive Schwarz and reduction of # sample mesh points.

Subdomains	99% SV Energy		
	$M$	MSE (%)	CPU time (s)
$\Omega_1$	—	0.0	95
$\Omega_2$	120	0.26	26
$\Omega_3$	60	0.43	17
$\Omega_4$	66	0.34	21
<b>Total</b>			<b>159</b>





- The Schwarz Alternating Method for Domain Decomposition-Based Coupling
- Extension to FOM\*-ROM<sup>#</sup> and ROM-ROM Coupling
- Numerical Examples
  - 2D Burgers Equation
  - 2D Shallow Water Equations
  - Teaser: 2D Euler Equations Riemann Problem
- Summary & Future Work





# 2D Shallow Water Equations (SWE)



Hyperbolic PDEs modeling **wave propagation** below a pressure surface in a fluid (e.g., atmosphere, ocean).

$$\begin{aligned} \frac{\partial h}{\partial t} + \frac{\partial(hu)}{\partial x} + \frac{\partial(hv)}{\partial y} &= 0 \\ \frac{\partial(hu)}{\partial t} + \frac{\partial}{\partial x} \left( hu^2 + \frac{1}{2}gh^2 \right) + \frac{\partial}{\partial y} (huv) &= -\mu v \\ \frac{\partial(hv)}{\partial t} + \frac{\partial}{\partial x} (huv) + \frac{\partial}{\partial y} \left( hv^2 + \frac{1}{2}gh^2 \right) &= \mu u \end{aligned}$$

## Problem setup:

- $\Omega = (-5, 5)^2$ ,  $t \in [0, 10]$ , Gaussian initial condition
- **Coriolis parameter**  $\mu \in \{-4, -3, -2, -1, 0\}$  for training, and  $\mu \in \{-3.5, -2.5, -1.5, -0.5\}$  for testing

## FOM discretization:

- Spatial discretization given by a first-order **cell-centered finite volume** discretization with  $N = 300$  elements in each dimension
- Implicit first order temporal discretization: **backward Euler** with fixed  $\Delta t = 0.01$
- Implemented in **Pressio-demoapps** (<https://github.com/Pressio/pressio-demoapps>)

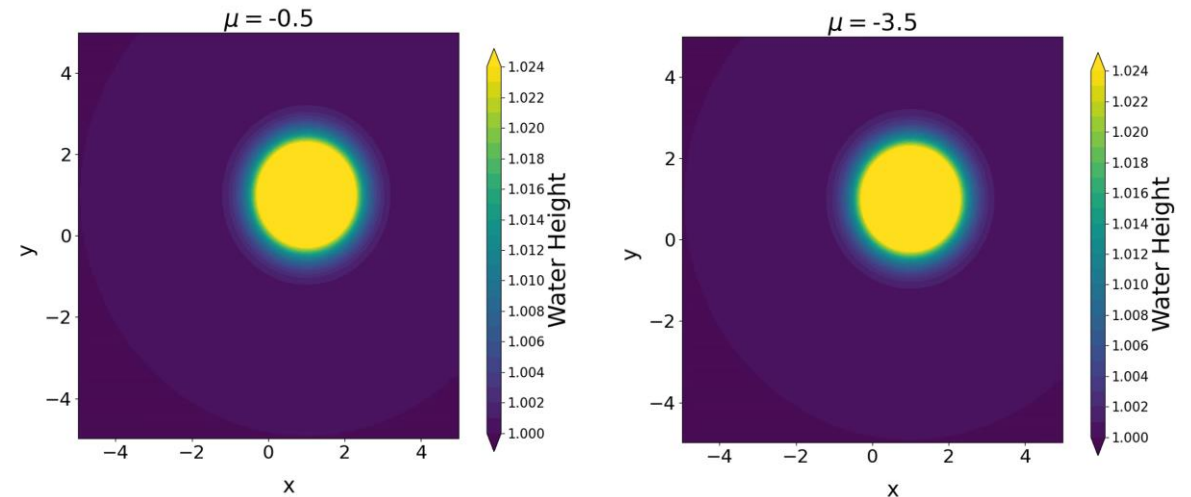


Figure above: FOM solutions to SWE for  $\mu = -0.5$  (left) and  $\mu = -3.5$  (right).



# Schwarz Coupling Details

**Green:** different from Burgers' problem

## Choice of domain decomposition

- **Non-overlapping** DD of  $\Omega$  into 4 subdomains coupled via **additive Schwarz**
  - **OpenMP parallelism** with 1 thread/subdomain
- **All-ROM** or **All-HROM** coupling via Pressio\*

## Snapshot collection and reduced basis construction

- **Single-domain FOM** on  $\Omega$  used to generate snapshots/POD modes

## Enforcement of boundary conditions (BCs) in ROM at Schwarz boundaries

- BCs are imposed **approximately** by fictitious ghost cell states
  - Implementing Neumann and Robin BCs is **challenging**
- **Ghost cells** introduce some overlap even with non-overlapping DD
  - $\Rightarrow$  **Dirichlet-Dirichlet non-overlapping Schwarz** is stable/convergent!

## Choice of hyper-reduction

- **Collocation** for hyper-reduction: min residual at small subset DOFs
- Assume **fixed budget of sample mesh points** at Schwarz boundaries

\*<https://github.com/Pressio/pressio-demoapps>

Figure right: non-overlapping DD w/ ghost cells creating overlap

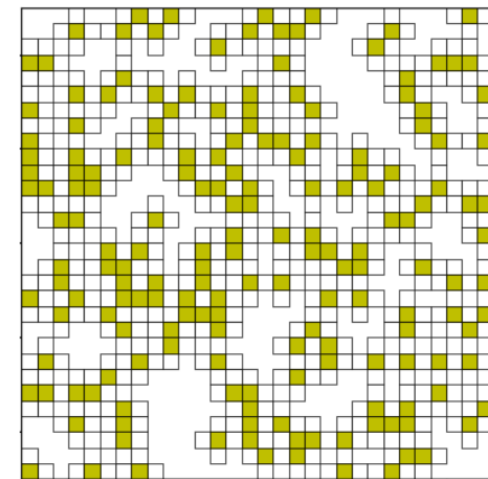
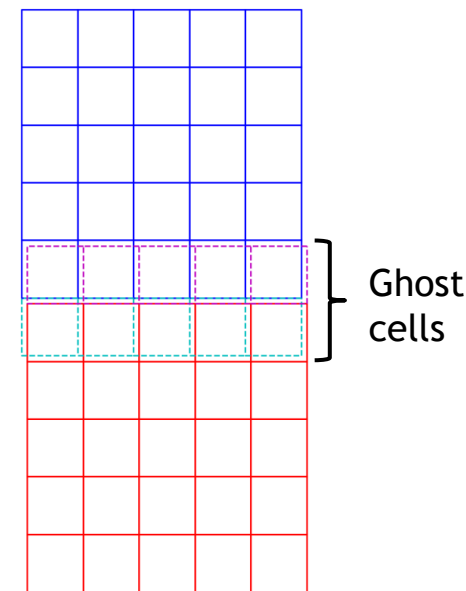


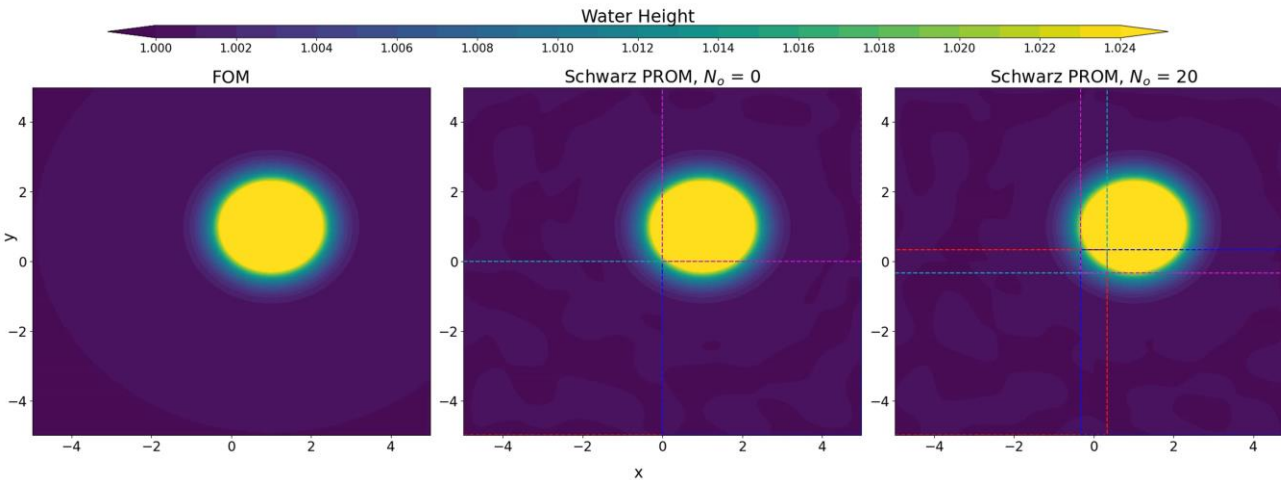
Figure above: sample mesh (yellow) and stencil (white) cells



# Schwarz All-ROM Domain Overlap Study



Study of Schwarz convergence for all-ROM coupling as a function of  $N_o :=$  cell width of overlap region (not including ghost cells).

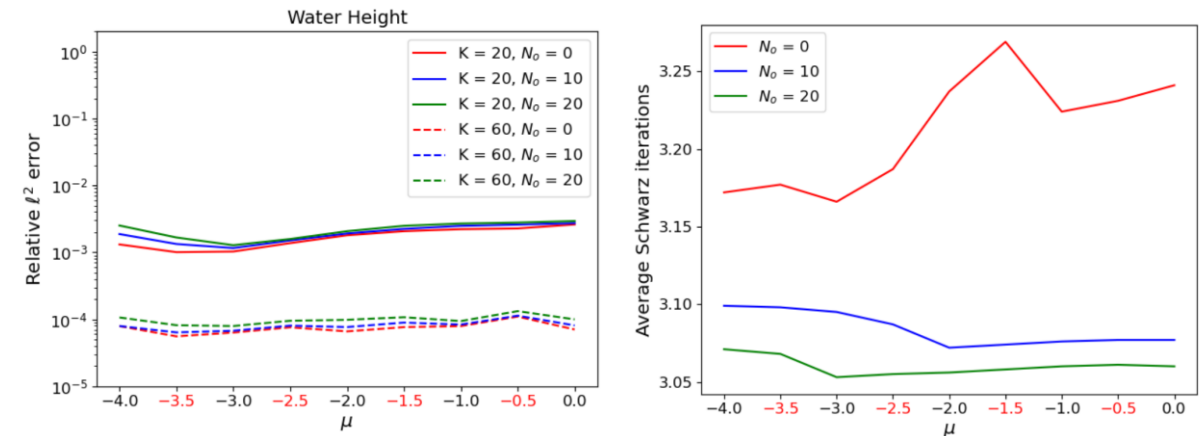


Movie above: FOM (left), 4 subdomain ROM coupled via non-overlapping Schwarz (middle), and 4 subdomain ROM coupled via overlapping Schwarz (right) for predictive SWE problem with  $\mu = -0.5$ . All ROMs have  $K = 80$  POD modes.

- Schwarz iterations decrease (very roughly) with  $N_o^{0.25}$  (figure, right) whereas evaluating  $r(q)$  scales with  $N_o^2$

➤  $\Rightarrow$  there is no reason not to do **non-overlapping coupling** for this problem

- Dirichlet-Dirichlet coupling with **no-overlap** ( $N_o = 0$ ) performs well with **no convergence issues** (movie, left) and **errors comparable to** Dirichlet-Dirichlet coupling with overlap (figure below, left)



Figures above: relative error and average # Schwarz iterations as a function of  $\mu$  and  $N_o$ . Black  $\mu$ : training, red  $\mu$ : testing.

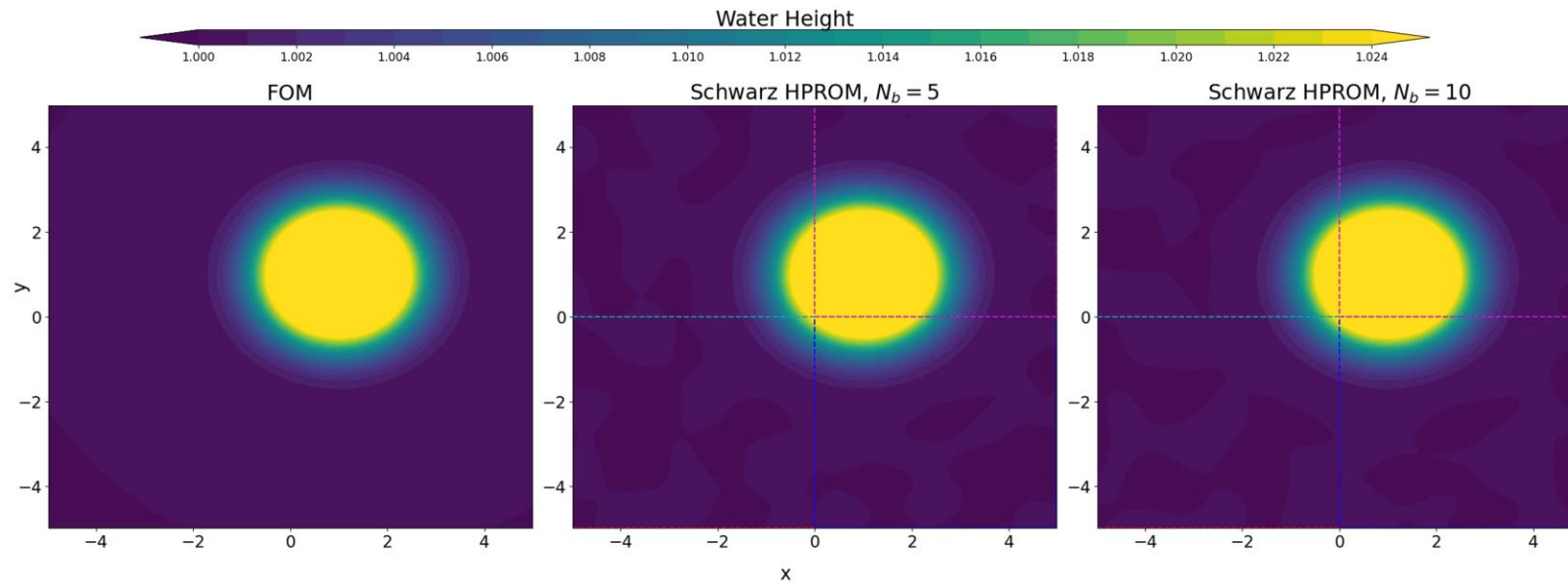


# Schwarz Boundary Sampling for All-HROM Coupling



**Key question:** how many Schwarz boundary points need to be included in **sample mesh** when performing HROM coupling?

- Naïve/sparsely-sampled Schwarz boundary results in **failure** to transmit coupling information during Schwarz



Movie above: FOM (left), all HROM with  $N_b = 5\%$  (middle) and all HROM with  $N_b = 10\%$  (left). ROMs have  $K = 100$  modes and  $N_s = 0.5\%N$  sample mesh points.

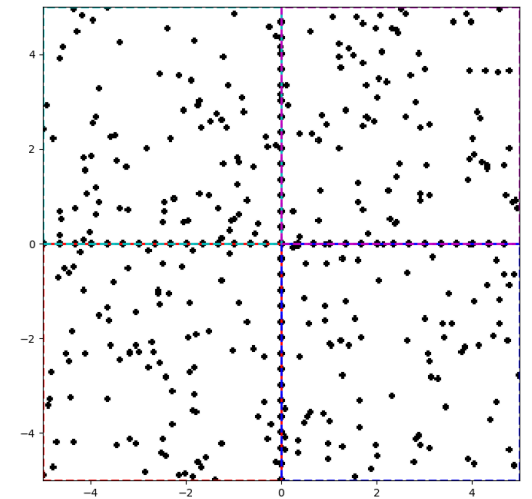
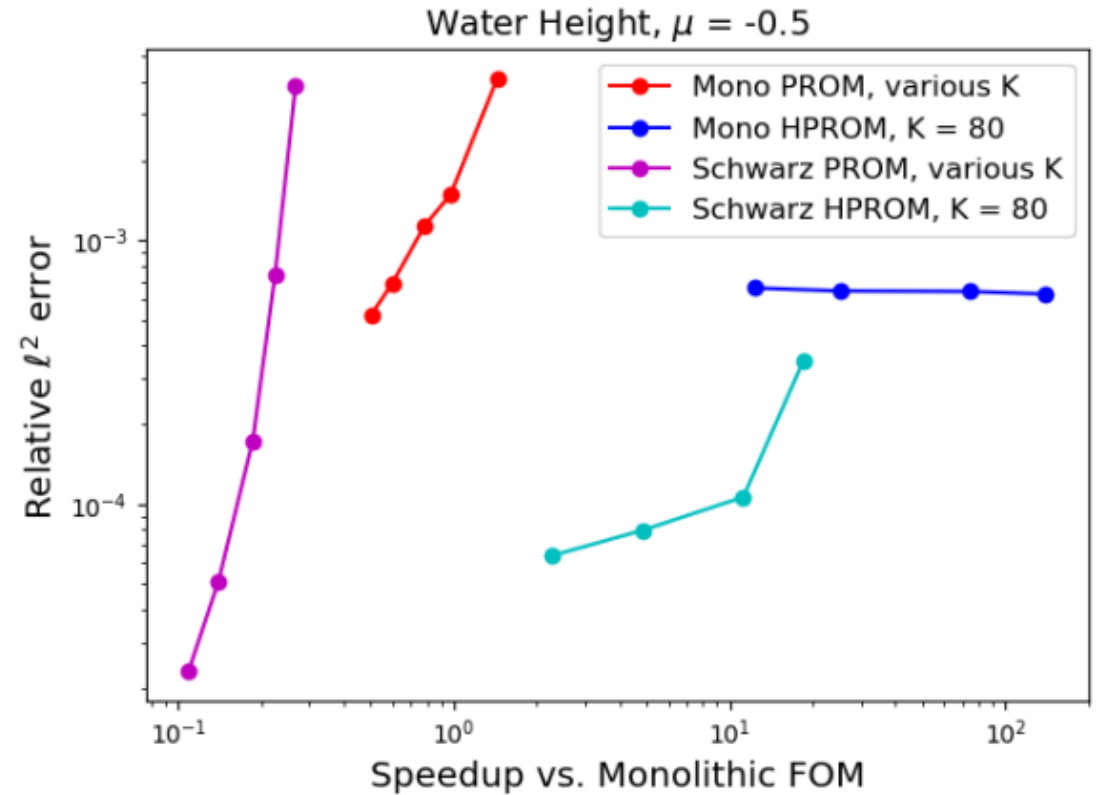
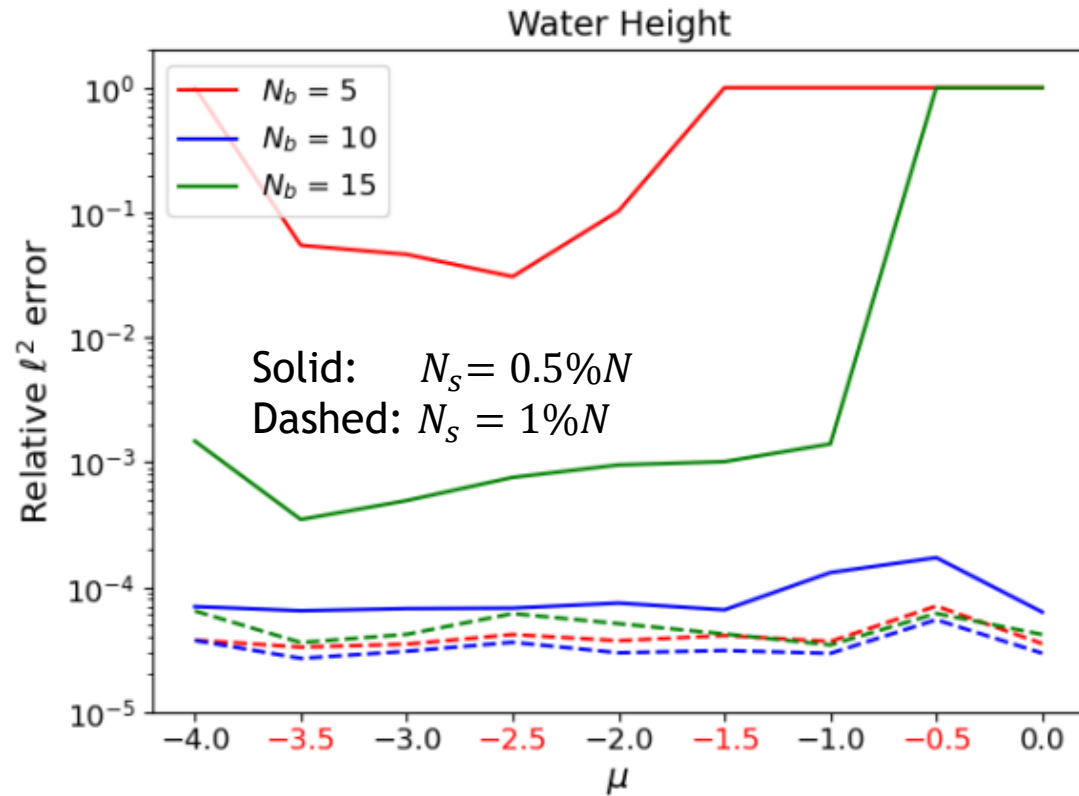


Figure above: example sample mesh with sampling rate  $N_b = 10\%$

- Including too many Schwarz boundary points ( $N_b$ ) in sample mesh given **fixed budget** of  $N_s$  sample mesh points may lead to **too few sample mesh points in interior**
- For SWE problem, we can get away with  **$\sim 10\%$  boundary sampling** (movie above, right-most frame)





- For a fixed ROM dimension, Schwarz delivers **lower error** and **comparable cost**!
- There are noticeable **cost savings** relative to **monolithic FOM**!
- Accuracy similar for **predictive  $\mu$**  (red) and **non-predictive  $\mu$**  (black) cases.

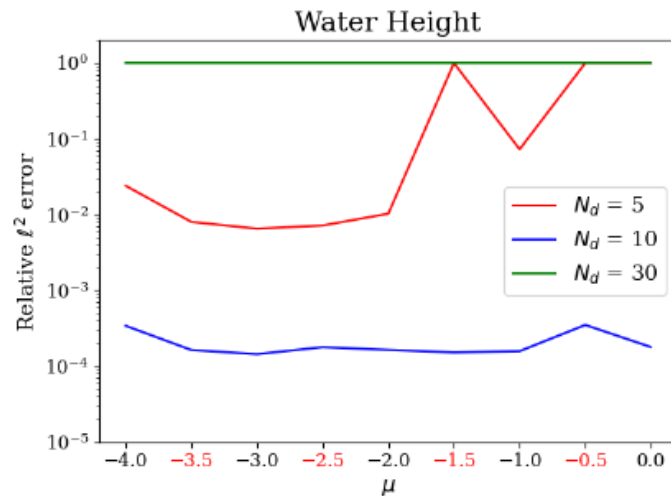


# Hyper-reduced ROMs: Impact of Boundary Sampling

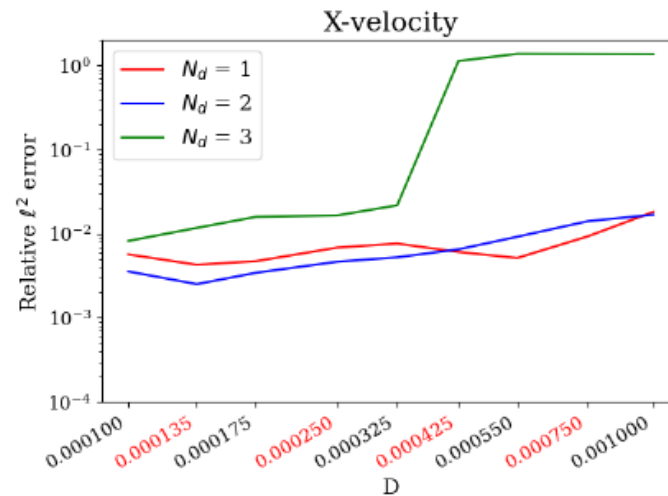


**Key result:** given a fixed “budget” of sample mesh points, there is a (problem-dependent) optimal number of sample mesh points to allocate to the Schwarz boundaries vs. the subdomain interiors.

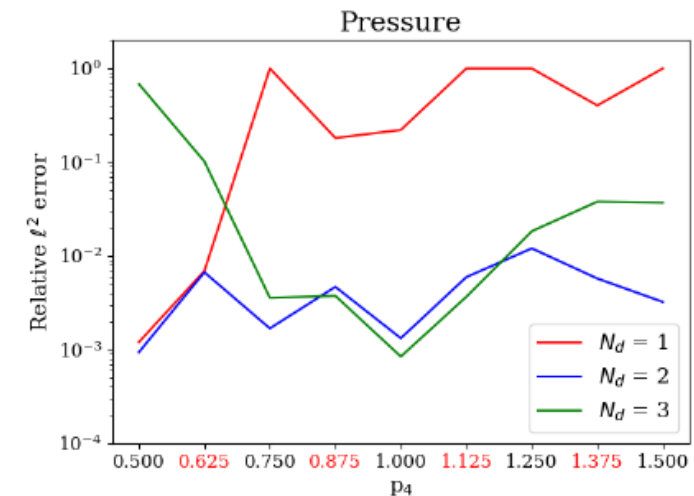
- There is a delicate balance of ensuring **BC transmission** together with an **accurate interior solutions**
- More **extensive boundary sampling** is required for problems with **shocks** (Burgers, Euler)



SWE,  $N_s = 0.5\%N$



Burgers',  $N_s = 3.75\%N$



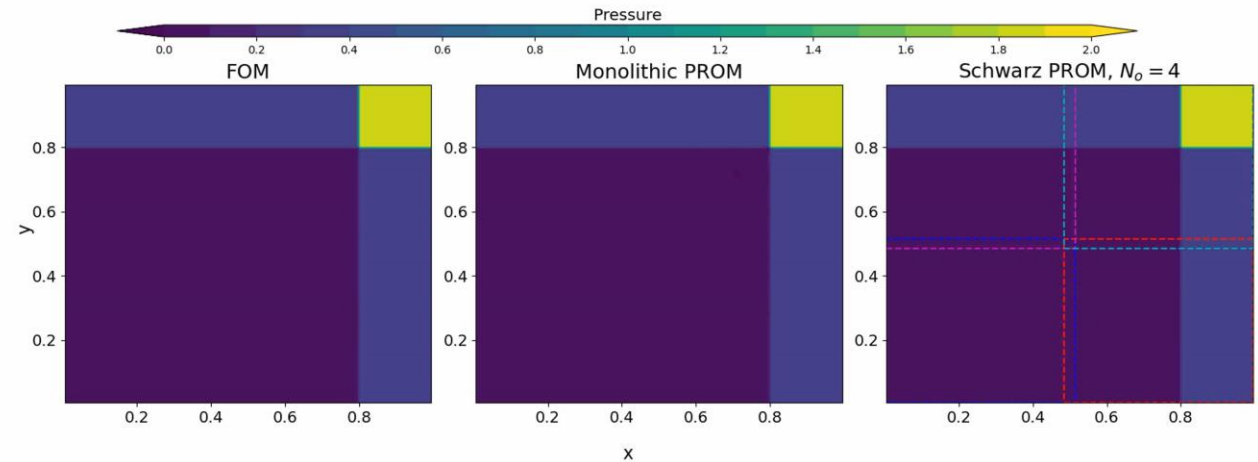
Euler,  $N_s = 5\%N$

Red parameter values are predictive.



$$\frac{\partial}{\partial t} \begin{pmatrix} \rho \\ \rho u \\ \rho v \\ \rho E \end{pmatrix} + \frac{\partial}{\partial x} \begin{pmatrix} \rho u \\ \rho u^2 + p \\ \rho uv \\ (E + p)u \end{pmatrix} + \frac{\partial}{\partial y} \begin{pmatrix} \rho v \\ \rho uv \\ \rho v^2 + p \\ (E + p)v \end{pmatrix} = \mathbf{0}$$

$$p = (\gamma - 1) \left( \rho E - \frac{1}{2} \rho (u^2 + v^2) \right)$$



### Problem setup:

- $\Omega = (0,1)^2$ ,  $t \in [0, 0.8]$ , homogeneous Neumann BCs
- Fix  $\rho_1 = 1.5$ ,  $u_1 = v_1 = 0$ ,  $p_3 = 0.029$
- Vary  $p_1$ ; IC from compatibility conditions\*
  - Training:  $p_1 \in [1.0, 1.25, 1.5, 1.75, 2.0]$
  - Testing:  $p_1 \in [1.125, 1.375, 1.625, 1.875]$

### FOM discretization:

- Spatial discretization given by a first-order **cell-centered finite volume** discretization with  $N = 300$  or  $N = 100$  elements in each dimension
- Implicit first order temporal discretization: **backward Euler** with fixed  $\Delta t = 0.005$
- Implemented in **Pressio-demoapps** (<https://github.com/Pressio/pressio-demoapps>)

### Preliminary results:

- Schwarz can **stabilize** unstable monolithic ROM for fixed dimension  $K$  (above)
- Since shock traverses all parts of domain, achieving **speedups** with Schwarz is **more difficult**

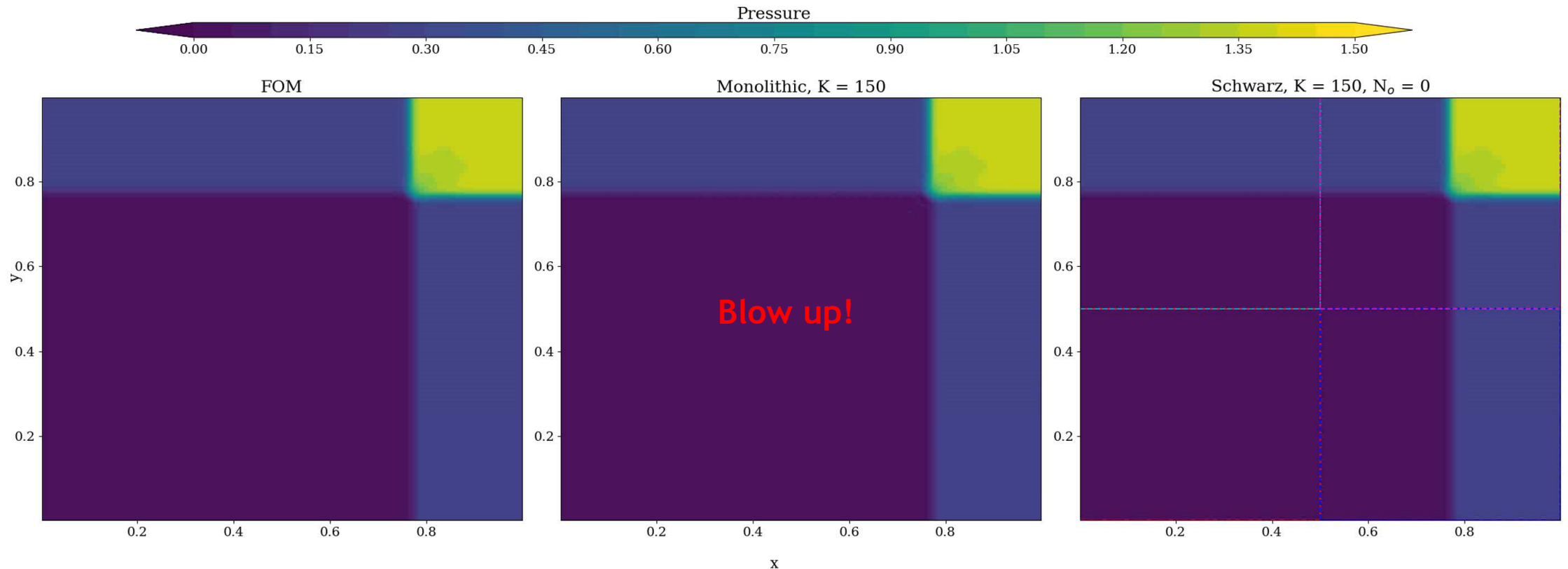
\*Schulz-Rinne, 1993.



# Unsampled ROMs: Stabilization Effects



**Key result:** domain decomposition + Schwarz coupling can stabilize an otherwise unstable monolithic solution



*Movie above:* monolithic vs. decomposed ROM for Euler problem with  $p_4 = 1.375$  (predictive regime).



The **Schwarz alternating method** has been developed for concurrent multi-scale coupling of **conventional** and **data-driven models**.

- 😊 Coupling is *concurrent* (two-way).
- 😊 *Ease of implementation* into existing massively-parallel HPC codes.
- 😊 “*Plug-and-play*” *framework*: simplifies task of meshing complex geometries!
  - 😊 Ability to couple regions with *different non-conformal meshes*, *different element types* and *different levels of refinement*.
  - 😊 Ability to use *different solvers (including ROM/FOM)* and *time-integrators* in different regions.
- 😊 *Scalable, fast, robust* on *real* engineering problems
- 😊 Coupling does not introduce *nonphysical artifacts*.
- 😊 *Theoretical* convergence properties/guarantees.

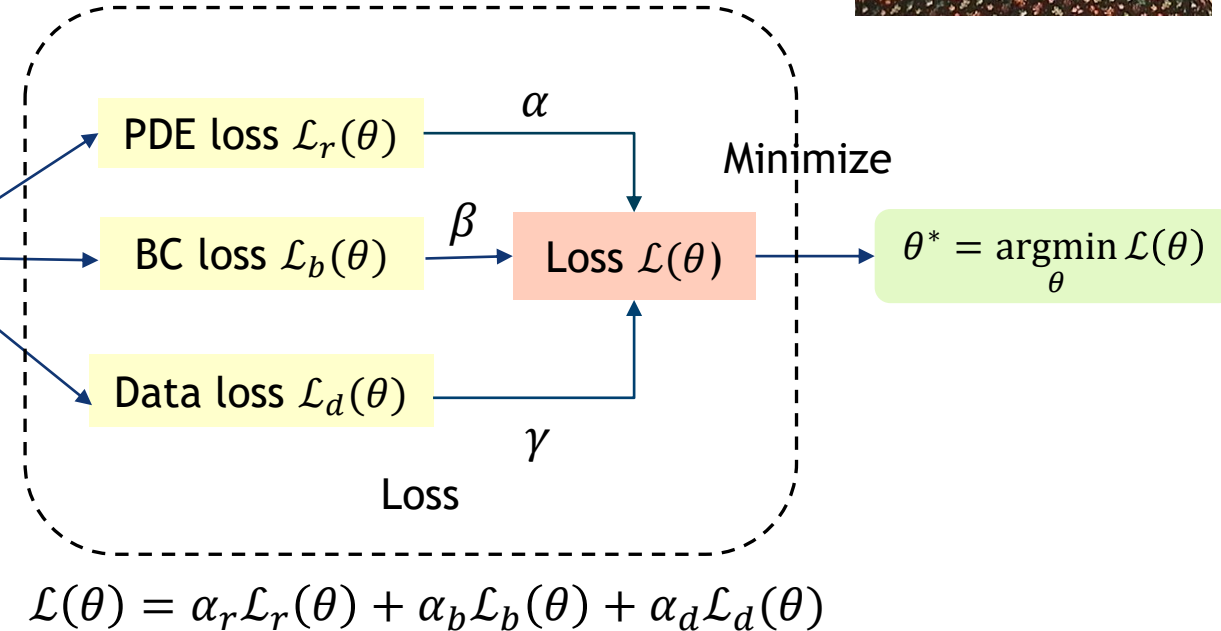
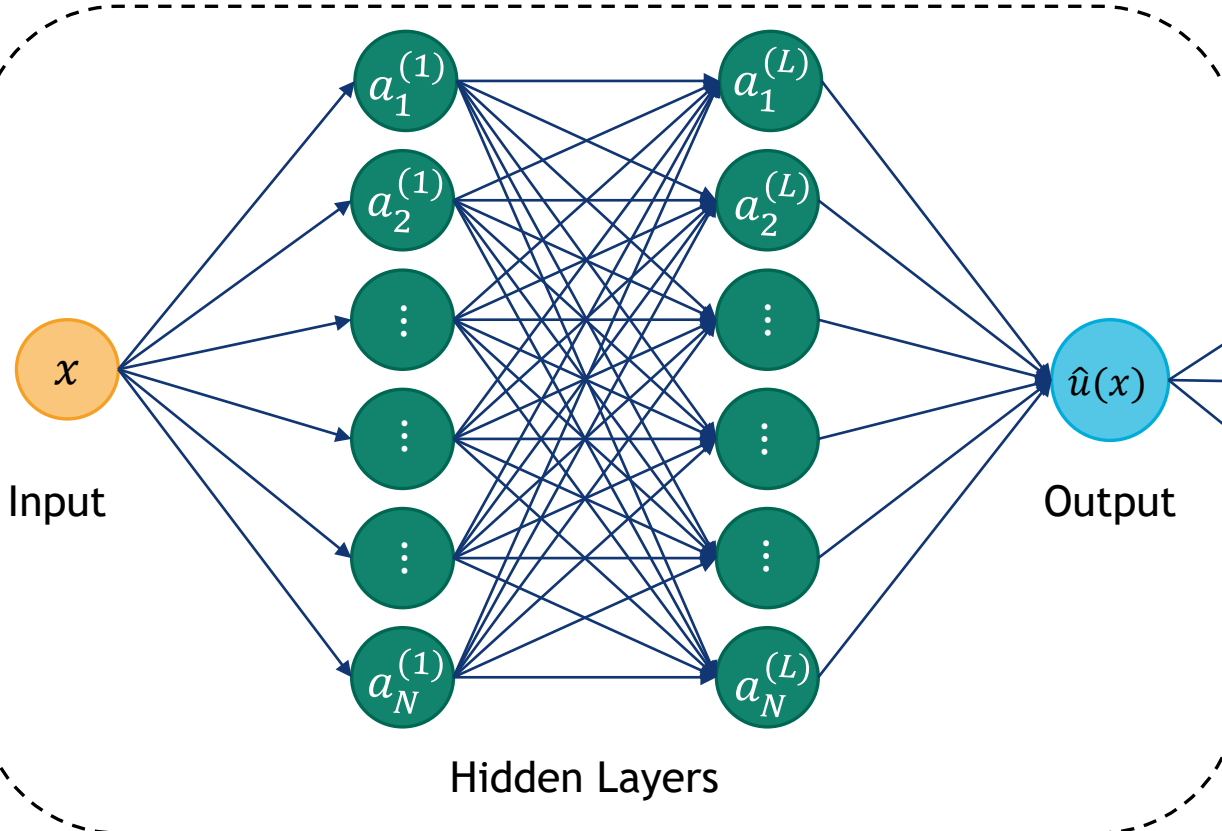


# Bonus: PINN-PINN and PINN-FOM coupling

Will Snyder  
Summer Intern  
Virginia Tech



Neural Network



*Focus thus far*

**Goal:** investigate the use of the Schwarz alternating method as a means to couple **Physics-Informed Neural Networks (PINNs)**

**Scenario 1:** use Schwarz to train subdomain PINNs (offline)

**Scenario 2:** use Schwarz to couple pre-trained subdomain PINNs/NNs (online)



## Bonus: PINN-PINN coupling

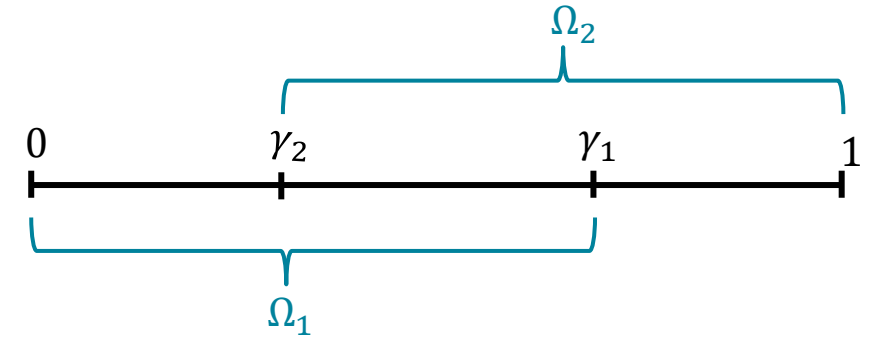


1D steady **advection-diffusion** equation on  $\Omega = [0,1]$ :

$$u_x - v u_{xx} = 1, \quad u(0) = u(1) = 0$$

PINNs are notoriously difficult to train for higher Peclet numbers!

→ *Can Schwarz help?*



Overlapping DD:  $\Omega = \Omega_1 \cup \Omega_2$  with boundary  $\partial\Omega = \{0,1\}$

### Schwarz PINN training algorithm:

**Loop** over subdomains  $\Omega_i$  until convergence of Schwarz method

**Train** PINN in  $\Omega_i$  with loss  $\mathcal{L}_i(\theta) = \alpha \mathcal{L}_{r,i}(\theta) + \beta \mathcal{L}_{b,i}(\theta) + \gamma \mathcal{L}_{d,i}(\theta)$

**Communicate** Dirichlet data between neighboring subdomains

**Update** boundary data on  $\gamma_i$  from neighboring subdomains

If **strong enforcement of Dirichlet BC (SDBC)**, set  $\hat{u}_{\Omega_i}(x, \theta) = NN_{\Omega_i}(x, \theta)$

If **weak enforcement of Dirichlet BC (WDBC)**, set  $\beta = 0$  and  $\hat{u}_{\Omega_i}(x, \theta) = v(x)NN_{\Omega_i}(x, \theta) + \psi(x)\hat{u}_{\Omega_j}(\gamma_j, \theta)$  where  $v(x)$  is chosen s.t.  $v(0) = v(\gamma_i) = v(1) = 0$  and  $\psi(x)$  is chosen s.t.  $v(\gamma_i) = 1$

$$\mathcal{L}_{r,i}(\theta) = \text{MSE}(-v \nabla_x^2 NN_{\Omega_i}(x, \theta) + \nabla_x NN_{\Omega_i}(x, \theta) - 1)$$

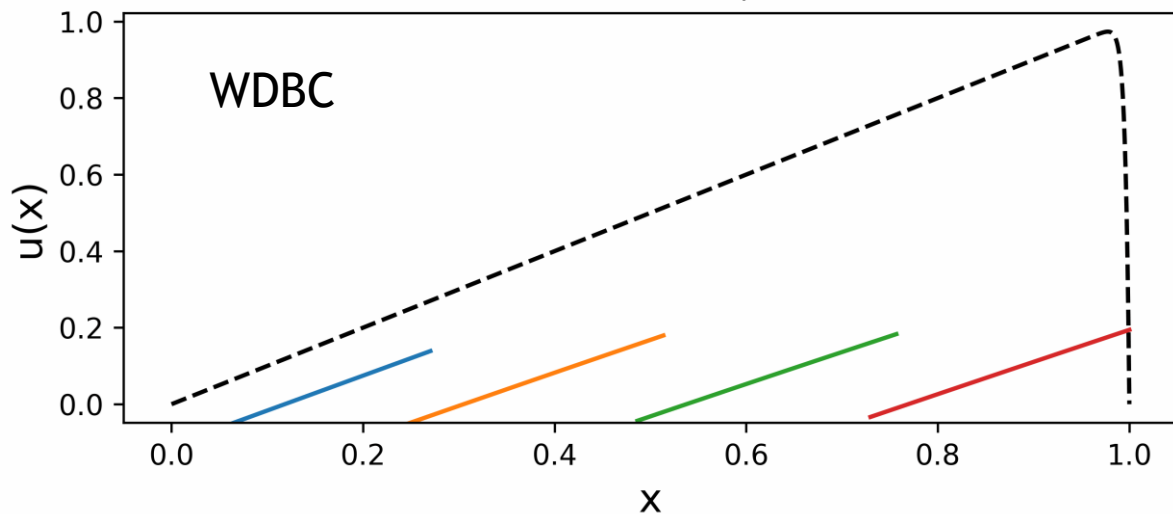
$$\mathcal{L}_{b,i}(\theta) = \text{MSE}(NN_{\Omega_i}(\partial\Omega, \theta)) + \text{MSE}(NN_{\Omega_i}(\gamma_i, \theta) - NN_{\Omega_j}(\gamma_i, \theta))$$



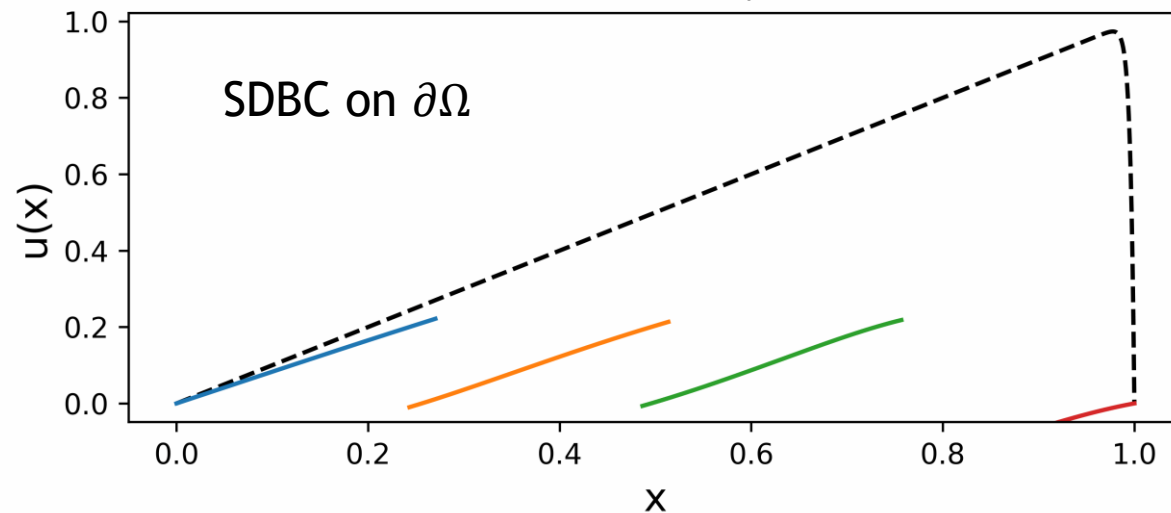
# Bonus: PINN-PINN coupling



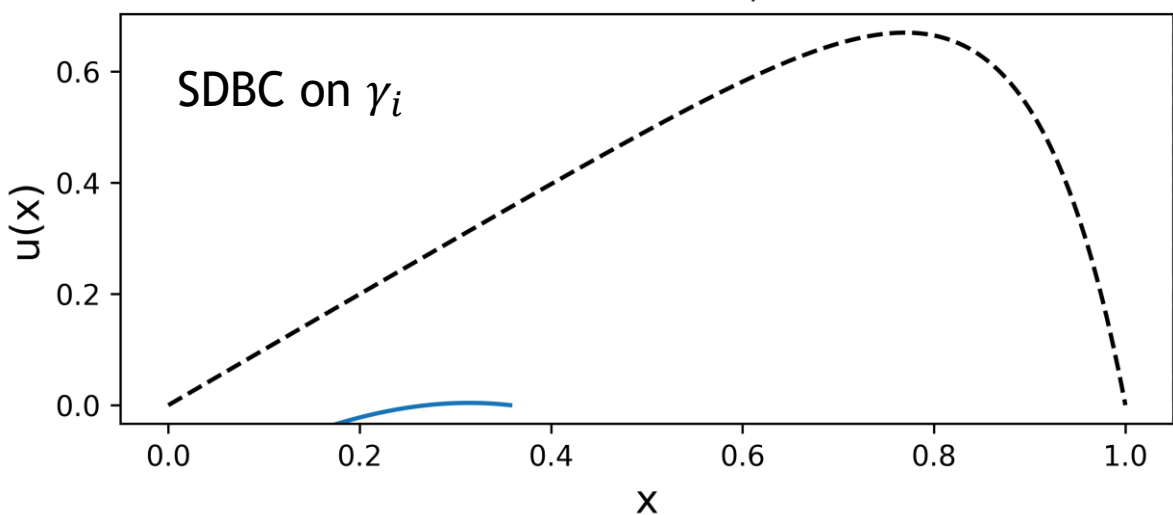
Schwarz iteration 1;  $Pe = 250$



Schwarz iteration 1;  $Pe = 250$

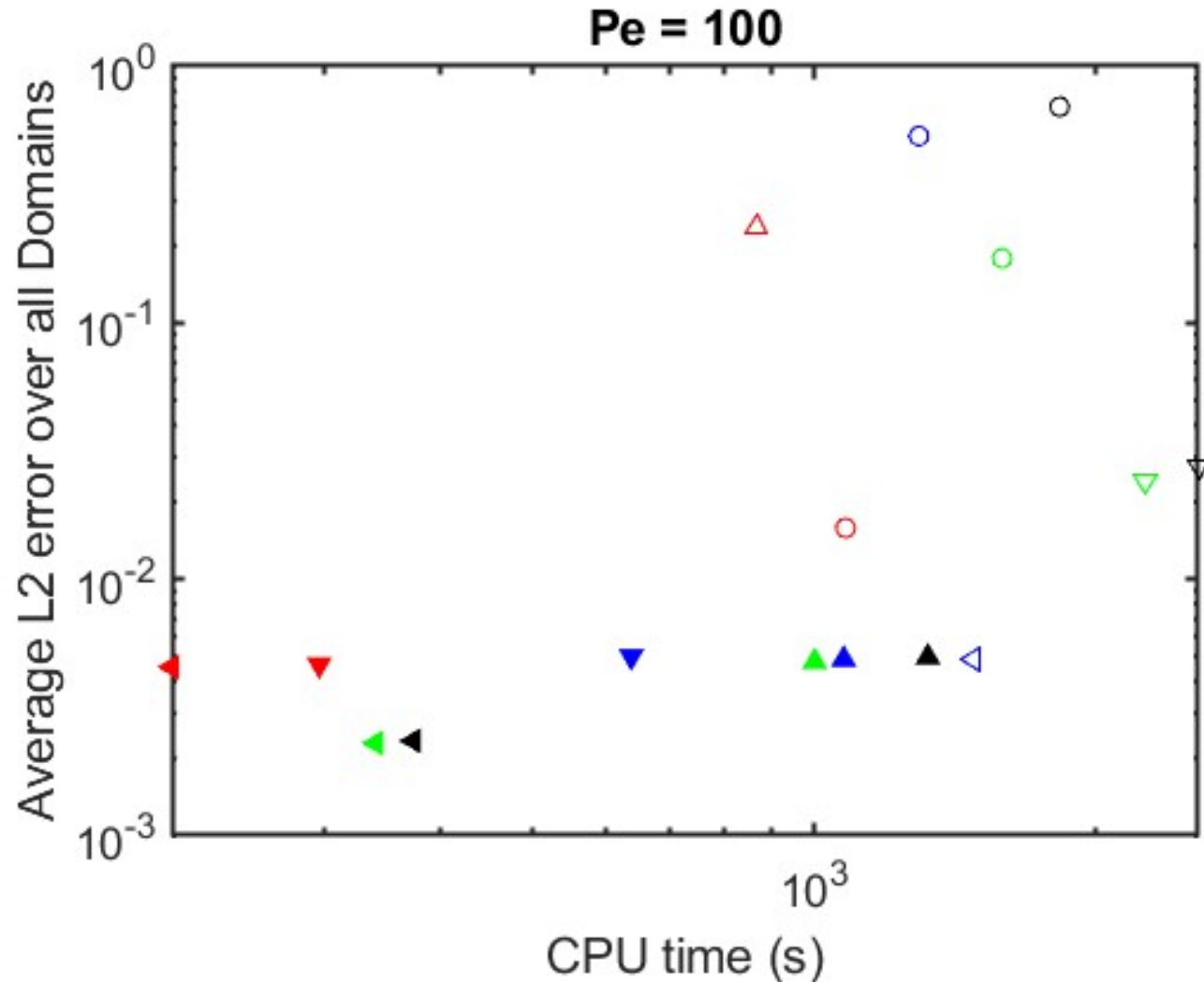


Schwarz iteration 1;  $Pe = 10$



- How **Dirichlet boundary conditions** are handled has a large impact on PINN convergence
- Convergence not improved in general with **increasing overlap**
- Increasing # **subdomains** in general will increase CPU time

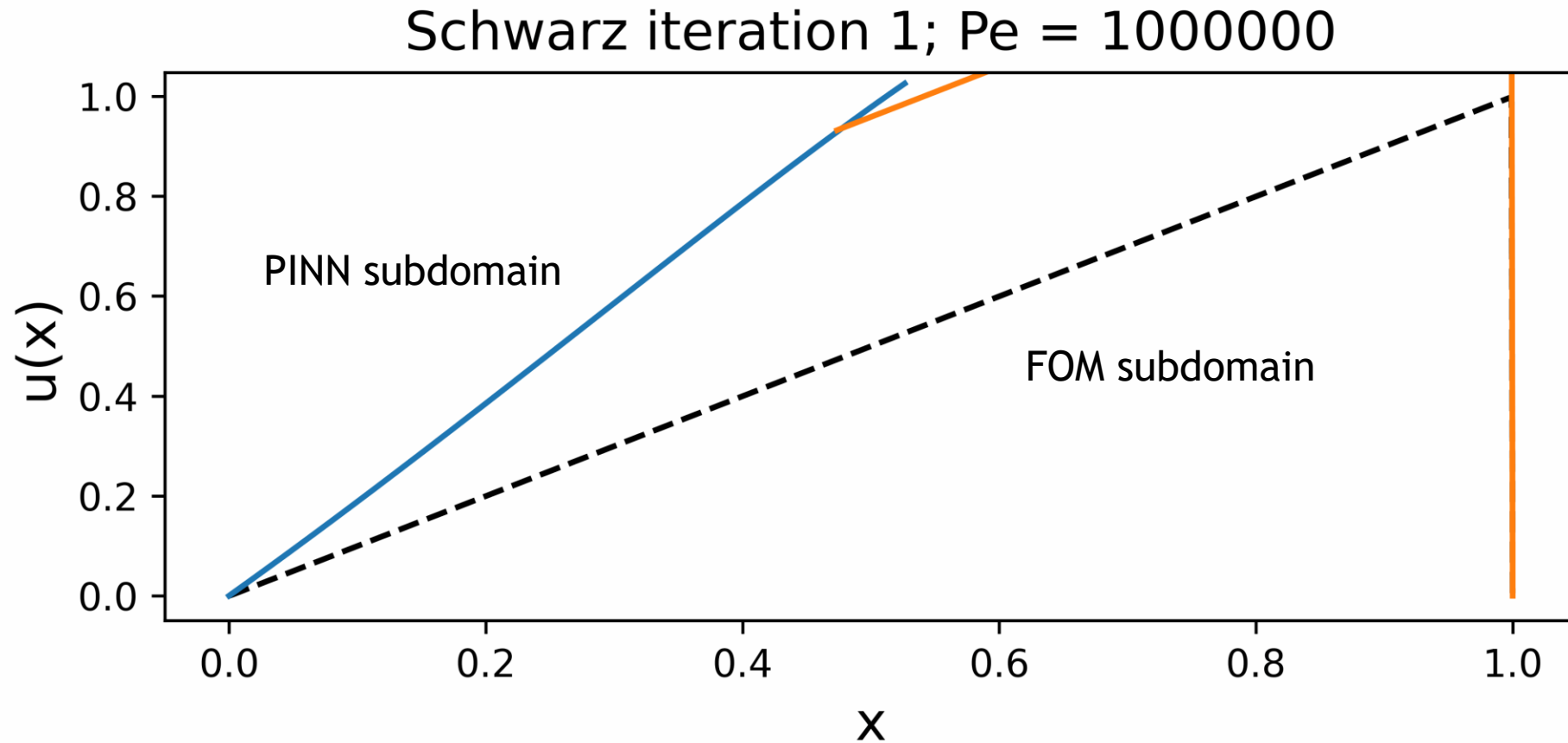




- 2  $\Omega$ , no snapshots, WDBC (unconverged)
- ▼ 2  $\Omega$ , no snapshots, SDBC
- △ 2  $\Omega$ , snapshots, WDBC (unconverged)
- ◄ 2  $\Omega$ , snapshots, SDBC
- 3  $\Omega$ , no snapshots, WDBC (unconverged)
- ▼ 3  $\Omega$ , no snapshots, SDBC
- ▲ 3  $\Omega$ , snapshots, WDBC
- ◁ 3  $\Omega$ , snapshots SDBC (unconverged)
- 4  $\Omega$ , no snapshots, WDBC (unconverged)
- ▽ 4  $\Omega$ , no snapshots, SDBC (unconverged)
- ▲ 4  $\Omega$ , snapshots, WDBC
- ◄ 4  $\Omega$ , snapshots SDBC
- 5  $\Omega$ , no snapshots, WDBC (unconverged)
- ▽ 5  $\Omega$ , no snapshots, SDBC (unconverged)
- ▲ 5  $\Omega$ , snapshots, WDBC
- ◄ 5  $\Omega$ , snapshots, SDBC

- Using **SDBC**s and **data loss** helps with PINN/NN convergence and accuracy





- PINN-FOM coupling gives **rapid PINN convergence** for **arbitrarily high Peclet numbers**
- PINN-FOM couplings works with **both WDBC and SDBC** configurations



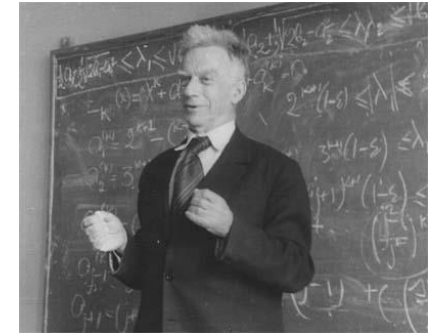
# Theoretical Foundation

Using the Schwarz alternating as a **discretization method** for PDEs is natural idea with a sound **theoretical foundation**.

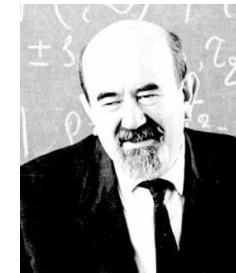
- **S.L. Sobolev (1936)**: posed Schwarz method for **linear elasticity** in variational form and **proved method's convergence** by proposing a convergent sequence of energy functionals.
- **S.G. Mikhlin (1951)**: **proved convergence** of Schwarz method for general linear elliptic PDEs.
- **P.-L. Lions (1988)**: studied convergence of Schwarz for **nonlinear monotone elliptic problems** using max principle.
- **A. Mota, I. Tezaur, C. Alleman (2017)**: proved **convergence** of the alternating Schwarz method for **finite deformation quasi-static nonlinear PDEs** (with energy functional  $\Phi[\varphi]$ ) with a **geometric convergence rate**.

$$\Phi[\varphi] = \int_B A(F, Z) dV - \int_B \mathbf{B} \cdot \boldsymbol{\varphi} dV$$

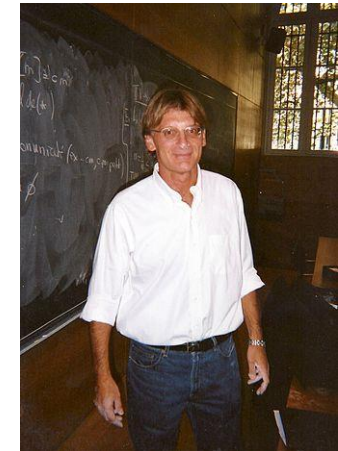
$$\nabla \cdot \mathbf{P} + \mathbf{B} = \mathbf{0}$$



S.L. Sobolev (1908 – 1989)



S.G. Mikhlin  
(1908 – 1990)



P.-L. Lions (1956-)



A. Mota, I. Tezaur, C. Alleman



# Convergence Proof\*



## 2 Formulation of the Schwarz Alternating Method

We start by defining the standard finite deformation variational formulation to establish notation before presenting the formulation of the coupling method.

### 2.1 Variational Formulation on a Single Domain

Consider a body as the open set  $\Omega \subset \mathbb{R}^2$  undergoing a motion described by the mapping  $x = \varphi(X; t) : \Omega \rightarrow \mathbb{R}^2$ ,  $X \in \Omega$ . Assume that the boundary of the body is  $\partial\Omega = \partial\Omega_D \cup \partial\Omega_N$  with unit normal  $N$ , where  $\partial\Omega_D$  is a displacement boundary,  $\partial\Omega_N$  is a traction boundary, and  $\partial\Omega_D \cap \partial\Omega_N = \emptyset$ . The prescribed boundary displacements or Dirichlet boundary conditions are  $\chi : \partial\Omega_D \rightarrow \mathbb{R}^2$ . The prescribed boundary tractions or Neumann boundary conditions are  $T : \partial\Omega_N \rightarrow \mathbb{R}^2$ . Let  $P = \text{Grad } \varphi$  be the deformation gradient. Let also  $\text{RB} : \Omega \rightarrow \mathbb{R}^2$  be the body force, with  $B$  the mass density in the reference configuration. Furthermore, introduce the energy functional

$$\Phi[\varphi] = \int_{\Omega} A(F, X) dX - \int_{\Omega} \text{RB} \cdot \varphi dV - \int_{\partial\Omega_N} T \cdot \varphi dS, \quad (1)$$

in which  $A(F, X)$  is the Helmholtz free energy density and  $X$  is a collection of internal variables. The weak form of the problem is obtained by minimizing the energy functional  $\Phi[\varphi]$  over the Sobolev space  $H^1(\Omega)$  that is comprised of all functions that are square-integrable and have square-integrable first derivatives. Define

$$S := \{\varphi \in H^1(\Omega) : \varphi = \chi \text{ on } \partial\Omega_D\} \quad (2)$$

and

$$V := \{\xi \in H^1(\Omega) : \xi = 0 \text{ on } \partial\Omega_D\} \quad (3)$$

where  $\xi \in V$  is a test function. The potential energy is minimized if and only if  $\Phi[\varphi] \leq \Phi[\varphi + \xi]$  for all  $\xi \in V$  and  $\varphi \in S$ . It is straightforward to show that the minimizer of  $\Phi[\varphi]$  in the mapping  $\varphi \in S$  that satisfies

$$D\Phi[\varphi](\xi) = \int_{\Omega} P : \text{Grad } \xi dV - \int_{\Omega} \text{RB} \cdot \xi dV - \int_{\partial\Omega_N} T \cdot \xi dS = 0, \quad (4)$$

where  $P = \partial A / \partial F$  denotes the first Piola-Kirchhoff stress. The Euler-Lagrange equation corresponding to the variational statement (4) is

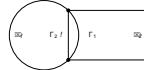


Figure 1: Two subdomains  $\Omega_1$  and  $\Omega_2$  with the corresponding boundaries  $\Gamma_1$  and  $\Gamma_2$  by the Schwarz alternating method.

that for  $i = 1$  and  $i = 2$  if  $n$  is odd, and  $i = 2$  and  $i = 1$  if  $n$  is even. Introduce the following definitions for each subdomain:

- Closure  $\bar{\Omega}_i := \Omega_i \cup \partial\Omega_i$
- Dirichlet boundary:  $\partial\Omega_i := \partial\Omega_i \cap \partial\Omega_D$
- Neumann boundary:  $\partial\Omega_i := \partial\Omega_i \cap \partial\Omega_N$
- Schwarz boundary:  $\Gamma_i := \partial\Omega_i \cap \Gamma$

Note that with these definitions we guarantee that  $\partial\Omega_1 \cap \partial\Omega_2 = \emptyset$ ;  $\partial\Omega_1 \cap \Gamma_1 = \emptyset$ ; and  $\partial\Omega_2 \cap \Gamma_2 = \emptyset$ .

Now define the spaces

$$S_i := \{\varphi \in H^1(\bar{\Omega}_i) : \varphi = \chi \text{ on } \partial\Omega_{i,D} \cup \partial\Omega_{i,N} \cup \Gamma_i\} \quad (5)$$

and

$$V_i := \{\varphi \in H^1(\bar{\Omega}_i) : \varphi = 0 \text{ on } \partial\Omega_{i,D} \cup \Gamma_i\} \quad (6)$$

where the symbol  $\partial\Omega_{i,N} \cap \Gamma_i$  denotes the projection from the subdomain  $\Omega_i$  onto the Schwarz boundary  $\Gamma_i$ . This projection operator plays a central role in the Schwarz alternating method. Its form and implementation are discussed in subsequent sections. For the moment it is sufficient to assume that the operator is able to project a field  $\varphi$  from one subdomain to the Schwarz boundary of the other subdomain.

The Schwarz alternating method solves a sequence of problems on  $\Omega_1$  and  $\Omega_2$ . The solution  $\varphi^{(n)}$  for the

$$\begin{aligned} 1. & \varphi_1^{(n)} = X_1^{(n)} \text{ in } \Omega_1, \varphi_1^{(n)} = \chi_1(X_1^{(n)}) \text{ on } \partial\Omega_{1,D}, &> \text{initiation for } \Omega_1 \\ 2. & \varphi_2^{(n)} = X_2^{(n)} \text{ in } \Omega_2, \varphi_2^{(n)} = \chi_2(X_2^{(n)}) \text{ on } \partial\Omega_{2,D}, &> \text{initiation for } \Omega_2 \\ 3. & \text{repeat} &> \text{Newton-Schwarz loop} \\ 4. & \begin{cases} \varphi_1^{(n+1)} = \left( K_{11}^{(n)} + K_{12}^{(n)} H_{21} \right) \begin{pmatrix} \varphi_2^{(n)} \\ H_{21} \varphi_2^{(n)} \end{pmatrix} \\ \varphi_2^{(n+1)} = \left( K_{21}^{(n)} + K_{22}^{(n)} H_{12} \right) \begin{pmatrix} \varphi_1^{(n)} \\ H_{12} \varphi_1^{(n)} \end{pmatrix} \end{cases} &> \text{linear system} \\ 5. & \varphi_1^{(n+1)} = \varphi_1^{(n)} + \Delta\varphi_1^{(n)} \\ 6. & \varphi_2^{(n+1)} = \varphi_2^{(n)} + \Delta\varphi_2^{(n)} \\ 7. & \text{until } \left\| \left( \left\| \varphi_1^{(n+1)} - \varphi_1^{(n)} \right\| \right)^2 + \left( \left\| \varphi_2^{(n+1)} - \varphi_2^{(n)} \right\| \right)^2 \right\|^{1/2} \leq \epsilon_{\text{tolerance}} &> \text{stop criterion} \end{aligned}$$

Algorithm 1: Illustrative Schwarz Method

[15], [16], [1]. Although we do not provide here formal convergence proofs for the remaining variants of the Schwarz method, we offer some numerical results illustrating their convergence in Section 4.

Consider the energy functional  $\Phi[\varphi]$  defined in (1). We will denote by  $(\cdot, \cdot)$  the usual  $L^2$  inner product over  $\Omega$ , that is,

$$(\psi_1, \psi_2) := \int_{\Omega} \psi_1 \cdot \psi_2 dV, \quad (35)$$

for  $\psi_1, \psi_2 \in W_0^{1,2}(\Omega)$ , with corresponding norm  $\|\cdot\|$ . The proof of the convergence of the Schwarz alternating method requires that the functional  $\Phi[\varphi]$  satisfy the following properties over the space  $S$  defined in (2):

1.  $\Phi[\varphi]$  is coercive.
2.  $\Phi[\varphi]$  is Fréchet differentiable, with  $\Phi'[\varphi]$  denoting its Fréchet derivative.
3.  $\Phi[\varphi]$  is strictly convex.
4.  $\Phi[\varphi]$  is lower semi-continuous.
5.  $\Phi'[\varphi]$  is uniformly continuous on  $K_n$ , where

$$K_n := \{\varphi \in S : \Phi[\varphi] \leq B, B \in \mathbb{R}, B < \infty\}. \quad (36)$$

It can be shown that the energy functional  $\Phi[\varphi]$  defined in (1) is strictly convex in  $S$  (property 3) provided that the Helmholtz energy density  $A(F, X)$  is a convex function of  $F$  and  $X$  (see, e.g., [15], [16], [1]).

**Theorem 1.** Assume that the energy functional  $\Phi[\varphi]$  satisfies properties 1–5 above. Consider the Schwarz alternating method of Section 2 defined by (9)–(13) and its equivalent form (39). Then

- (a)  $\Phi[\tilde{\varphi}^{(0)}] \geq \Phi[\tilde{\varphi}^{(1)}] \geq \dots \geq \Phi[\tilde{\varphi}^{(n-1)}] \geq \Phi[\tilde{\varphi}^{(n)}] \geq \dots \geq \Phi[\varphi]$ , where  $\varphi$  is the minimizer of  $\Phi[\varphi]$  over  $S$ .
- (b) The sequence  $\{\tilde{\varphi}^{(n)}\}$  defined in (39) converges to the minimizer  $\varphi$  of  $\Phi[\varphi]$  in  $S$ .
- (c) The Schwarz minimum values  $\Phi[\tilde{\varphi}^{(n)}]$  converge monotonically to the minimum value  $\Phi[\varphi]$  in  $S$  starting from any initial guess  $\tilde{\varphi}^{(0)}$ .

**Remark 1** By the coercivity of  $\Phi[\varphi]$ , it follows from the Lax-Milgram theorem that a unique minimizer to the functional over  $S$  exists, i.e., the minimization of  $\Phi[\varphi]$  is well-posed.

**Remark 2** By the Stampacchia theorem, the minimization of  $\Phi[\varphi]$  in  $S$  is equivalent to finding  $\varphi \in S$  such that

$$(\Phi'[\varphi], \xi - \varphi) \geq 0 \quad (37)$$

for all  $\xi \in S$ .

**Remark 3** Recall that the strict convexity property of  $\Phi[\varphi]$  can be written as

$$\Phi[\psi_1] - \Phi[\psi_2] - (\Phi'[\psi_2], \psi_1 - \psi_2) \geq 0, \quad (38)$$

for  $\psi_1, \psi_2 \in S$ . From (36), remark that if  $\Phi[\varphi]$  is strictly convex over  $S \cap B \subset B$  such that  $B < \infty$ , we can find an  $\alpha_B > 0$  such that  $\forall \psi_1, \psi_2 \in K_B$  we have

$$\Phi[\psi_1] - \Phi[\psi_2] - (\Phi'[\psi_2], \psi_1 - \psi_2) \geq \alpha_B \|\psi_1 - \psi_2\|^2. \quad (39)$$

**Remark 4** By property 5, the uniform continuity of  $\Phi'[\varphi]$ , there exists a modulus of continuity  $\omega > 0$ , with  $\omega : K_B \rightarrow K_B$ , such that

$$\|\Phi'[\varphi_1] - \Phi'[\varphi_2]\| \leq \omega(\|\varphi_1 - \varphi_2\|). \quad (40)$$

for  $\varphi_1, \varphi_2 \in K_B$ . By definition,  $\omega(t) \rightarrow 0$  as  $t \rightarrow 0$ .

**Remark 5** It was shown in [15] that in the case  $\Omega_1 \cap \Omega_2 \neq \emptyset$ ,  $\forall \varphi \in S$ , there exist  $\zeta_1 \in \partial\Omega_1$  and  $\zeta_2 \in \partial\Omega_2$  such that

$$\varphi = \zeta_1 + \zeta_2. \quad (41)$$

and

$$\max\{\|\zeta_1\|, \|\zeta_2\|\} \leq C_0 \|\varphi\|, \quad (42)$$

for some  $C_0 > 0$  independent of  $\varphi$ .

**Remark 6** Note that (39) can be written as

$$(\Phi'[\varphi^{(n)}], \varphi^{(n)} - \varphi) = 0, \quad \text{for } \varphi^{(n)} \in \tilde{S}_n, \varphi^{(n)} \in S, \quad (43)$$

for  $n \in \{1, 2, 3, \dots\}$  and  $\alpha \in \{0, 1, 2, \dots\}$  (recall from (6) the relation between  $n$  and  $\alpha$ ). This is due to the uniqueness of the solution to each minimization problem over  $S$ , and the definition of  $\varphi^{(n)}$  as the minimizer of  $\Phi[\varphi]$  over  $\tilde{S}_n$ .

**Remark 7** Let  $\varphi^{(n)} \in \tilde{S}_n$  and let  $\xi \in S$ . By Remark 5, there exist  $\zeta_1 \in \partial\Omega_1$  and  $\zeta_2 \in \partial\Omega_2$  such that

$$(\Phi'[\varphi^{(n)}], \xi) - (\Phi'[\varphi^{(n)}], \zeta_1 + \zeta_2) = 0. \quad (44)$$

Again using (37) and also (39) one finds

$$(\Phi'[\varphi^{(n)}], \Phi'[\varphi^{(n)}] - \zeta_1) = (\Phi'[\varphi^{(n)}], \xi) \leq \|(\Phi'[\varphi^{(n)}] - \Phi'[\varphi^{(n)}])\| \cdot \|\zeta_1\|, \quad (45)$$

and substituting (45) into (41) we finally obtain that

$$(\Phi'[\varphi^{(n)}], \xi) \leq C_0 \|\Phi'[\varphi^{(n)}] - \Phi'[\varphi^{(n)}]\| \cdot \|\xi\|, \quad (46)$$

$\forall \xi \in S$ .

**Remark 8** For part (a) of Theorem 1, recall the definition of geometric convexity:

$$K_{n+1} \subseteq CK_n, \quad (47)$$

$\forall n \in \{0, 1, 2, \dots\}$  for some  $C > 0$ , where

$$K_n := \{\varphi^{(n+1)} - \varphi^{(n)}\}. \quad (48)$$

**Remark 9** Recall from the definition of continuity that if  $\Phi'[\varphi]$  is Lipschitz continuous at  $\varphi^{(n)}$  near  $\varphi$ , then there exists a constant  $K > 0$  such that

$$\|\Phi'[\varphi^{(n)}] - \Phi'[\varphi]\| \leq K, \quad (49)$$

Considering that  $\Phi'[\varphi] = 0$  since  $\varphi$  is the minimizer of  $\Phi[\varphi]$ , (49) is equivalent to

$$\|\Phi'[\varphi^{(n)}]\| \leq K \|\varphi^{(n)} - \varphi\|. \quad (50)$$

### Proof of Theorem 1

**Proof of (a).** Let  $\varphi^{(0)} := \arg \min_{\varphi \in \tilde{S}_0} \Phi[\varphi]$ . By (40),  $\varphi^{(0)} \in \tilde{S}_0$ . Let  $\varphi^*$  be the minimizer of  $\Phi[\varphi]$  over  $S$  and suppose  $\Phi[\varphi^*] > \Phi[\varphi^{(0)}]$ . But this is a contradiction, since we can take  $\varphi^* = \varphi^{(0)}$ . Hence, it cannot be that  $\Phi[\varphi^{(0)}] < \Phi[\varphi^*]$  where  $\varphi^* = \arg \min_{\varphi \in S} \Phi[\varphi]$ . It follows by induction that

$$\Phi[\varphi^{(n)}] \leq \Phi[\varphi^{(n-1)}] \quad (51)$$

for  $n \in \{1, 2, 3, \dots\}$ . Now let  $\varphi$  be the minimizer of  $\Phi[\varphi]$  over  $S$ . Since the problem is well-posed  $\varphi$  is unique. Hence  $\Phi[\varphi] \leq \Phi[\varphi^{(n)}]$  for all  $n \in \{1, 2, 3, \dots\}$ .  $\square$

$$\lim_{n \rightarrow \infty} \|\varphi^{(n)} - \varphi^{(n-1)}\| = 0. \quad (52)$$

from which we can conclude that  $\varphi^{(n)} - \varphi^{(n-1)} \rightarrow 0$  as  $n \rightarrow \infty$ .

We must now show that  $\varphi^{(n)}$  converges to  $\varphi$ , the minimizer of  $\Phi[\varphi]$  on  $S$ . By (51) with  $\psi_1 = \varphi$  and  $\psi_2 = \varphi^{(n)}$ , we have

$$\|\varphi - \varphi^{(n)}\|^2 \leq \frac{1}{\alpha_B} \left( \Phi[\varphi] - \Phi[\varphi^{(n)}] - (\Phi'[\varphi^{(n)}], \varphi - \varphi^{(n)}) \right). \quad (53)$$

Since  $\varphi$  is the minimum of  $\Phi[\varphi]$ , by (a) we have that  $\Phi[\varphi] \leq \Phi[\varphi^{(n)}]$ . It follows that

$$\Phi[\varphi] - \Phi[\varphi^{(n)}] - (\Phi'[\varphi^{(n)}], \varphi - \varphi^{(n)}) \leq - \left( \Phi'[\varphi^{(n)}], \varphi - \varphi^{(n)} \right) = (\Phi'[\varphi^{(n)}], \varphi^{(n)} - \varphi). \quad (54)$$

Substituting (54) into (53) we have

$$\|\varphi - \varphi^{(n)}\|^2 \leq \frac{1}{\alpha_B} (\Phi'[\varphi^{(n)}], \varphi^{(n)} - \varphi). \quad (55)$$

Now by (42) Remark 7,

$$(\Phi'[\varphi^{(n)}], \varphi^{(n)} - \varphi) \leq C_0 \|\Phi'[\varphi^{(n)}] - \Phi'[\varphi^{(n)}]\| \cdot \|\varphi^{(n)} - \varphi\|. \quad (56)$$

Substituting (56) into (55) leads to

$$\|\varphi^{(n)} - \varphi\| \leq \frac{C_0}{\alpha_B} \|\Phi'[\varphi^{(n)}] - \Phi'[\varphi^{(n)}]\|. \quad (57)$$

Applying the uniform continuity assumption (50), we obtain

$$\|\varphi^{(n)} - \varphi\| \leq \frac{C_0}{\alpha_B} \left( \|\varphi^{(n)} - \varphi\| \right). \quad (58)$$

By (58),  $\|\varphi^{(n)} - \varphi\| = 0$  as  $n \rightarrow \infty$ . From this we obtain the result, namely that  $\varphi^{(n)} \rightarrow \varphi$  in  $S$ .

**Proof of (b).** This follows immediately from (a) and (58).

**Proof of (c).** By (b), for large enough  $n$ , there exists some  $C_1 > 0$  independent of  $n$  such that

$$\|\varphi^{(n)} - \varphi\| \leq C_1 \|\varphi^{(n-1)} - \varphi^{(n-2)}\|. \quad (59)$$

for  $n \in \{1, 2, 3, \dots\}$ . Now let  $\varphi$  be the minimizer of  $\Phi[\varphi]$  over  $S$ . Since the problem is well-posed  $\varphi$  is unique. Hence  $\Phi[\varphi] \leq \Phi[\varphi^{(n)}]$  for all  $n \in \{1, 2, 3, \dots\}$ .  $\square$

Let us choose  $C_1$  such that  $C_1 > \alpha_B/K$ , where  $K$  is the Lipschitz continuity constant in (50). Combining (59) with (50) leads to

$$\frac{1}{\alpha_B} (\Phi'[\varphi^{(n)}], \varphi^{(n)} - \varphi) \geq \|\varphi^{(n-1)} - \varphi^{(n)}\|^2 \geq \frac{1}{\alpha_B} \|\varphi^{(n)} - \varphi\|^2. \quad (60)$$

Remark that [50]

$$\tilde{S}_n = \varphi^{(n-1)} + \tilde{V}_n \quad \text{for } \varphi^{(n-1)} \in \tilde{S}_{n-1} \Rightarrow \varphi^{(n-1)} \in \tilde{S}_n. \quad (61)$$

**Theorem 1.** Assume that the energy functional  $\Phi[\varphi]$  satisfies properties 1–5 above. Consider the Schwarz alternating method of Section 2 defined by (9)–(13) and its equivalent form (39). Then

(a)  $\Phi[\tilde{\varphi}^{(0)}] \geq \Phi[\tilde{\varphi}^{(1)}] \geq \dots \geq \Phi[\tilde{\varphi}^{(n-1)}] \geq \Phi[\tilde{\varphi}^{(n)}] \geq \dots \geq \Phi[\varphi]$ , where  $\varphi$  is the minimizer of  $\Phi[\varphi]$  over  $S$ .

(b) The sequence  $\{\tilde{\varphi}^{(n)}\}$  defined in (39) converges to the minimizer  $\varphi$  of  $\Phi[\varphi]$  in  $S$ .

(c) The Schwarz minimum values  $\Phi[\tilde{\varphi}^{(n)}]$  converge monotonically to the minimum value  $\Phi[\varphi]$  in  $S$  starting from any initial guess  $\tilde{\varphi}^{(0)}$ .

(d) If  $\Phi'[\varphi]$  is Lipschitz continuous in a neighborhood of  $\varphi$ , then the sequence  $\{\varphi^{(n)}\}$  converges geometrically to the minimizer  $\varphi$ .  $\square$

**Proof.** See Appendix A.  $\square$

Finally, while most of works cited above present their analysis for the specific case of two subdomains, extension to multiple subdomains is a general straightforward. The case of multiple subdomains is considered specifically in Lions [15], Badoia [14], and Li-Shun and Evans [14].

**4 Numerical Examples**

In this section, we present numerical examples of the behavior of the Schwarz alternating method for two different implementations. First, we briefly describe the two implementations, one in MATLAB and the other in the open-source software FEniCS (code [17]). Next, we discuss the error estimates used throughout the numerical examples. Then, we continue with four examples that demonstrate different features of the Schwarz alternating method and our implementation. The first example, a one-dimensional singular bar, is used to demonstrate the behavior of the four Schwarz variants of Section 2.4. The second example, a cuboid body of square base, aims to study the effect of the size of the overlap region on the convergence of the method. The objective of the third example is a method to find, in a single step, the numerical error in the results and to demonstrate the ability of the method to couple different element topologies. The last example is a bar

under a point load. The objective of the fourth example is to study the effect of the size of the overlap region on the convergence of the method. The objective of the fifth example is a method to find, in a single step, the numerical error in the results and to demonstrate the ability of the method to couple different element topologies. The last example is a bar

under a point load. The objective of the fifth example is a method to find, in a single step, the numerical error in the results and to demonstrate the ability of the method to couple different element topologies. The last example is a bar

under a point load. The objective of the fifth example is a method to find, in a single step, the numerical error in the results and to demonstrate the ability of the method to couple different element topologies. The last example is a bar

under a point load. The objective of the fifth example is a method to find, in a single step, the numerical error in the results and to demonstrate the ability of the method to couple different element topologies. The last example is a bar

under a point load. The objective of the fifth example is a method to find, in a single step, the numerical error in the results and to demonstrate the ability of the method to couple different element topologies. The last example is a bar

under a point load. The objective of the fifth example is a method to find, in a single step, the numerical error in the results and to demonstrate the ability of the method to couple different element topologies. The last example is a bar

under a point load. The objective of the fifth example is a method to find, in a single step, the numerical error in the results and to demonstrate the ability of the method to couple different element topologies. The last example is a bar

under a point load. The objective of the fifth example is a method to find, in a single step, the numerical error in the results and to demonstrate the ability of the method to couple different element topologies. The last example is a bar

under a point load. The objective of the fifth example is a method to find, in a single step, the numerical error in the results and to demonstrate the ability of the method to couple different element topologies. The last example is a bar

under a point load. The objective of the fifth example is a method to find, in a single step, the numerical error in the results and to demonstrate the ability of the method to couple different element topologies. The last example is a bar

under a point load. The objective of the fifth example is a method to find, in a single step, the numerical error in the results and to demonstrate the ability of the method to couple different element topologies. The last example is a bar

under a point load. The objective of the fifth example is a method to find, in a single step, the numerical error in the results and to demonstrate the ability of the method to couple different element topologies. The last example is a bar

under a point load. The objective of the fifth example is a method to find, in a single step, the numerical error in the results and to demonstrate the ability of the method to couple different element topologies. The last example is





- Like for quasistatics, dynamic alternating Schwarz method converges provided each single-domain problem is **well-posed** and **overlap region** is **non-empty**, under some **conditions** on  $\Delta t$ .
- **Well-posedness** for the dynamic problem requires that action functional  $S[\boldsymbol{\varphi}] := \int_I \int_{\Omega} L(\boldsymbol{\varphi}, \dot{\boldsymbol{\varphi}}) dV dt$  be **strictly convex** or **strictly concave**, where  $L(\boldsymbol{\varphi}, \dot{\boldsymbol{\varphi}}) := T(\dot{\boldsymbol{\varphi}}) + V(\boldsymbol{\varphi})$  is the Lagrangian.
  - This is studied by looking at its second variation  $\delta^2 S[\boldsymbol{\varphi}_h]$
- We can show assuming a **Newmark** time-integration scheme that for the **fully-discrete** problem:

$$\delta^2 S[\boldsymbol{\varphi}_h] = \mathbf{x}^T \left[ \frac{\gamma^2}{(\beta \Delta t)^2} \mathbf{M} - \mathbf{K} \right] \mathbf{x}$$

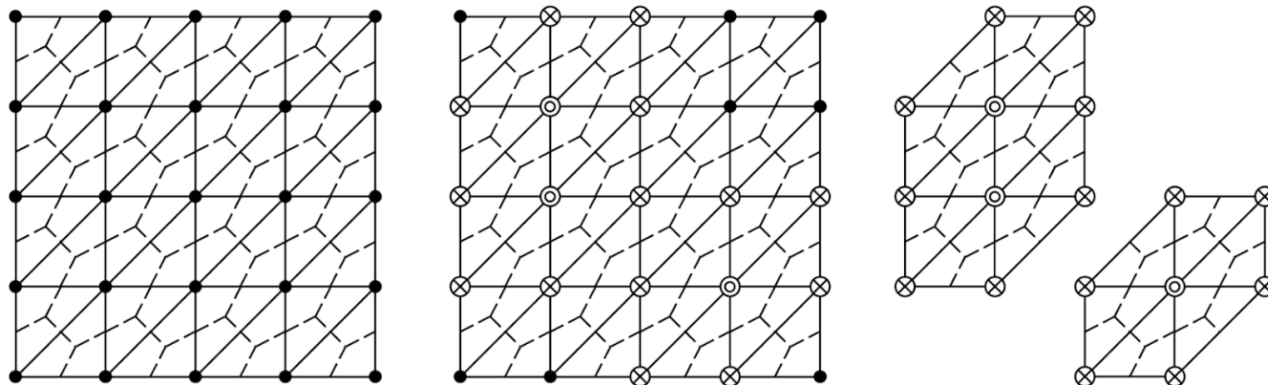
- $\delta^2 S[\boldsymbol{\varphi}_h]$  can always be made positive by choosing a **sufficiently small**  $\Delta t$
- Numerical experiments reveal that  $\Delta t$  requirements for **stability/accuracy** typically lead to automatic satisfaction of this bound.



- **Project-then-approximate** paradigm (as opposed to approximate-then-project)

$$\begin{aligned} r_k(q_k, t) &= W^T r(\tilde{u}, t) \\ &= \sum_{e \in \mathcal{E}} W^T L_e^T r_e(L_{e+} \tilde{u}, t) \end{aligned}$$

- $L_e \in \{0,1\}^{d_e \times N}$  where  $d_e$  is the **number of degrees of freedom** associated with each mesh element (this is in the context of meshes used in first-order hyperbolic problems where there are  $N_e$  mesh elements)
- $L_{e+} \in \{0,1\}^{d_e \times N}$  selects degrees of freedom necessary for **flux reconstruction**
- Equality can be **relaxed**



Augmented reduced mesh:  $\odot$  represents a selected node attached to a selected element; and  $\otimes$  represents an added node to enable the full representation of the computational stencil at the selected node/element



# ECSW: Generating the Reduced Mesh and Weights



- Using a subset of the same snapshots  $u_i, i \in 1, \dots, n_h$  used to generate the **state basis**  $V$ , we can train the reduced mesh
- Snapshots are first **projected** onto their associated basis and then **reconstructed**

$$c_{se} = W^T L_e^T r_e \left( L_e + \left( u_{ref} + V V^T (u_s - u_{ref}) \right), t \right) \in \mathbb{R}^n$$

$$d_s = r_k(\tilde{u}, t) \in \mathbb{R}^n, \quad s = 1, \dots, n_h$$

- We can then form the **system**

$$\mathbf{C} = \begin{pmatrix} c_{11} & \dots & c_{1N_e} \\ \vdots & \ddots & \vdots \\ c_{n_h 1} & \dots & c_{n_h N_e} \end{pmatrix}, \quad \mathbf{d} = \begin{pmatrix} d_1 \\ \vdots \\ d_{n_h} \end{pmatrix}$$

- Where  $\mathbf{C}\xi = \mathbf{d}, \xi \in \mathbb{R}^{N_e}, \xi = \mathbf{1}$  must be the solution
- Further relax the equality to yield **non-negative least-squares problem**:

$$\xi = \arg \min_{x \in \mathbb{R}^n} \|\mathbf{C}x - \mathbf{d}\|_2 \text{ subject to } x \geq \mathbf{0}$$

- Solve the above optimization problem using a **non-negative least squares solver** with an **early termination condition** to **promote sparsity** of the vector  $\xi$





Key idea behind OpInf: circumvent the burden of implementing intrusive ROMs in HPC codes by combining projection-based ROM and machine learning (ML).

- Start with a physics-based FOM that can be written to have a specific structure, e.g., quadratic structure:

$$\dot{\mathbf{q}} + \mathbf{A}\mathbf{q} + \mathbf{H}(\mathbf{q} \times \mathbf{q}) = \mathbf{0}$$

- Use lens of projection to define the functional form of a ROM for (1):

$$\dot{\hat{\mathbf{q}}} + \hat{\mathbf{A}}\hat{\mathbf{q}} + \hat{\mathbf{H}}(\hat{\mathbf{q}} \otimes \hat{\mathbf{q}}) = \mathbf{0}$$

- Learn ROM operators in (2) from FOM data by solving the following least-squares minimization problem:

$$\min_{\hat{\mathbf{A}}, \hat{\mathbf{H}}} \left\| \dot{\hat{\mathbf{Q}}}^T + \hat{\mathbf{Q}}^T \hat{\mathbf{A}}^T + (\hat{\mathbf{Q}} \otimes \hat{\mathbf{Q}})^T \hat{\mathbf{H}}^T \right\|_F^2$$

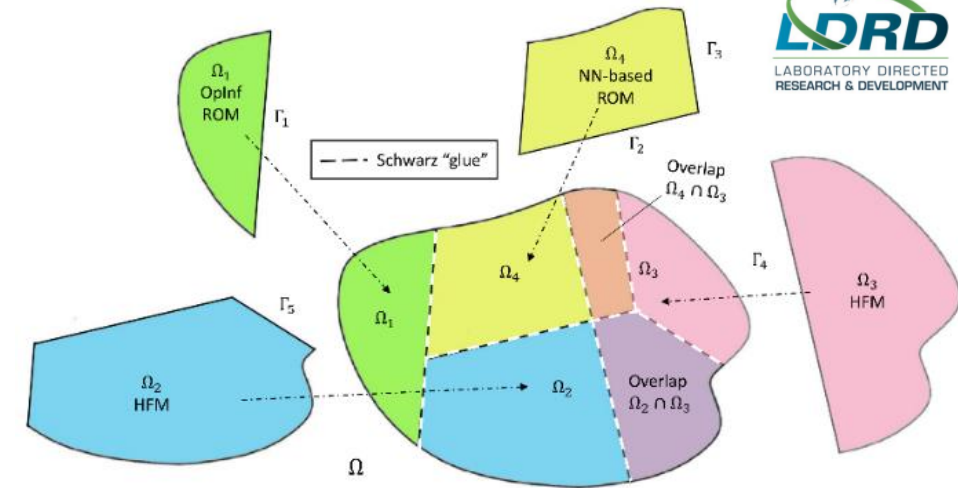
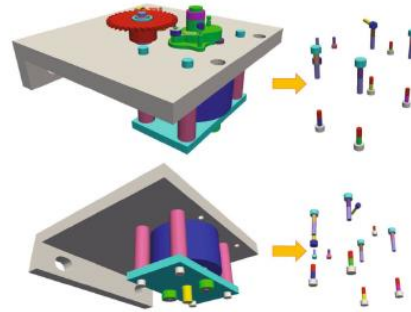


# New Project: Adaptive Hybrid modElS via domAin Decomposition (AHEAD)

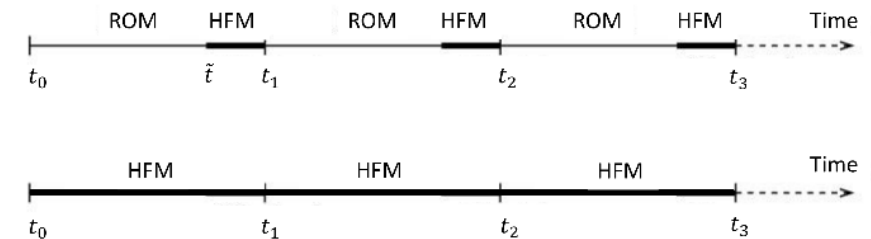
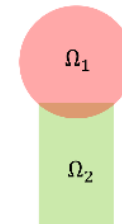
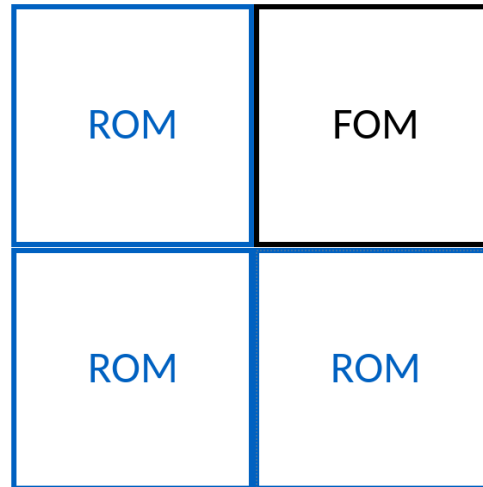
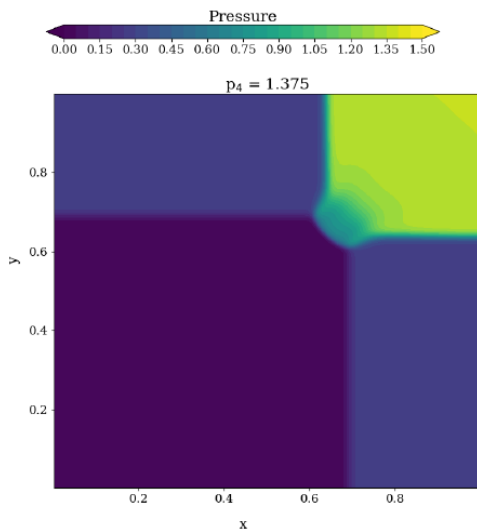


## Goals (for solid mechanics exemplars):

- Simplify meshing via Schwarz + DD
- Extend Schwarz to **non-intrusive ROMs** (Operator Inference, NN)
- Development of **automated criteria** to determine appropriate use of less refined or reduced-order models without sacrificing accuracy, enabling **real-time transitions** between different model fidelities



Example sample DD and ROM/FOM assignment.



On-the-fly model switching in our DD workflow.

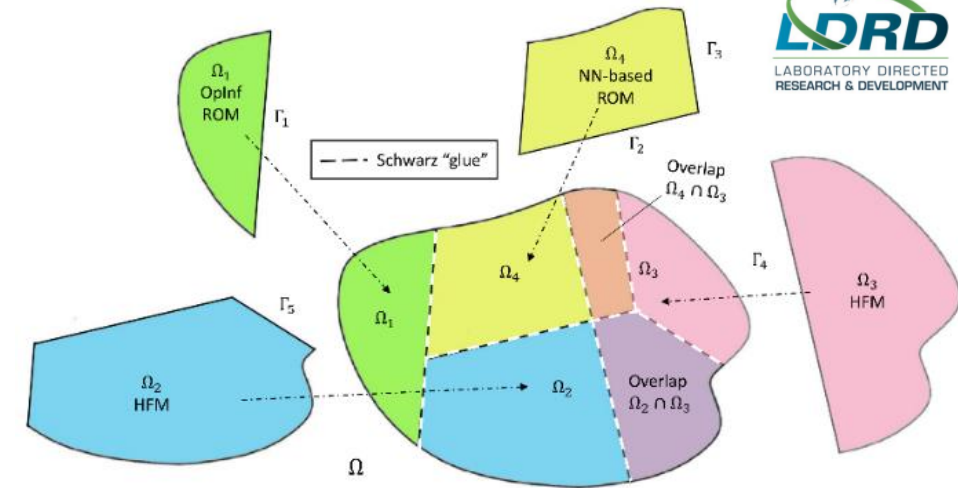
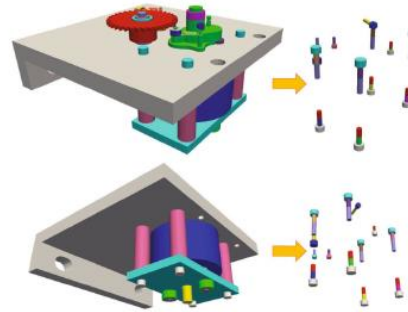


# New Project: Adaptive Hybrid modElS via domAin Decomposition (AHEAD)

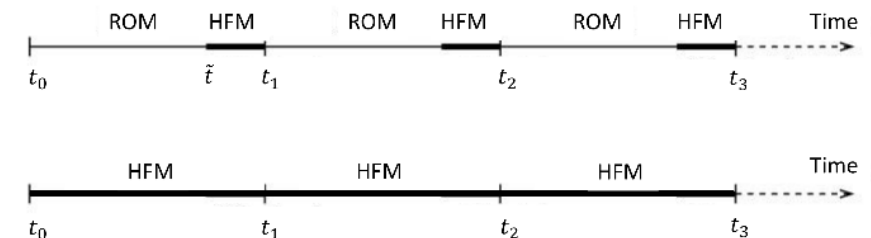
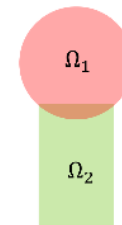
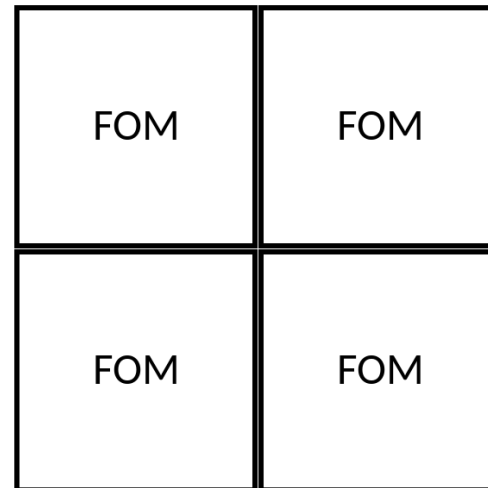
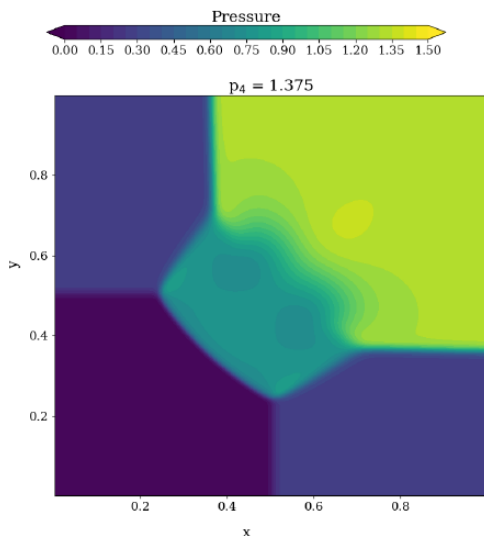


## Goals (for solid mechanics exemplars):

- Simplify meshing via Schwarz + DD
- Extend Schwarz to **non-intrusive ROMs** (Operator Inference, NN)
- Development of **automated criteria** to determine appropriate use of less refined or reduced-order models without sacrificing accuracy, enabling **real-time transitions** between different model fidelities



Example sample DD and ROM/FOM assignment.



On-the-fly model switching in our DD workflow.

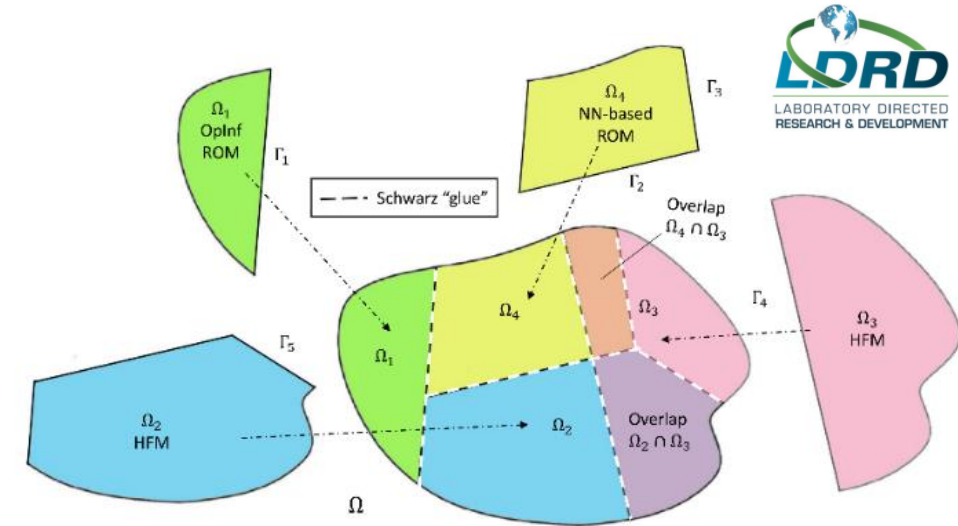
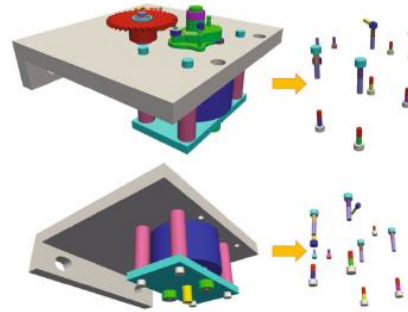


# New Project: Adaptive Hybrid modElS via domAin Decomposition (AHEAD)

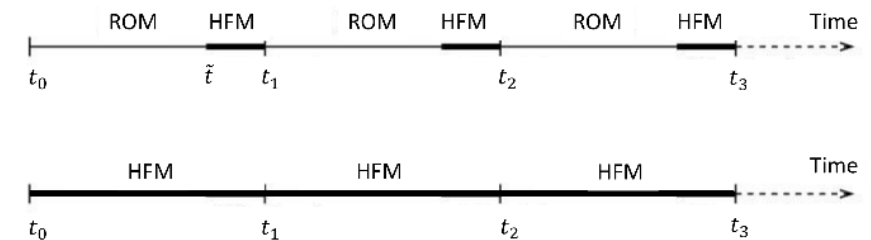
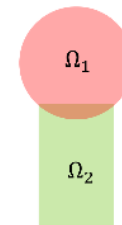
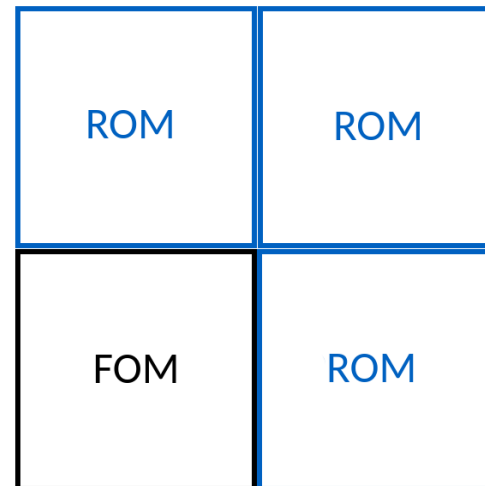
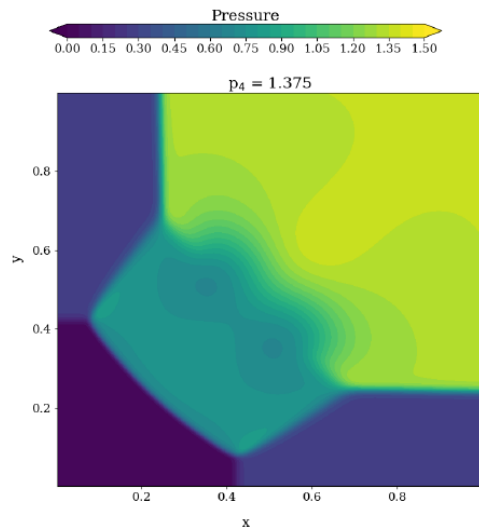


## Goals (for solid mechanics exemplars):

- Simplify meshing via Schwarz + DD
- Extend Schwarz to **non-intrusive ROMs** (Operator Inference, NN)
- Development of **automated criteria** to determine appropriate use of less refined or reduced-order models without sacrificing accuracy, enabling **real-time transitions** between different model fidelities



Example sample DD and ROM/FOM assignment.



On-the-fly model switching in our DD workflow.



# 1D Linear Elastic Wave Propagation in a Clamped Beam



- **1D linear elastic beam** geometry  $\Omega = (-0.5, 0.5)$ , clamped at both ends, with prescribed initial condition,  $\Delta x = 1 \times 10^{-3}$ ,  $\Delta t = 1 \times 10^{-7}$ ,  $T_{max} = 1 \times 10^{-3}$  and  $\nu = 0$ .
- Very **stringent test** for discretization/coupling methods and ROMs.
- **Overlapping DD**:  $\Omega_1 = (-0.5, 0.25)$  and  $\Omega_2 = (-0.25, 0.5)$
- **Prediction across different initial conditions (ICs)**:
  - Train with data from symmetric Gaussian IC (10K snapshots)
  - Predict with rounded square initial condition
- **Linear Oplnf**, with **regularization**  $\gamma = 1 \times 10^{-11}$

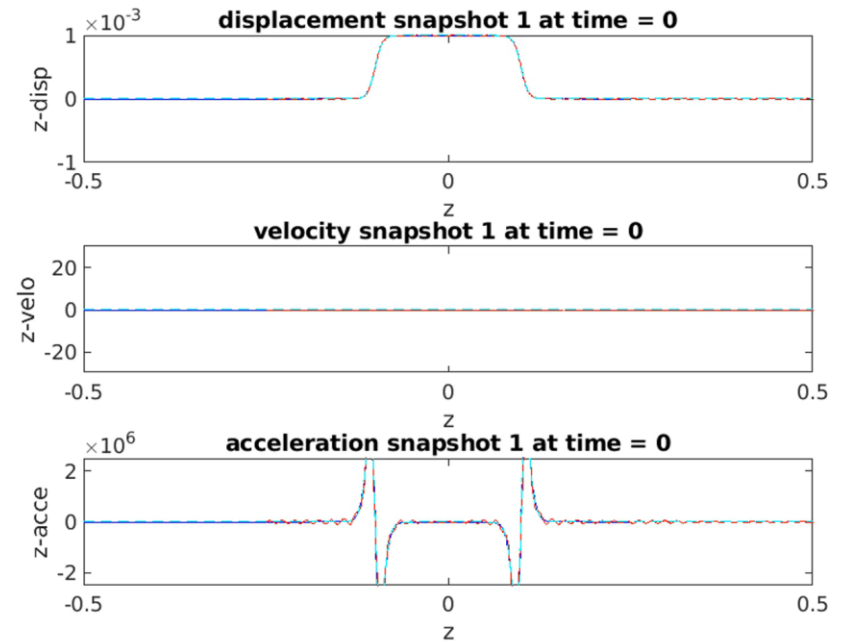


Figure above: cyan = exact analytical, blue/red = FOM/Oplnf computed.

**Key result:** similar accuracy for predictive and reproductive cases. Convergence with basis size  $M$  is observed

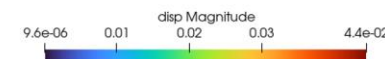
	Reproductive			Predictive		
	Displacement	Velocity	Acceleration	Displacement	Velocity	Acceleration
FOM-FOM	6.50e-3	8.02e-2	2.5e-1	6.5e-3	8.02e-2	2.52e-1
FOM-Oplnf ( $M = 15$ )	6.30e-2	4.50e-1	8.18e-1	7.48e-2	5.21e-1	8.82e-1
FOM-Oplnf ( $M = 30$ )	1.44e-2	1.66e-1	4.46e-1	1.70e-2	2.01e-1	5.25e-1
FOM-Oplnf ( $M = 60$ )	6.11e-3	7.67e-2	2.38e-1	6.53e-3	8.02e-2	2.60e-1

Table left: relative errors w.r.t. exact analytical solution

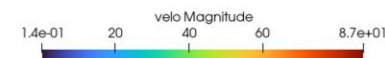


# 3D Hyperelastic Torsion Problem

- **Dynamic nonlinear hyperelastic bar** subjected to high degree of *torsion*
- **Saint-Venant Kirchhoff** material model, which gives rise to PDEs with *cubic nonlinearities*.
- **Overlapping DD** of  $\Omega$  into *two subdomains*, discretized with *nonconformal HEX8 meshes*
- Evaluated **reproductive FOM-OpInf** couplings with *linear, quadratic and cubic OpInf ROMs* built from 2K snapshots.
- **Best displacement relative errors** (quadratic OpInf): 1.94% in  $\Omega_1$  and 3.78% in  $\Omega_2$



FOM-FOM

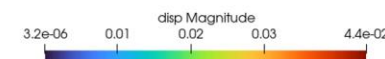
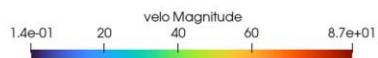


**Key result:** quadratic and cubic OpInf models can produce **stable** and **accurate** solutions (whereas linear OpInf blows up) but are extremely **sensitive** to  $\gamma$ .



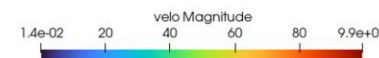
FOM-OpInf

( $M = 60, \gamma = 5 \times 10^{-3}$ )



FOM-QOpInf

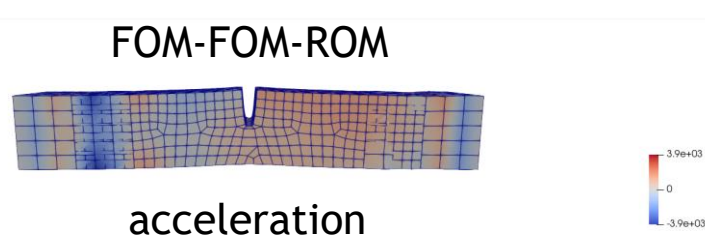
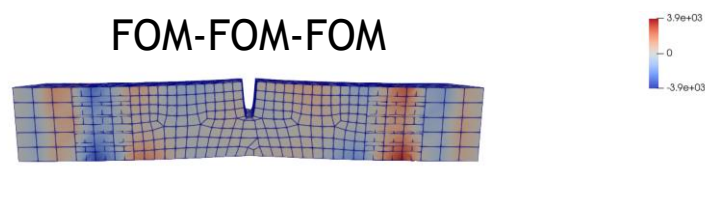
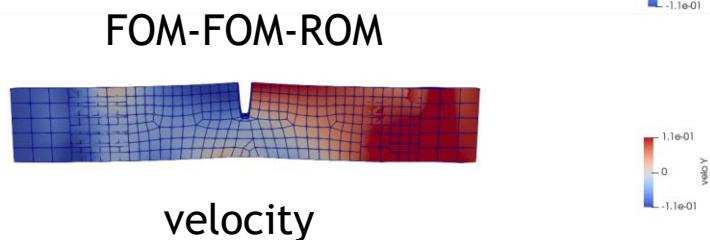
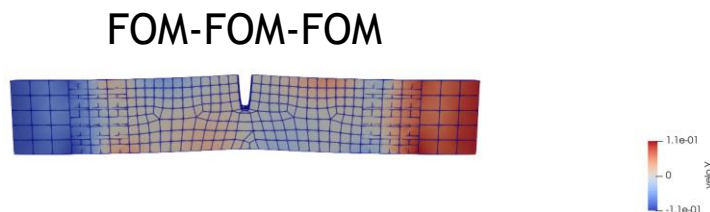
( $M = 30, \gamma = 5 \times 10^{-3}$ )



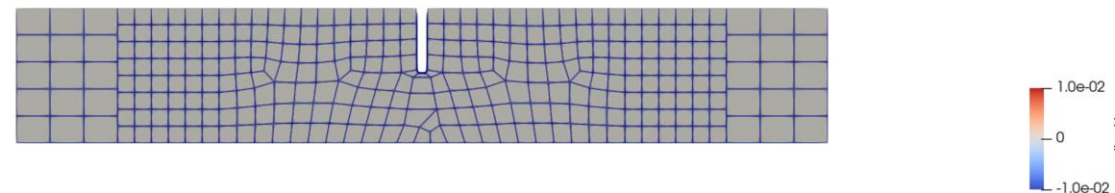


# 3D Hyperelastic Laser Weld Problem

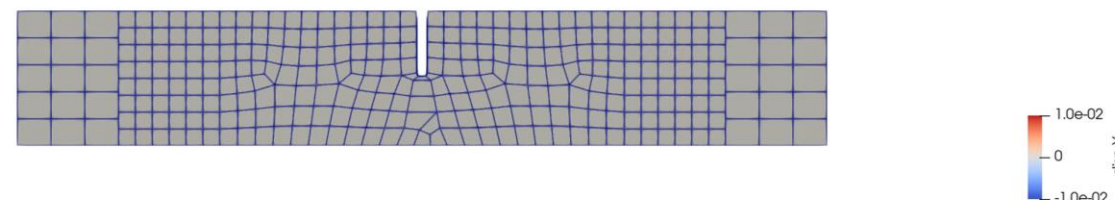
- **Nonlinear hyperelastic laser weld** geometry pulled dynamically from both ends at rate of  $0.1t$  and run to  $T_{max} = 0.1$  with  $\Delta t = 0.001$ .
- **Neohookean material model**, which gives rise to PDE with *non-polynomial nonlinearities*
- **Overlapping** DD of  $\Omega$  into *three subdomains*, discretized with *nonconformal HEX8 meshes*
- FOM in  $\Omega_1$  and  $\Omega_2$ , **linear OpInf** ROM with  $M = 20$  in  $\Omega_3$ 
  - Problem is *nonlinear* but dynamics away from laser weld are *linear*.
- **Reproductive** problem, **regularization**  $\gamma = 1 \times 10^{-4}$
- **Relative errors in y-displacement:** 0.61% in  $\Omega_1$ , 4.4% in  $\Omega_2$  and 14% in  $\Omega_3$



FOM-FOM-FOM



FOM-FOM-ROM



Movies above:  $y$ -displacement for coupled models.

**Key result:** linear OpInf ROMs within coupled FOM-ROM models can give **reasonably accurate results** for nonlinear problems if used in appropriate (linear dynamics) regions.

Figures left:  $y$ -velocity and  $y$ -acceleration solutions at final time.



## Summary:

- Schwarz has been **demonstrated** for coupling of FOMs and (H)ROMs
- **Computational gains** can be achieved by coupling **HROMs** and using the **additive Schwarz** variant
- Interesting **new results** regarding **interface sampling** & **non-overlapping transmission BCs** for CCFV

## Ongoing & future work:

- Extension to **other applications** (fasteners, laser welds)
- **Rigorous analysis** of why Dirichlet-Dirichlet BC “work” when employing non-overlapping Schwarz with discretizations that employ ghost cells
- Learning of “**optimal**” **transmission conditions** to ensure **structure preservation**
- Extension of Schwarz to enabling coupling of **non-intrusive ROMs** (e.g., OpInf, Neural Networks)
- Development of **automated criteria** to determine appropriate use of less refined or reduced-order models without sacrificing accuracy, enabling **real-time transitions** between different model fidelities → **New project: AHEAD LDRD**

